CRC Report No. A-126

ABILITY OF MODELS TO REPRODUCE THE OBSERVED CHANGES IN OZONE IN THE SOCAB DUE TO EMISSIONS REDUCTIONS FROM COVID-19

Final Report

March 2022

COORDINATING RESEARCH COUNCIL, INC.
5755 NORTH POINT PARKWAY • SUITE 265 • ALPHARETTA, GA 30022

The Coordinating Research Council, Inc. (CRC) is a non-profit corporation supported by the petroleum and automotive equipment industries. CRC operates through the committees made up of technical experts from industry and government who voluntarily participate. The four main areas of research within CRC are: air pollution (atmospheric and engineering studies); aviation fuels, lubricants, and equipment performance; heavy-duty vehicle fuels, lubricants, and equipment performance (e.g., diesel trucks); and light-duty vehicle fuels, lubricants, and equipment performance (e.g., passenger cars). CRC's function is to provide the mechanism for joint research conducted by the two industries that will help in determining the optimum combination of petroleum products and automotive equipment. CRC's work is limited to research that is mutually beneficial to the two industries involved. The final results of the research conducted by, or under the auspices of, CRC are available to the public.

Prepared for:

Coordinating Research Council
Alpharetta, Georgia

Prepared by:

Ramboll US Consulting, Inc.
7250 Redwood Blvd., Suite 105
Novato, California 94945

February 2022
1690021197

CRC A-126: ABILITY OF MODELS TO REPRODUCE THE OBSERVED CHANGES IN OZONE IN THE SOCAB DUE TO EMISSIONS REDUCTIONS FROM COVID-19 – FINAL REPORT

Bright ideas. Sustainable change.

CRC A-126: Ability of Models to Reproduce the Observed Changes in Ozone in the SoCAB due to Emissions Reductions from COVID-19 – Final Report

Ramboll
7250 Redwood Boulevard
Suite 105
Novato, CA 94945
USA

T +1 415 899 0700
https://ramboll.com

CONTENTS

Table of Figures

Table of Tables

APPENDICES

ACRONYMS AND ABBREVIATIONS

AMET	Atmospheric Model Evaluation Tool
ARB	California Air Resource Board
AQMP	Air Quality Management Plan
AQ	Air Quality
AQS	Air Quality System
BC	Boundary Condition
CARB	California Air Resources Board
CMAQ	Community Multiscale Air Quality modeling system
COVID	Coronavirus disease
COVID-19	Coronavirus disease of 2019
DVB	Design Value in Base year
DBF	Design Value in Future year
EPA	Environmental Protection Agency
GCM	Global Chemistry Model
GEOS-Chem	Goddard Earth Observing System (GEOS) global chemistry model
LCC	Lambert Conformal Conic projection
LSM	Land Surface Model
MCIP	Meteorology-Chemistry Interface Processor
MDA8	Daily-Maximum 8-hr Average
MEGAN	Model of Emissions of Gases and Aerosols in Nature
MOVES	Motor Vehicle Emissions Simulator
MPE	Model Performance Evaluation
MSKF	Multi-Scale Kain-Fritsch Cumulus Parameterization
NAAQS	National Ambient Air Quality Standard
NCAR	National Center for Atmospheric Research
NCEP	National Center for Environmental Prediction
NEI	National Emissions Inventory
NMB	Normalized Mean Bias
NME	Normalized Mean Error
NO_2	Nitrogen Dioxide
NO_X	Oxides of Nitrogen
NOAA	National Oceanic and Atmospheric Administration
O_3	Ozone
PBL	Planetary Boundary Layer
PGM	Photochemical Grid Model
PM	Particulate Matter
PPB	Parts Per Billion
PPM	Parts Per Million
QA	Quality Assurance
QC	Quality Control
SCAQMD	South Coast Air Quality Management District
SCC	Source Classification Code
SIP	State Implementation Plan
SMOKE	Sparse Matrix Kernel Emissions modeling system
SoCAB	South Coast Air Basin
Tpd	tons per day
VCP	Volatile Consumer Products
VMT	Vehicle Miles Traveled

VOC	Volatile Organic Compounds
WRF	Weather Research Forecast model
4HMDA8	4th highest maximum daily average 8-hour

EXECUTIVE SUMMARY

ES.1 Introduction

The South Coast Air Basin (SoCAB) of southern California has some of the highest ozone levels in the U.S. and the most days per year that exceed the ozone National Ambient Air Quality Standard (NAAQS). Photochemical grid model (PGM) modeling is used to determine the level of emission reductions of oxides of nitrogen (NO_X) and volatile organic compounds (VOC) in the SoCAB needed to attain the ozone NAAQS by the required dates. The SoCAB ozone attainment control strategy is focused on NO_X emissions reductions as attainment cannot be reached using VOC emission reductions alone. Mobile sources are by far the largest NO_X emissions source sector and the emission control requirements needed for ozone attainment in the SoCAB highly influence mobile source tailpipe emissions standards. The South Coast Air Quality Management District (SCAQMD) uses the Community Multiscale Air Quality (CMAQ) PGM to estimate the level of NO_X and VOC emissions reduction needed to attain the ozone NAAQS in the future attainment years. CMAQ is first applied for a base meteorological year and the model ozone estimates are compared against concurrent ozone observations in a model performance evaluation. CMAQ is then applied for a future year emissions scenario and the observed current year ozone levels are projected to the future year using the relative changes in the CMAQ base and future year ozone modeling results following procedures recommended by the U.S. Environmental Protection Agency (EPA). The model performance evaluation that compares the base year CMAQ modeling results with concurrent observations matched by time and location is termed an operational evaluation. Another type of evaluation is called a dynamic evaluation that evaluates whether PGM concentration estimates can respond to changes in emissions the same way as is observed.

In response to the COVID-19 pandemic, there have been substantial reductions in many activities (e.g., driving, manufacturing, goods movement) that generate ozone and fine particulate matter ($PM_{2.5}$) precursor emissions across the world. This has resulted in a real-world experiment of a sudden reduction in emissions that allows an assessment of how air quality has responded to the reductions in emissions. The level of NO_X emission reductions in the SoCAB caused by the response to COVID-19 pandemic was comparable to levels expected in approximately 5 years in the future under the ozone attainment control plans. We used the COVID-19 caused emission reductions in 2020 to perform a dynamic evaluation of the procedures used to project future year ozone concentrations using CMAQ modeling that are used to define the NO_X and VOC control plan for ozone attainment.

ES.2 Methodology

The June-July 2019 and 2020 modeling periods were selected that satisfied the following episode selection criteria: (1) periods in two years that had measurable emissions changes due to COVID-19 restrictions between 2020 and an earlier year; (2) regulatory significance for ozone formation potential (i.e., includes days with ozone close to the current year ozone design values); (3) meteorologically non-anomalous and similar conditions for periods in the two years; and (4) absence of confounding factors such as wildfires. Google mobility data indicated that the largest effect on transportation in the SoCAB due to the response to the COVID-19 pandemic occurred in late March and April, with a lessening but continued effect as the summer progressed. In addition, TROPOMI and OMI satellite NO_2 column data indicated that NO_2 columns were lower in June and July 2020 than previous years for the SoCAB even after considering meteorology and non-COVID related emission trends. We analyzed the regional meteorology for May – August 2020 including the 850 mb temperature (T850) which is the most descriptive parameter for determining the ozone formation potential in the SoCAB. High T850 gives an indication of the strength of the temperature inversion that can trap pollutants near the surface as well as the presence of high temperatures and slow wind speeds, all of which lead to higher ozone formation. We found that May 2020 had much higher T850 than the previous five years especially May 2019 which was wet and cold, and August 2020 had higher monthly T850 than the previous five years. In addition, August-October 2020 had an intense wildfire season throughout California. For these reasons we restrict our modeling and analysis to June and July 2020 and also modeled June and July 2019 to perform the dynamic model evaluation.

The modeling component of this study was accomplished with the WRF meteorological model and the CMAQ photochemical grid air quality model. The WRF and CMAQ extents for the 12-km and 4-km resolution modeling extents are displayed in Figure ES 1a. Figure ES 1b is a closer look at the SoCAB study region with ozone monitors indicated and counties labeled.

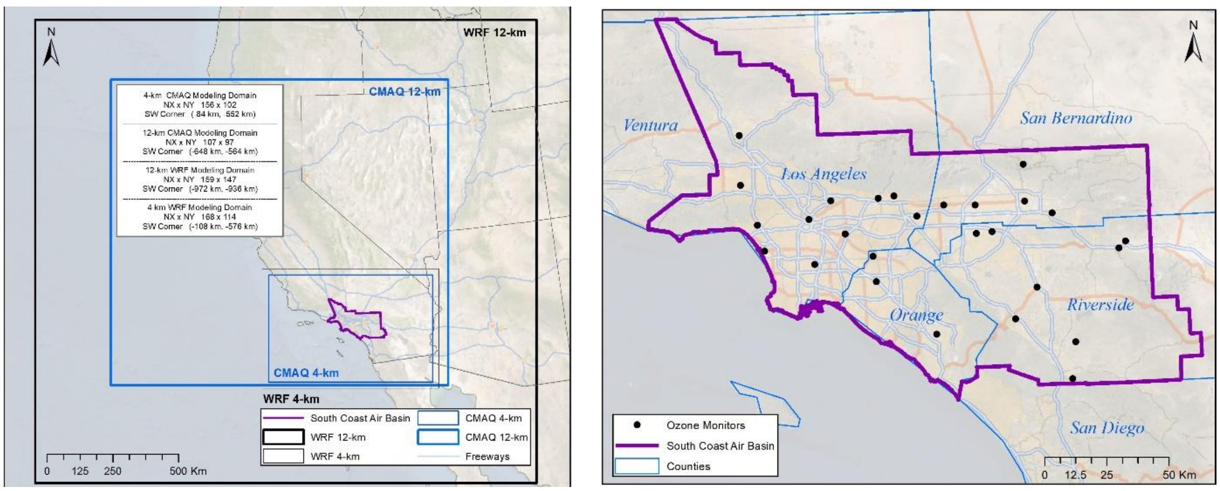

(**a**) (**b**)

Figure ES 1. Study area: (a) Geographic extents and modeling domain parameters; (b) South Coast Air Basin study region with monitor locations and SoCAB counties.

Anthropogenic emissions for California were from the ARB 2020 emissions inventory (EI) that assumed no effects from the COVID-19 pandemic (i.e., business as usual, BAU). These emissions are available in a "pre-merged" format, which means they are stored by individual source sectors (e.g., on-road mobile, aircraft) which facilitates applying different COVID-19 scaling factors to the different emission source sectors. Biogenic emissions were based on the Model of Emissions of Gases And Aerosols From Nature (MEGAN) v3.1 biogenic emissions model with ARB's adjusted urban leaf area index (LAI) using the 12/4-km WRF meteorological data. Fire emissions were based on the Fire INventory from NCAR (FINN). Emissions for the Mexico region in the 4-km domain were from the South Coast Air Quality Management Plan (2016 AQMP). Figure ES 2 displays the anthropogenic by-sector emissions breakdown for the SoCAB for the ARB 2020 EI. Any sector with less than 1% contribution to the total is not displayed. The period average is June 1 – July 31, 2020.

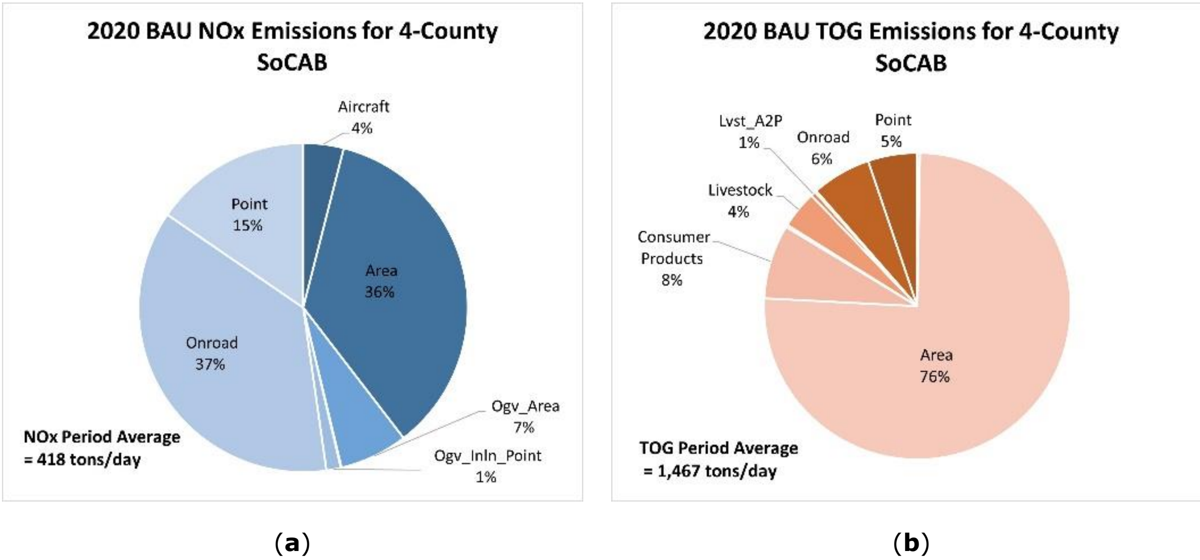

Figure ES 2. 4-county South Coast Air Basin 2020 BAU emissions by sector: (a) NOx emissions; (b) TOG emissions.

Three emissions scenarios were developed for CMAQ modeling on the 12/4-km domains:

1. 2019 Base Case: Actual emissions for June-July 2019;
2. 2020 BAU Case: 2020 business as usual scenario that represents emissions in 2020 had the COVID-19 pandemic not occurred; and
3. 2020 COVID Case: Actual 2020 emissions that reflect the reduced activity due to the response to the COVID-19 pandemic.

2019 Base emission were obtained by scaling the ARB 2020 BAU emissions for onroad emissions only. The CEPAM onroad 2019 adjustment factors were: NOx = 1.11, TOG = 1.07, and CO = 1.10. These factors were applied uniformly over the 4-km domain to the onroad emissions for each hour. 2020 BAU emissions were taken directly from the ARB 2020 emissions without any scaling adjustment since these emissions were compiled prior to the pandemic and do not account for pandemic effects.

A bottom-up approach was employed for the 2020 COVID case emissions. The 2020 BAU emissions were adjusted with sector specific COVID adjustment factors based on changes in activity. The sector with the largest NOx reductions is onroad and the primary data source used to derive the onroad scaling factor was the U.S. Energy Information Administration (EIA) refinery gasoline and diesel sales in California. EIA June and July 2020/2019 fuel sale ratios were 77% for gasoline and 84% for diesel. Figure ES 3 provides a summary of the emissions for the three model scenarios for NOx and TOG in panels (a) and (b), respectively. Note that the TOG emissions adjustments are less than 1% between the 3 scenarios, since they are dominated by area sources that had a minimal COVID adjustment and the change in onroad VOC (-27.2 tpd) is partially offset by an increase in the consumer products (+12.1 tpd).

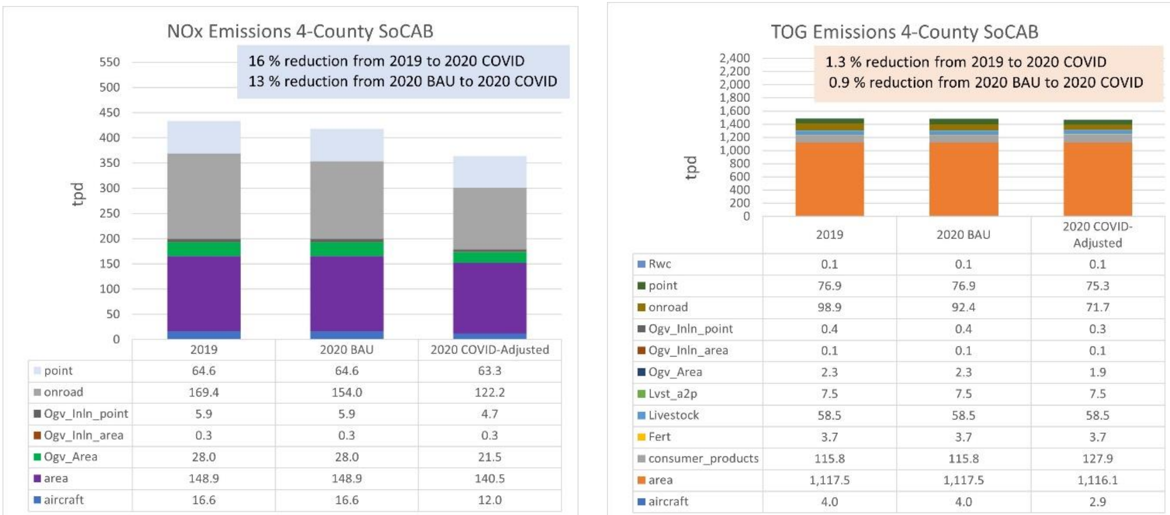

	2019	2020 BAU	2020 COVID-Adjusted
point	64.6	64.6	63.3
onroad	169.4	154.0	122.2
Ogv_Inln_point	5.9	5.9	4.7
Ogv_Inln_area	0.3	0.3	0.3
Ogv_Area	28.0	28.0	21.5
area	148.9	148.9	140.5
aircraft	16.6	16.6	12.0

	2019	2020 BAU	2020 COVID-Adjusted
Rwc	0.1	0.1	0.1
point	76.9	76.9	75.3
onroad	98.9	92.4	71.7
Ogv_Inln_point	0.4	0.4	0.3
Ogv_Inln_area	0.1	0.1	0.1
Ogv_Area	2.3	2.3	1.9
Lvst_a2p	7.5	7.5	7.5
Livestock	58.5	58.5	58.5
Fert	3.7	3.7	3.7
consumer_products	115.8	115.8	127.9
area	1,117.5	1,117.5	1,116.1
aircraft	4.0	4.0	2.9

(**a**) (**b**)

Figure ES 3. 4-county South Coast Air Basin 2019, 2020 BAU, and 2020 COVID emissions comparison by sector: (a) NOx emissions; (b) TOG emissions.

The 2019 and 2020 adjustment factors were applied to the pre-merged 2020 BAU emissions files. Figure ES 4 examples of the spatial distribution of the merged gridded NO_X emissions ($NO_X \approx NO + NO_2$) on June 10, 2020, at 0:00 UTC in moles/sec per 4-km grid cell. Figure ES 4a are emissions for the 2020 BAU scenario and Figure ES 4b is ratio of the 2020 COVID to 2020 BAU NO_X emissions. Note that the conversion factor from moles/sec to tons/day for NO_X is 4.38. Figure ES 4a shows that the highest NOx emissions come from the Los Angeles region as well as along the coast to San Diego. Figure ES 4b shows that NOx reductions are approximately 8% over the Pacific due to the OGV reductions and shows a range of reductions throughout the domain and approximately a 10 – 15% reduction over the SoCAB. For Mexico the 2020 BAU/ 2020 COVID ratio is one since those emissions were unadjusted.

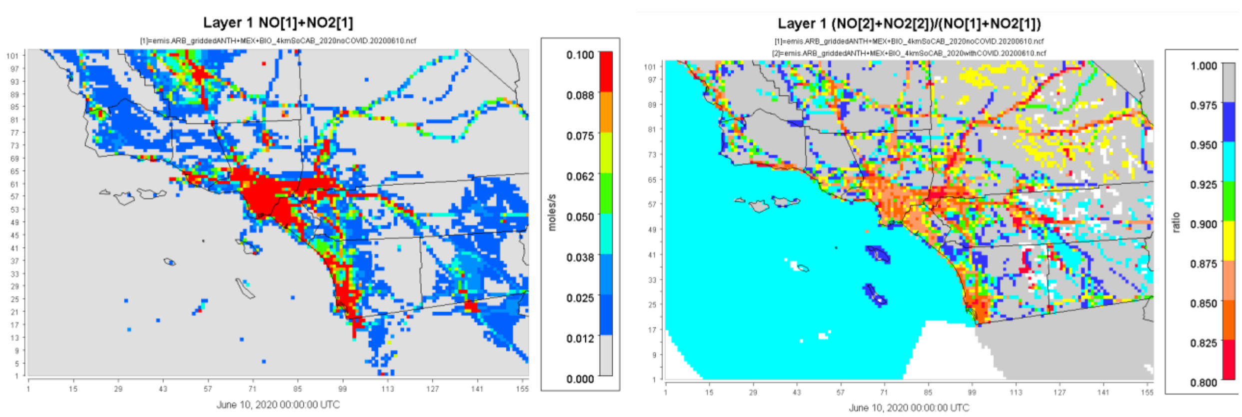

(**a**) (**b**)

Figure ES 4. Example of model-ready NOx emissions on the 4-km domain: (a) 2020 BAU NOx emissions; (b) 2020 BAU/2020 COVID NOx emissions ratio.

CMAQ version 5.2.1 was run from June through July (with a 10-day spin-up in May) for the 12-km and 4-km modeling domains and the 2019 and 2020 emissions scenarios. An operational model evaluation was performed, and ozone model performance was generally within typical thresholds based on historical PGM applications.

ES.3 Dynamic Evaluation Results

This study had two main goals: (1) to perform a dynamic model evaluation of the CMAQ model to determine whether it can reproduce the observed ozone response due to the sudden emissions reductions associated with the COVID-19 pandemic; and (2) to examine the impacts of the COVID-19 emissions reductions in the SoCAB with CMAQ. The first goal is accomplished by considering the two actual emission scenarios that occurred (i.e., 2019 Base and 2020 COVID) and comparing the modeled responses and observed ozone responses. The second goal is accomplished by comparing the CMAQ results for the two 2020 modeled scenarios (i.e., 2020 COVID and 2020 BAU emission scenarios).

For the dynamic evaluation, EPA's recommended procedures were followed for projecting future year ozone design values for an ozone attainment demonstration. EPA recommends using model ozone estimates in a relative rather than absolute sense for making future year ozone projections to reduce potential effects model bias may have on the projected future year ozone. Fractional changes in air pollutant concentrations between the model future year and model base year are calculated, these ratios are called relative response factors (RRFs). The RRFs are multiplied by base year observed ozone design value (DVB) to project a future year ozone design value (DVF) at each monitoring site:

$$DVF = RRF \times DVB$$

We calculate RRFs as one would do for projecting future year ozone design values, only instead of using modeling results for a base and future year emissions scenario with the same meteorological inputs, we use the modeling results for the 2019 Base Case and 2020 COVID Case that have different meteorology. We also calculate observation based RRFs using the 2019 and 2020 ozone observations in a consistent fashion as the modeled RRFs. The dynamic evaluation then compares the modeled and observed RRFs to determine whether the modeled ozone estimates between 2019 Base and 2020 COVID Cases responds in the same fashion as observed.

Following EPA's ozone modeling guidance, the RRFs are calculated using an average of the 10 highest (T10) modeled MDA8 ozone days in the two modeling years for each SoCAB grid cell that contains a monitor to obtain a modeled/observed pair of RRFs at each monitoring site. In addition, for all model grid cells we calculate T10 modeled RRFs over all the SoCAB grid cells. Figure ES 5 presents the results of the dynamic evaluation as a spatial plot that compares gridded CMAQ RRFs with observed RRFs at monitoring sites across the SoCAB. Over much of the SoCAB, the modeled and observed RRFs are consistent and estimate that T10 modeled day ozone increased between 2019 and 2020 with some exceptions: (1) The two furthest east monitors in the SoCAB (Banning Airport and Morongo) where both the modeled and observed RRFs agree that ozone is reduced; (2) Sites near the coast (e.g., West LA, LAX and Compton) where the model estimates ozone increases (RRF > 1.15), while the observed RRFs decreased; (3) At five additional locations throughout the basin where both modeled and observed changes were small to moderate but may change in the opposite direction (i.e., Crestline and Perris where the model estimates essentially no change in the RRFs and the observed RRFs indicate a slight reduction; Azusa and Reseda where the observed RRFs indicates no change and the model estimates a 5-10% increase; and, Fontana where observed RRF indicates a decrease of 2-5% and the model estimates an increase of 2-5%).

Thus, the only monitors that indicate a regionally consistent and substantial discrepancy between the modeled and observed RRFs are the three southwestern Los Angeles County sites near the coast (i.e., West LA, LAX and Compton). Besides these three sites, there is general agreement between CMAQ and the observed ozone responses as shown in the scatter plot in Figure ES 5 which compares the observed and modeled RRFs excluding the three coastal sites discussed above. This suggests that CMAQ is broadly able to replicate the observed ozone increase between 2019 and 2020 (that include the COVID-19 emissions reductions) within the framework of EPA’s recommended ozone projection procedures used in a modeled attainment demonstration. In general, the model response is weaker than the observed response (i.e., regression slope < 1) and responses at individual sites may vary (R^2 = 0.2). Note that the average modeled and observed RRFs in the scatter plot are both 1.07 which indicate an average 7% increase in ozone in 2020 compared to 2019.

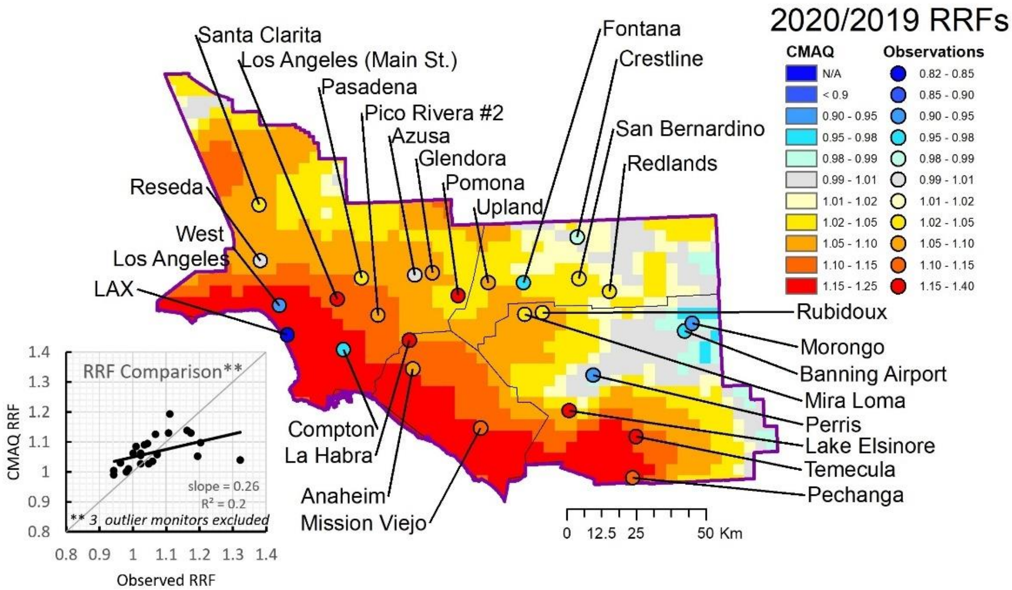

Figure ES 5. Dynamic evaluation that compares CMAQ versus observed RRFs based on T10 modeled MDA8 ozone days.

Note that the analysis in Figure ES 5 has year-specific meteorology for the two modeling years in the RRF calculations. Although the modeling periods of June-July 2019 and 2020 were selected to obtain modeling episodes in two different years with similar meteorology, there will still be differences and the extent to which the meteorology affected the increase in ozone between 2019 and 2020 is investigated next. Figure ES 6 compares two sets of modeled RRFs. Figure ES 6a is the same as Figure ES 5 (i.e., 2020 COVID/2019 Base) and Figure ES 6b is 2020 COVID/2020 BAU (which has emissions reductions but the same meteorology for both cases). Note that the 2020 BAU NO_X emissions are approximately 4% lower than the 2019 Base emissions (i.e., the RRFs in Figure ES 6a are based on a 17% difference whereas Figure ES 6b is based on a 13% difference between the scenarios), so it is not a perfect one-to-one comparison, nevertheless, it is useful to get a sense of the relative magnitude of meteorological versus emissions impacts. RRF deviations from unity for the dynamic meteorological case (i.e., Figure ES 6a) compared to the static meteorological case (i.e., Figure ES 6b) are much larger, which suggest that meteorology plays the dominant role in causing higher ozone in 2020 than 2019. In addition, the spatial pattern is quite different between the two figures. Figure ES 6b shows regions of VOC-sensitive (yellow) and NO_X-sensitive (blue) ozone formation chemical regimes clearly delineated.

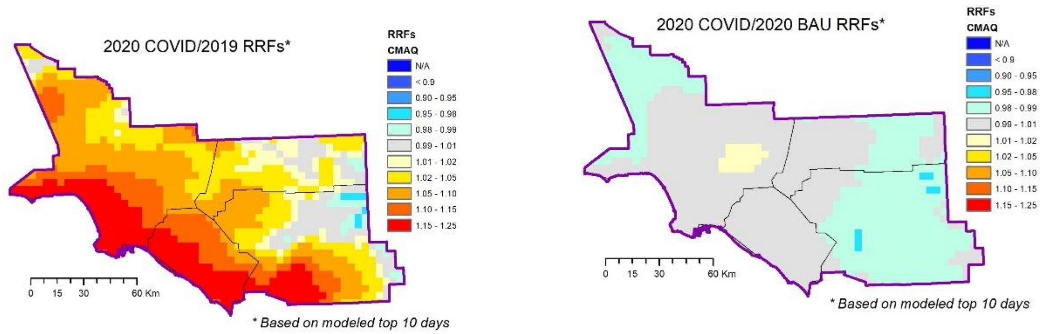

(**a**) (**b**)

Figure ES 6. CMAQ derived RRFs (a) 2020 COVID/2019 Base; (b) 2020 COVID/2020 BAU.

ES.4 Impacts of the COVID-19 Emissions Reductions in the SoCAB

The CMAQ-predicted impacts of the COVID-19 emissions reductions on the two-month average MDA8 ozone concentrations are shown in Figure ES 7. Grey shading represents minimal differences; cool shades represent ozone decreases and warm shades represent ozone increases. The domain-wide maximum is 0.81 ppb, and the domain-wide minimum is -1.33 ppb. The ozone response to the ~13% NO_X reduction clearly delineates the average extent of the modeled VOC-sensitive versus NO_X-sensitive chemical regimes within the SoCAB. The area of ozone increases encompasses the southeastern quadrant of Los Angeles County and stretches into San Bernardino and Orange Counties. The area of ozone decreases occurs over a larger area that includes Santa Clarita Valley, most of San Bernardino, Riverside, and southern Orange Counties. Although the area of ozone decrease is larger than the area of ozone increase, a vast majority of the population resides in the area of ozone increases.

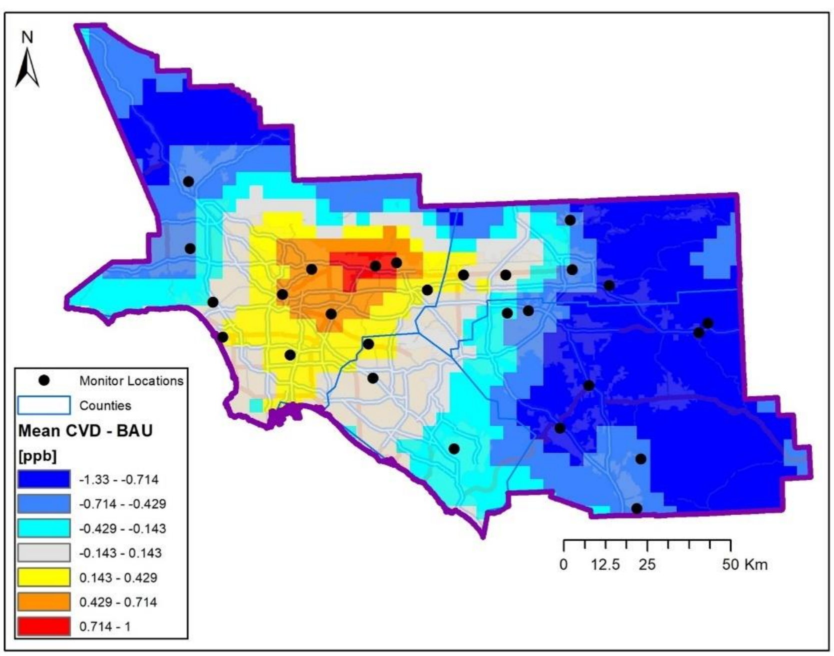

Figure ES 7. Period-average June 1 – July 31 impacts of the COVID-19 emissions reductions on MDA8 ozone, estimated by CMAQ.

ES.5 Conclusions

1. Using procedures that are used to make future year ozone projections, the CMAQ ozone changes between 2019 and 2020 are generally consistent with the observed ozone changes which lends confidence in future year ozone projection methodologies;

2. Meteorology played the major role in the increases in ozone between 2019 and 2020;

3. The reduction in NO_X emissions due to the response of the COVID pandemic caused ozone increases in Los Angeles County and into western San Bernardino County, with more widespread ozone decreases further east;

4. Ozone formation in parts of the SoCAB is still VOC-sensitive and the locations where NO_X reductions cause ozone increases occur in areas with some of the highest population density in the SoCAB;

5. The evaluation of VOC/NO_X emission control strategies to attain the ozone NAAQS needs to examine ozone levels in the intervening years between current and the attainment year to better understand whether ozone may be getting worse or cause more population exposure to high ozone concentrations rather than focusing solely on ozone levels in the far-off attainment year.

1.0 INTRODUCTION

In response to the COVID-19 pandemic, there have been substantial reductions in many activities (e.g., driving, manufacturing, goods movement) that generate ozone and fine particulate matter ($PM_{2.5}$) precursor emissions around the world. This has resulted in a real-world experiment of a sudden reduction in emissions that allows an assessment of how the observed air quality responded to the reductions in emissions and whether air quality models can reproduce such changes.

1.1 Purpose

The Coordinated Research Council (CRC) has initiated Project A-126 to examine the effects of the emission reduction due to COVID on ozone air quality in the South Coast Air Basin (SoCAB) of Southern California and whether the models used to define future year ozone attainment emission control strategies can reproduce the observed ozone changes in response to the sudden emission changes.

The South Coast Air Quality Management District (SCAQMD) develops Air Quality Management Plans (AQMPs) that, among other things, include control plans for oxides of nitrogen (NO_X) and Volatile Organic Compounds (VOC) designed to achieve attainment of the ozone National Ambient Air Quality Standards (NAAQS) by the required dates. These control plans in turn drive the emissions standards for motor vehicles and other sources in the United States (U.S.). Thus, it is important that the models used to develop the ozone control plans respond to emission changes the same way as observed ozone responds to changes in emissions. This aspect of the evaluation of photochemical grid models (PGMs) is termed a Dynamic Evaluation and the sudden emission changes in 2020 due to COVID-19 mitigation strategies offer a unique real-world opportunity to conduct such a Dynamic Evaluation in the SoCAB.

1.2 Trends in SoCAB Ozone Concentrations

Figure 1-1 displays the trend in the SoCAB-wide highest maximum daily average 8-hour (MDA8) ozone Design Value (DV[1]) over the last 40 years. The SoCAB ozone DV trend shows a steep decline in ozone DVs from 250 ppb in 1980 to a low of 102 ppb in 2014. However, there was a slowing of the downward trend in ozone DVs around the year 2000 and even an increase starting in 2016. Figure 1-2 displays the ozone DV and 4th highest MDA8 ozone concentration trends over the last two decades. There is considerable year-to-year variation in ozone concentrations as shown in the 4th highest MDA8 ozone in Figure 1-2 that is not as evident in the ozone DV trends due to the 3-year averaging of the ozone DV. Given that, with the possible exception of the 2008-2009 recession and 2020 COVID-19 response, the year-to-year changes in emissions is more gradual yet there are large yearly variations in the 4th high MDA8 ozone, the year-to-year variations of meteorology is a major driver of ozone levels in the SoCAB.

[1] An ozone DV is defined as the three-year average of the 4th highest MDA8 ozone concentration at a monitoring site.

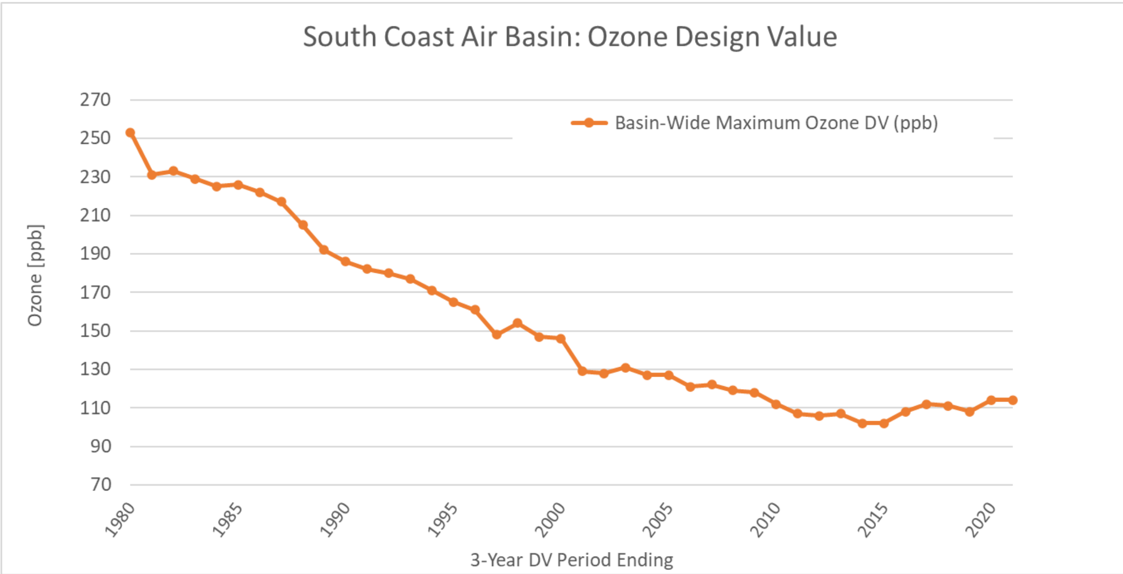

Figure 1-1. Trends in SoCAB-wide maximum ozone design values 1980-2020.

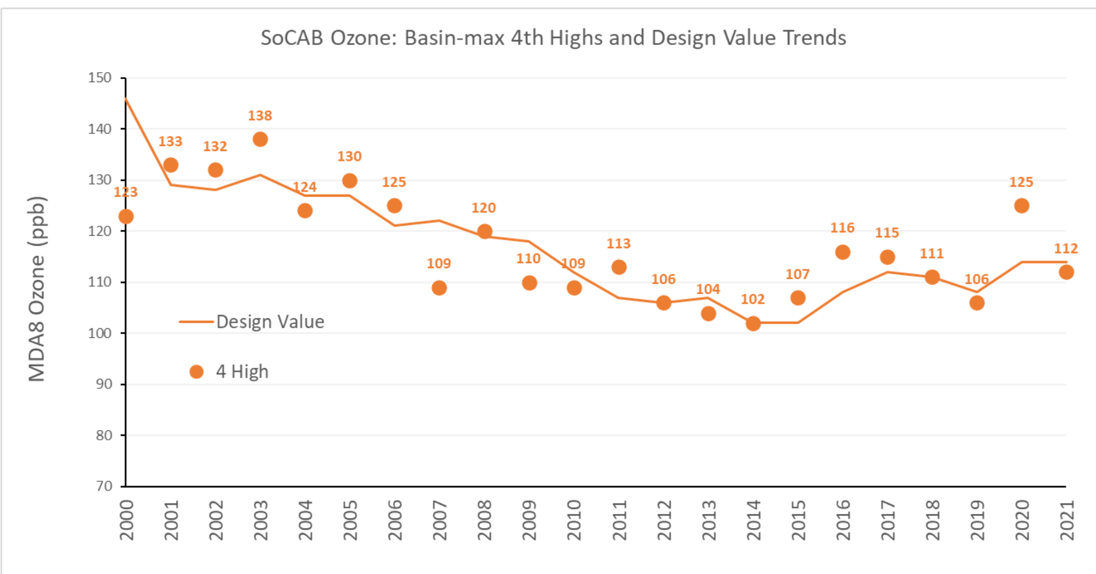

Figure 1-2. Trends in SoCAB-wide maximum ozone DV (line) and 4th highest MDA8 ozone concentrations (symbols with values) over the last two decades.

The fourth highest MDA8 ozone in 2020 was 125 ppb that was the highest value since 2006 (Figure 1-2). Despite the emission reductions due to the shelter-in-place order in response to the COVID-19 pandemic, 2020 had some of the highest ozone concentrations in the SoCAB in decades. Figure 1-3 displays the number of ozone exceedance days per year in the SoCAB over the last 30 years with 2020 having 157 exceedance days that was the most since 1997. A discussion of the potential causes of high ozone in 2020 is provide in Chapter 9.0 where we analyze the anomalously high number of bad air days as shown in Figure 1-3 as well as the anomalous 4th high MDA8 in 2020 as shown in Figure 1-2.

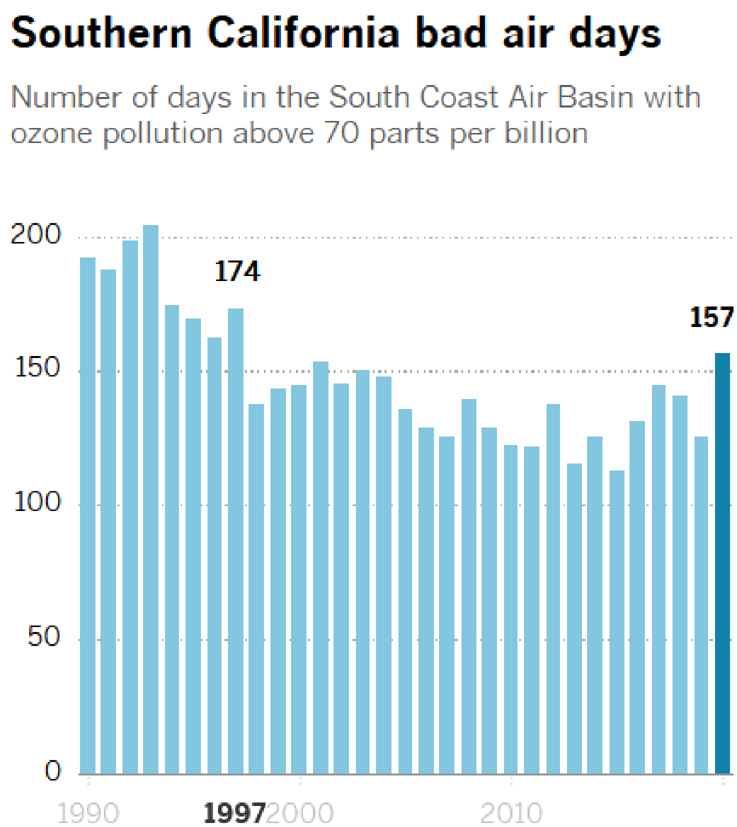

Figure 1-3. Number of days per year in the SoCAB that MDA8 ozone exceeded 70 ppb ozone NAAQS.[2]

1.3 Overview of Approach

The June and July 2019 and 2020 periods were modeled using the Community Multiscale Air Quality modeling system (CMAQ) photochemical grid model that has been used in the most recent Air Quality Management Plans (AQMPs) for the SoCAB (e.g., the 2016 AQMP[3] and 2012 AQMP[4] as well as the 2022 AQMP[5] in preparation). The Weather Research Forecast (WRF) meteorological model was used to generate CMAQ meteorological inputs for the mid-May through July period in 2019 and 2020. Three emissions scenarios were developed that are primarily based on ARB 2020 emissions platform[6]:

- <u>2019 Base Case</u>: Actual 2019 emissions;
- <u>2020 Business As Usual (BAU) Case</u>: Emissions that would have occurred in 2020 without the COVID-19 shelter-in-place order; and
- <u>2020 COVID Case</u>: Actual 2020 emissions that occurred that include the effects of the COVID-19 shelter-in-place order on emissions.

[2] https://www.latimes.com/california/story/2020-12-06/2020-la-air-quality-southern-california-pollution-analysis
[3] http://www.aqmd.gov/home/air-quality/clean-air-plans/air-quality-mgt-plan/final-2016-aqmp
[4] http://www.aqmd.gov/home/air-quality/clean-air-plans/air-quality-mgt-plan/final-2012-air-quality-management-plan
[5] http://www.aqmd.gov/home/air-quality/clean-air-plans/air-quality-mgt-plan#
[6] Jeremy Avise, personal communication

The methodologies to derive the emissions scenarios are described in detail in Chapter 5.0 A model evaluation was conducted that compared the CMAQ results to the concurrent measured ozone and NO_X concentrations.

Observed air quality and meteorological and modeling data were analyzed to determine the potential causes of the high ozone concentrations in 2020 and whether current PGM ozone estimates respond to the changes in emissions the same way as was observed.

This Report is organized as follows:

- Chapter 2 discusses the episode selection;
- Chapter 3 details the WRF meteorological modeling;
- Chapter 4 summarize the preliminary CMAQ modeling that used a top-down approach to implement the effects COVID-19 had on emissions in 2020;
- Chapter 5 discusses the approach for developing the 2019 base case, 2020 BAU case and 2020 COVID case emissions using a bottom-up approach for accounting for the COVID-19 effect on activity and subsequently emissions in 2020;
- Chapter 6 discusses the CMAQ bottom-up modeling approach;
- Chapter 7 presents the operational model performance evaluation;
- Chapter 8 assess the ability of the CMAQ ozone estimates to respond to changes in emissions due to COVID-19 in the same way as observed;
- Chapter 9 provides additional analysis of the causes of high ozone in 2020 based on ambient data;
- Chapter 10 summarizes conclusions and recommendations; and
- Chapter 11 presents references.

Additional information is provided in Appendices.

2.0 EPISODE SELECTION

To assess the effect of the emission changes due to the response to the COVID-19 pandemic on ozone concentrations in the SoCAB, we model periods with and without the COVID-19 effects that have similar meteorological and ozone formation potential conditions. This requires modeling a period before the 2020 COVID-19 effects and modeling a period in 2020 when the response to the COVID-19 pandemic affected emissions.

2.1 2020 Period with COVID-19 Effects on Emissions

The shelter-in-place orders in response to the COVID-19 pandemic in the SoCAB came out in mid-March 2020 and resulted in a dramatic drop in transportation and other activities that generate emissions. This is shown in the county-level Google mobility data in Figures 2-2 through 2-4. Figure 2-1 presents the counties where the mobility data were analyzed and an outline of the SoCAB. Figure 2-2 and Figure 2-3 show that in mid-March there was a 20% drop in grocery and pharmacy trips and a 40% drop in trips for retail/recreation, workplace, transit stations and parks with an increase in residential trips. The reductions in trips for grocery/pharmacy and parks is almost recovered by May 2020, but trips for retail/recreation and workplace continued to be suppressed through the summer and into September 2020. The Google mobility data indicate that the largest effect on transportation occurred in late March and April, with a lessening of the effect as the summer progressed, but some effects occurred throughout the summer of 2020.

Figure 2-4 displays Aura OMI satellite NO_2 column measurements from January through September and the years 2015 through 2020. There is a sudden drop in the satellite measured NO_2 column in mid-March 2020, with 2020 NO_2 in the SoCAB continuing to be mostly below the other years until around August 2020.

Although the Google mobility data suggest the largest reduction in transportation sources occurred in April 2020, the highest ozone levels in the SoCAB that drive the ozone attainment emission control plans occur later in the summer (June-August) so modeling April would not provide regulatory relevant information regarding whether models used for attainment demonstration modeling can reproduce the observed changes in ozone in response to changes in emissions caused by the COVID-19 pandemic mitigation strategies.

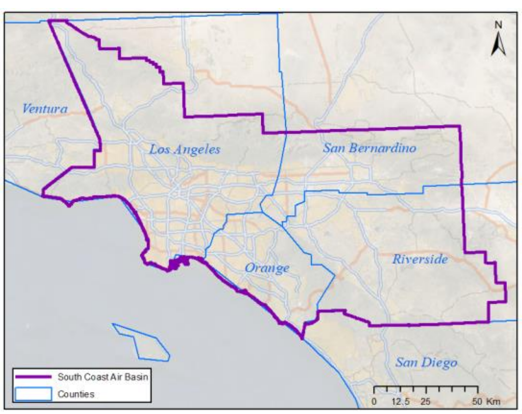

Figure 2-1. SoCAB with county outlines.

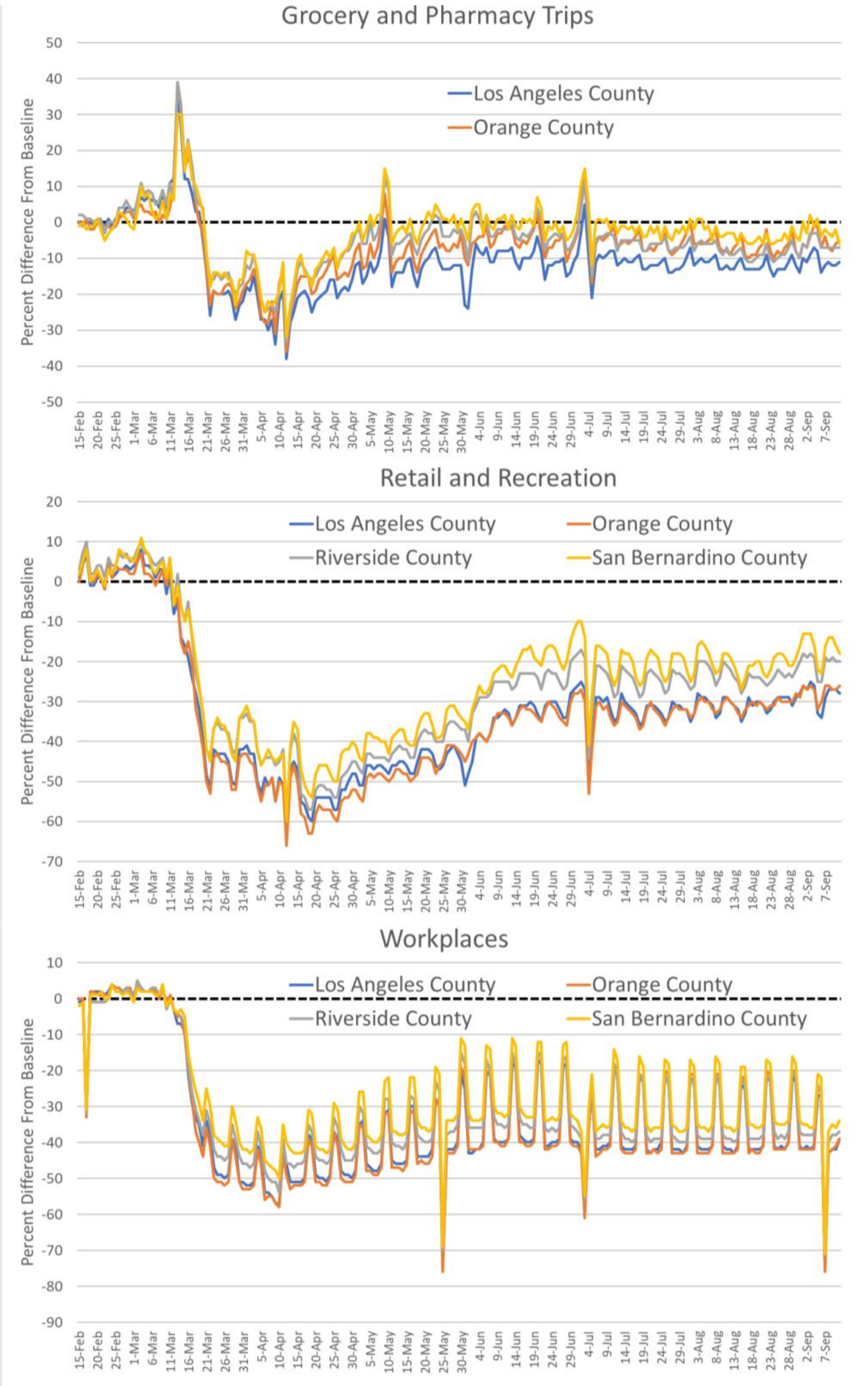

Figure 2-2. Google daily mobility data for counties in the SoCAB from February to September 2020.

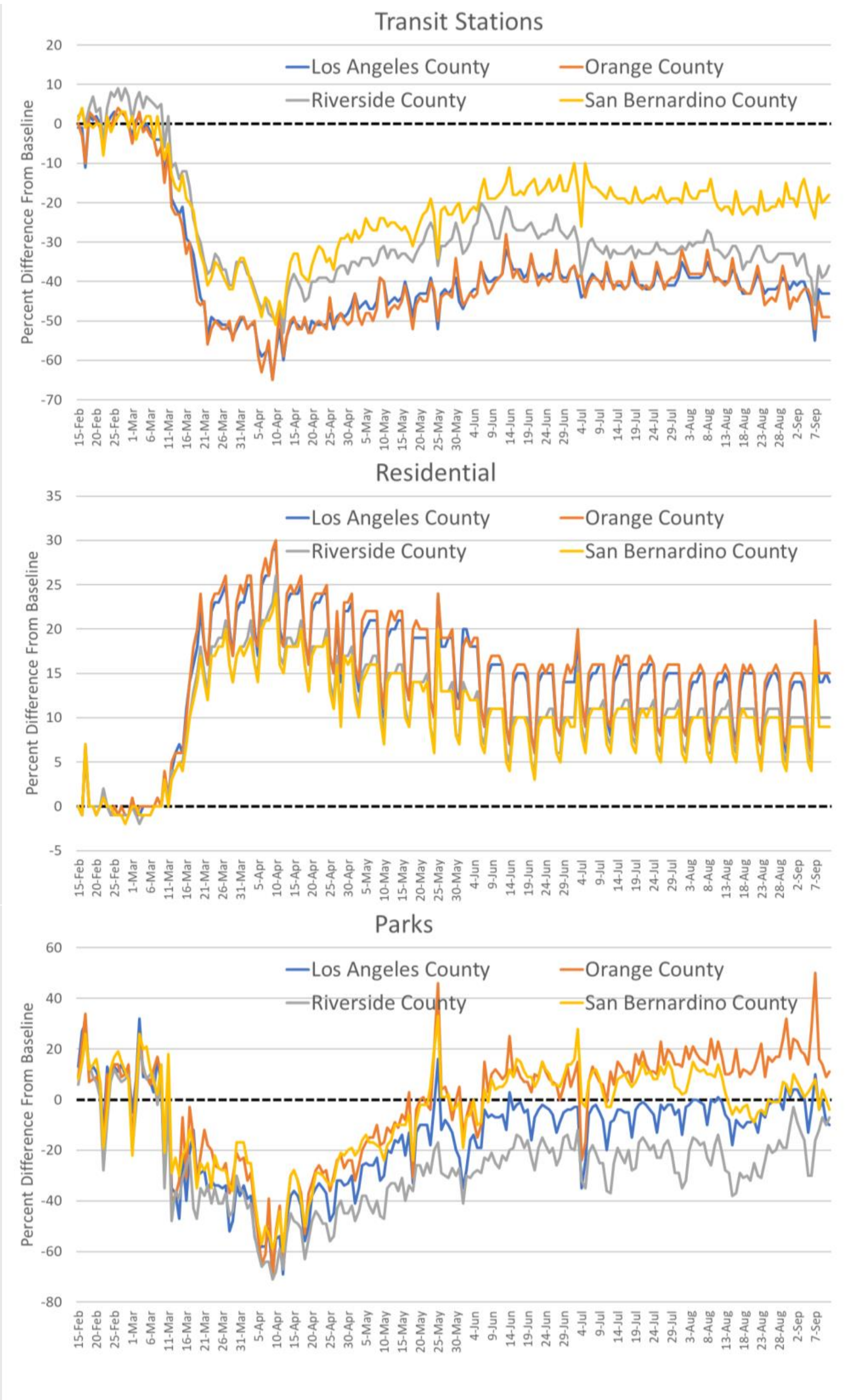

Figure 2-3. Google daily mobility data for counties in the SoCAB from February to September 2020.

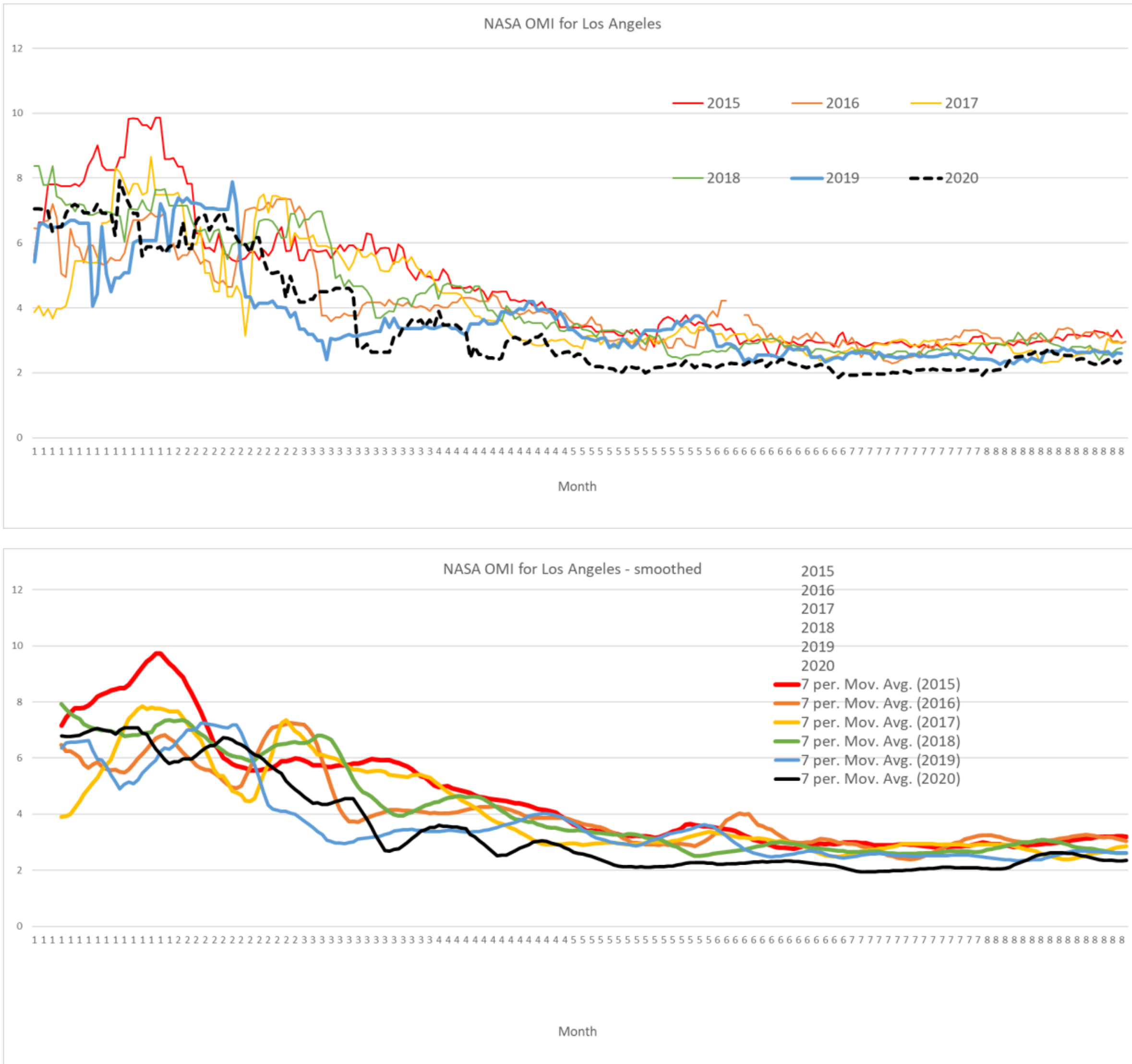

Figure 2-4. Satellite NO_2 column measurements for Los Angeles and January to August 2015 through 2020 from the Aura satellite.[7]

[7] https://aura.gsfc.nasa.gov/index.html

2.2 Meteorological Characterization

The single most descriptive parameter for determining the ozone formation potential of the atmosphere in the SoCAB is the 850 mb temperature (T850). High T850 gives an indication of the strength of the temperature inversion that can trap pollutants near the surface as well as the presence of high temperatures and slow wind speeds, all of which lead to higher ozone formation. Figure 2-5 compares the May-August monthly T850 for the San Diego upper-air sounding and the 6-year period of 2015-2020. May 2020 had a much higher T850 than the previous five years, especially May 2019 that was wet and cold. The T850 in June and July 2016-2018 are higher than the other years, but the monthly average June and July T850 values in 2019 and 2020 are comparable. August 2020 had the highest August monthly T850 value of the six years analyzed.

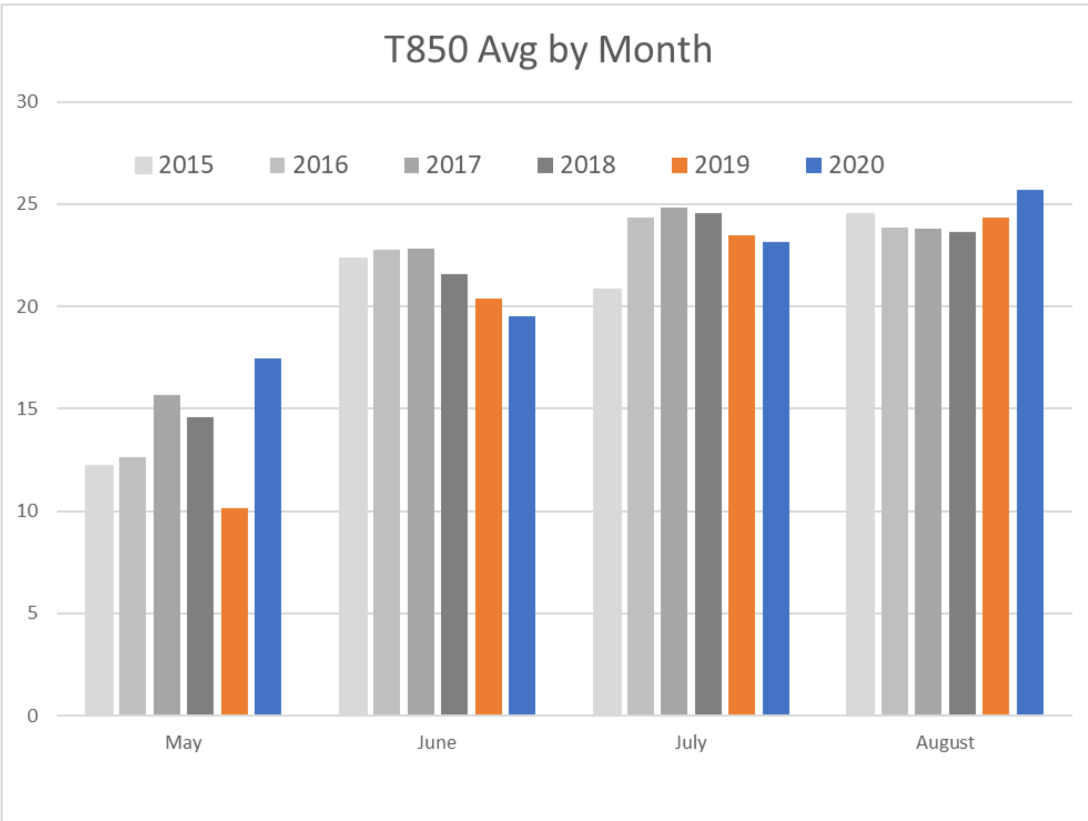

Figure 2-5. Monthly average 850 mb temperature (C) for May through August and 2015 through 2020 at the San Diego upper-air sounding location.

Figure 2-6 compares the distribution of temperatures at the Ontario inland site for the months of May through August and the 2019 and 2020 years. May 2019 was much colder and wetter than May 2020, so comparison of ozone results between the two years for May would not be useful. There is much more overlap in the temperature distributions for 2019 and 2020 and the months of June and July with the median/means being with a few degrees of each other. August 2020 was much warmer than August 2019 with the median in 2020 approximately the same as the 75th percentile in 2019. Ozone formation in August 2020 was also contaminated by emissions from wildfires.

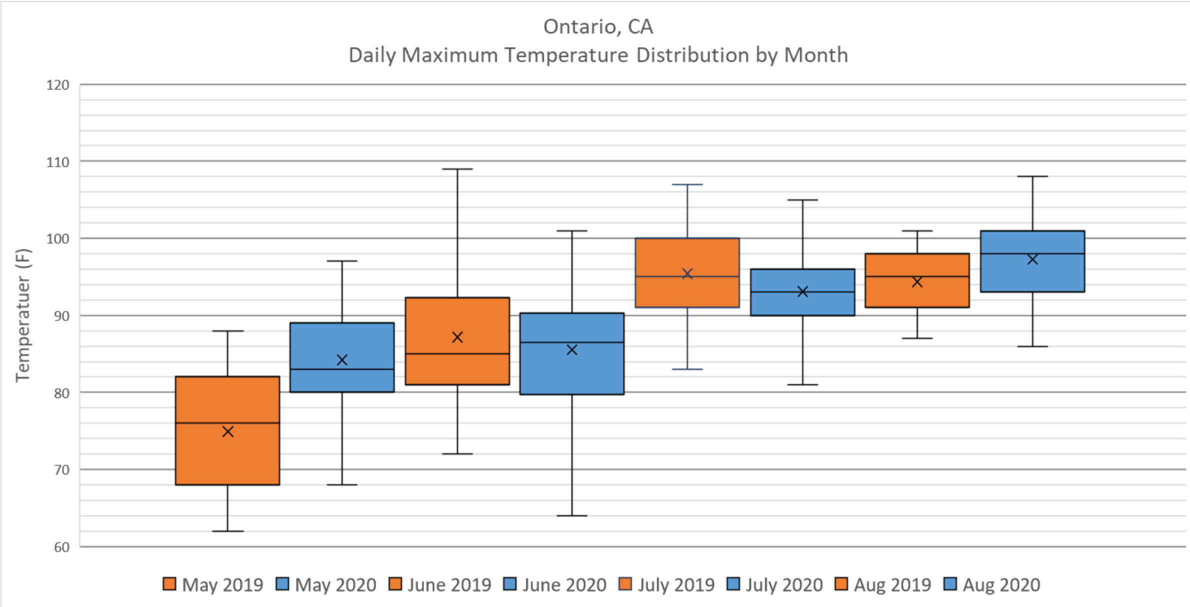

Figure 2-6. Distribution of temperatures at Ontario during the months of May, June, July and August during 2019 and 2020. Boxes are 25-75%, whiskers are max/min, median is bar and mean is cross.

2.3 Selection of Modeling Period for Analysis

The June-July 2019 and 2020 modeling periods were selected for the modeling and data analyses in this study for the following reasons:

- April 2020 was too early in the year so ozone modeling would not represent the highest ozone levels that are used to determine the ozone emission control plans for the SoCAB.
- May 2020 was much hotter and drier than the previous 5 years and had much higher occurrence oof conditions conducive to ozone formation than previous years.
- August 2020 was also hotter and had higher ozone formation potential meteorological conditions than previous years. Smoke from wildfires also likely affected ozone concentrations in the SoCAB in August and September.[8]
- Of previous years to 2020, 2019 would have emissions most like 2020 had the COVID-19 pandemic not occurred.

[8] https://www.fire.ca.gov/incidents/2020/

3.0 METEOROLOGICAL MODELING

The Weather Research Forecast (WRF) prognostic meteorological model was used to generate meteorological inputs for CMAQ and the mid-May through July period in 2019 and 2020.

3.1 WRF Modeling Domain

WRF was operated on a western U.S. 36-km grid resolution domain (d01), a California 12-km grid resolution domain (d02) and a 4-km grid resolution domain for the SoCAB (d03). The WRF 4-km SoCAB domain was defined to align with and completely contain the 4-km SoCAB CMAQ modeling domain used by the SCAQMD in their AQMP modeling. Similarly, the WRF 12-km California domain was aligned with and defined larger than the California Air Resources Board (CARB) CMAQ 12-km California domain. Table 4-1 provides the projection parameters and the domain definitions for the SCAQMD/AQMP 4-km and CARB 12-km CMAQ modeling domains and the WRF 36/12/4-km modeling domains. The WRF 12/4-km modeling domains are shown in Figure 3-1.

Table 3-1. Definitions of the SCAQMD/AQMP 4-km and CARB 12-km CMAQ modeling domains and the WRF 36/12/4-km modeling domains.

Projection Definition	
Projection	Lambert Conic Conformal (LCC)
Latitude of Origin	37 N
Central Meridian	120.5 W
Standard Parallel	30N, 60 N
4-km SCAQMD/AQMP CMAQ Modeling Domain	
NX x NY	156 x 102
SW Corner	(-84 km, -552 km)
12-km CARB CMAQ Modeling Domain	
NX x NY	107 x 97
SW Corner	(-648 km, -564 km)
36-km WRF Modeling Domain	
NX x NY	88 x 78
SW Corner	(-1584 km, -1404 km)
12-km WRF Modeling Domain	
NX x NY	159 x 147
SW Corner	(-972 km, -936 km)
4-km WRF Modeling Domain	
NX x NY	168 x 114
SW Corner	(-108 km, -576 km)

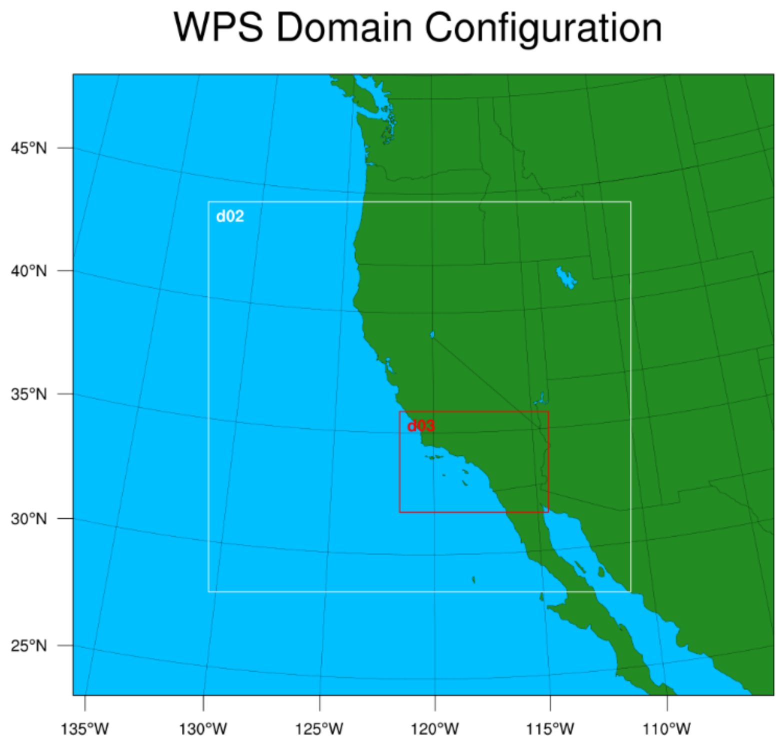

Figure 3-1. WRF 12-km (d02) and 4-km (d03) grid resolution modeling domains used to develop meteorology for mid-May through July in 2019 and 2020.

3.2 WRF Physics Options

Table 3-2 lists the WRF physics options used for the mid-May-July 2019 and 2020 36/12/4-km WRF simulations. We selected the hybrid sigma-pressure coordinate system to reduce numerical errors over the complex terrain in the SoCAB modeling domains that ranges from sea level to over 11,000 feet for Mount San Gorgonio. The Noah Land-Surface Model (LSM) and Yonsei University (YSU) Planetary Boundary Layer (PBL) models were used. The multi-scale Kain Fritsch (MSKF) cumulus parameterization was used in all three domains.

Table 3-2. WRF v4.1.4 physics options used in the 2019 and 2020 SoCAB modeling.

WRF Physics Option	Option Selected	Notes
Vertical Coordinate System	Hybrid Sigma-Pressure	Hybrid Sigma-Pressure coordinate (Park et al., 2019)
Microphysics	WRF Single-Moment 6-class (WSM6)	A scheme with ice, snow and graupel processes suitable for high-resolution simulations.
Longwave Radiation	RRTMG	Rapid Radiative Transfer Model. An accurate scheme using look-up tables for efficiency. Accounts for multiple bands, and microphysics species.
Shortwave Radiation	RRTMG	Rapid Radiative Transfer Model. An accurate scheme using look-up tables for efficiency. Accounts for multiple bands, and microphysics species.
Surface Layer Physics	MM5 similarity	Based on Monin-Obukhov with Carslon-Boland viscous sub-layer and standard similarity functions from look-up tables
LSM	Noah	NCEP/NCAR land surface model with soil temperature and moisture in four layers, fractional snow cover and frozen soil physics.
PBL scheme	Yonsei University (YSU)	Non-local-K scheme with explicit entrainment layer and parabolic K profile in unstable mixed layer
Cumulus parameterization	MSKF WRF	Multi-Scale Kain-Fritsch (MSKF) cumulus parameterization includes feedback of subgrid cloud information to the radiation schemes.

3.3 WRF Model Performance Evaluation

In this section we present a limited WRF model performance evaluation (MPE). The MPE focuses on: (1) WRF's ability to reproduce the 850 mb temperatures (T850) from the observed upper-air soundings at San Diego (Marine Corps Air Station Miramar; KNKX) and the Vandenburg Air Force Base (KVBG) near Lompoc; and (2) WRF's ability to reproduce surface meteorological observations across the SoCAB.

3.3.1 Upper Air T850 Evaluation

The top panel in Figure 3-2 shows T850 for WRF (orange) and observations (blue) at KNKX for June 1 – July 31 for both 2019 and 2020. The bottom panel in Figure 3-2 shows T850 bias (WRF-observations) at KNKX for the same two periods. These upper-air instruments are launched twice daily at 00:00 and 12:00 UTC (5:00 PM and 5:00 AM PDT, respectively). WRF T850 performance at KNKX is excellent, with nearly all hours falling within ±2 °C bias. Monthly mean bias and error statistics (Table 3-3) at KNKX show that monthly error for the 4 months never exceeds 0.9 °C (worst performing month is June 2019; MB: -0.70 °C; ME: 0.87 °C).

Figure 3-3 shows the same T850 time series as in Figure 3-2, but for the KVBG station. WRF T850 performance at KVBG is similar to KNKX, with bias rarely exceeding ±2 °C. As seen at KNKX, monthly error for the 4 months at KVBG never exceeds 0.9 °C (see Table 3-3). At both stations, T850 performance is better in July than June for both 2019 and 2020. Finally, T850 agreement appears quite good when observed T850 is above 20 °C, a key condition for producing high ozone concentrations.

We conclude from this T850 model performance evaluation that the WRF meteorology is adequately representing observed 850 mb temperatures, especially during the warmest days when ozone formation potential in the SoCAB is highest.

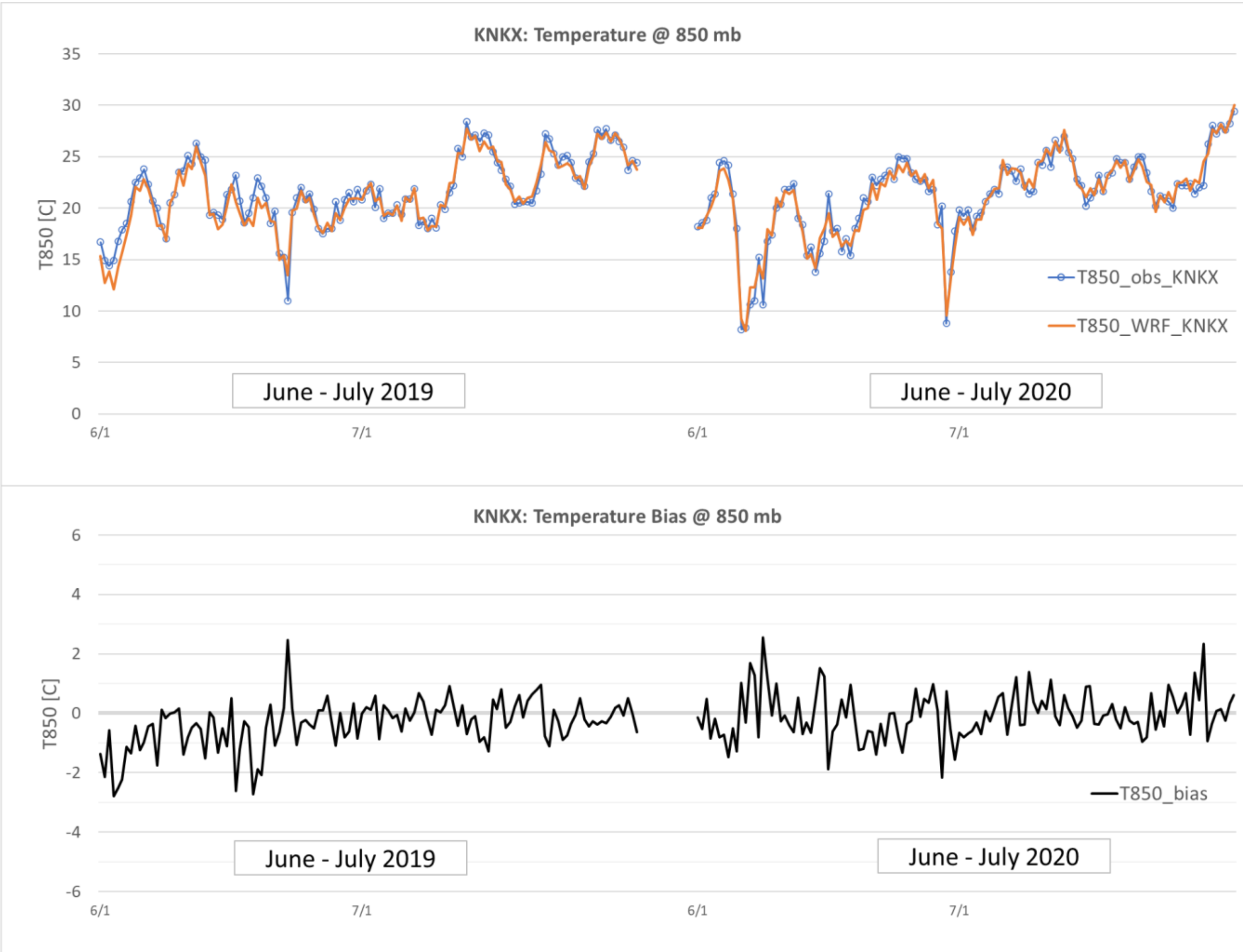

Figure 3-2. Top panel: T850 for observations (blue) and WRF (orange) at KNKX for June-July 2019 and June-July 2020. Bottom panel: T850 bias (WRF-observations) at KNKX for June-July 2019 and June-July 2020.

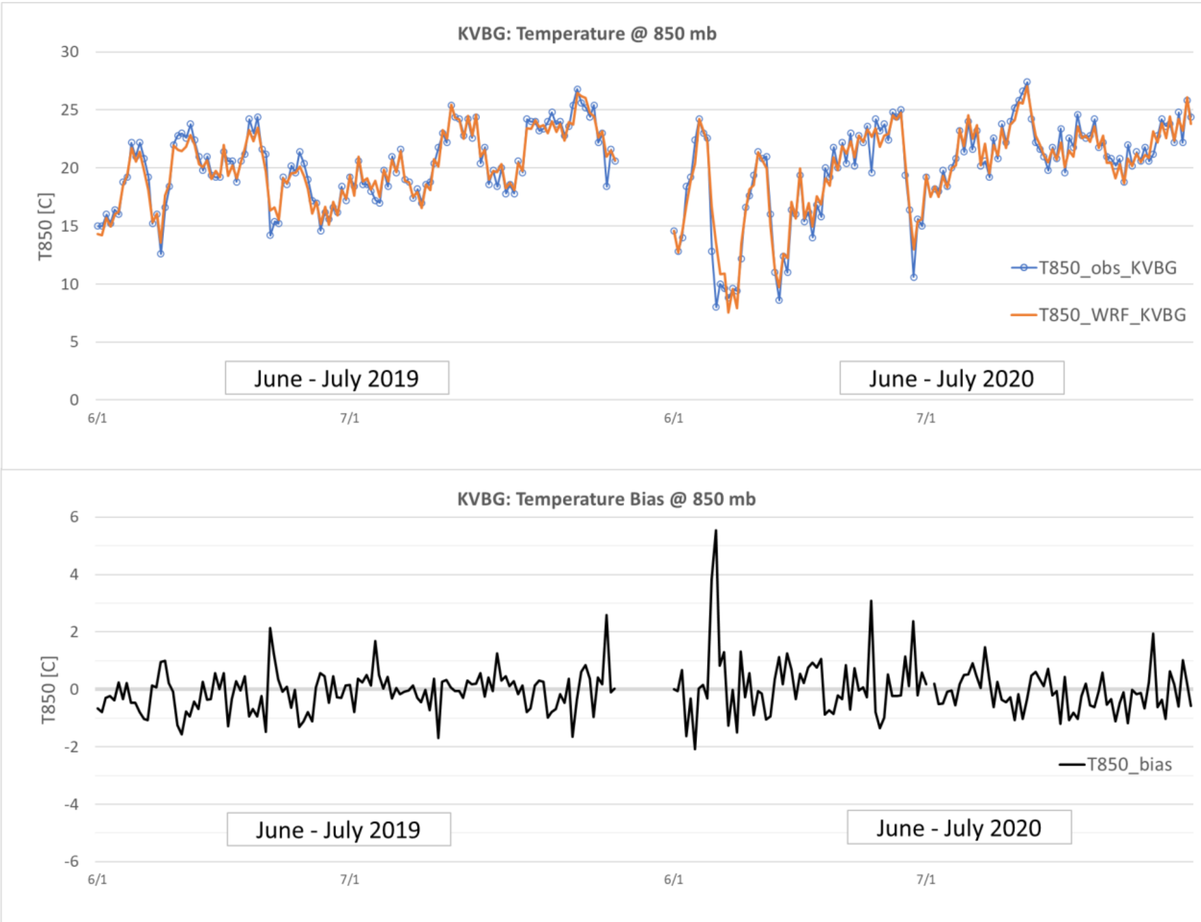

Figure 3-3. Top panel: T850 for observations (blue) and WRF (orange) at KVBG for June-July 2019 and June-July 2020. Bottom panel: T850 bias (WRF-observations) at KVBG for June-July 2019 and June-July 2020.

Table 3-3. T850 monthly mean bias (MB) and mean error (ME) at KNKX and KVBG for June and July for 2019 and 2020.

Station	June 2019		July 2019		June 2020		July 2020	
	MB (°C)	ME (°C)	MB (°C)	ME (°C)	MB (°C)	ME (°C)	MB (°C)	ME (°C)
KNKX	-0.70	0.87	-0.06	0.41	-0.16	0.75	0.04	0.51
KVBG	-0.24	0.59	0.04	0.46	0.21	0.84	-0.11	0.51

3.3.2 Surface Meteorological Evaluation

A quantitative evaluation of the WRF surface model performance was conducted at surface meteorological monitoring sites within the SoCAB using METSTAT. METSTAT (Ramboll, 2013) is a publicly available evaluation software that was used to calculate monthly bias and error statistical performance metrics for surface wind speed and direction, temperature and humidity and compares them to a set of commonly used meteorological model performance benchmarks.

3.3.2.1 Meteorological Model Performance Benchmarks

METSTAT calculates meteorological performance statistics for a meteorological model simulation and compares then to performance benchmarks to help interpret the model performance and put it in context with the performance of past meteorological model applications. Table 3-4 lists the meteorological model performance benchmarks for simple (Emery et al., 2001) and complex (Kemball-Cook et al., 2005; McNally, 2009) situations. The simple condition benchmarks were developed by analyzing well-performing meteorological model evaluation results for simple, mostly flat terrain conditions and simple meteorological conditions (e.g., stationary high pressure) that were conducted to support air quality modeling studies (e.g., ozone SIP modeling). The complex benchmarks were developed during the Western Regional Air Partnership (WRAP) first round of regional haze modeling and are performance benchmarks for more complicated conditions, such as the complex terrain of the Rocky Mountains and Alaska (Kemball-Cook et al., 2005). McNally (2009) analyzed multiple annual runs that included complex terrain conditions and suggested an alternative set of benchmarks for temperature under more complex conditions.

The WRF evaluation metrics were calculated on a monthly time frame for wind speed, wind direction, temperature, and humidity at the surface using all 63 surface observation sites in the SoCAB 4-km domain and at individual sites. The WRF surface meteorological model performance metrics were compared against the simple and complex model performance benchmarks using “soccer plots.” Soccer plots use two WRF performance metrics as X-axis and Y-axis values (e.g., temperature bias as X, and temperature error as Y) along with the performance benchmarks. The closer the symbols are to the zero origin, the better the model performance. These plots make it easy to see when the two WRF statistical performance metrics fall within the benchmarks.

Table 3-4. Meteorological model performance benchmarks for simple and complex conditions.

Parameter	Emery et al. (2001)	Kemball-Cook et al. (2005)	McNally (2009)
Conditions	Simple	Complex	Complex
Temperature Bias	≤ ±0.5 K	≤ ±2.0 K	≤ ±1.0 K
Temperature Error	≤ 2.0 K	≤ 3.5 K	≤ 3.0 K
Humidity Bias	≤ ±0.8 g/kg	≤ ±1.0 g/kg	≤ ±1.0 g/kg
Humidity Error	≤ 2.0 g/kg	≤ 2.0 g/kg	≤ 2.0 g/kg
Wind Speed Bias	≤ ±0.5 m/s	≤ ±1.5 m/s	(not addressed)
Wind Speed RMSE	≤ 2.0 m/s	≤ 2.5 m/s	(not addressed)
Wind Dir. Bias	≤ ±10 degrees	(not addressed)	(not addressed)
Wind Dir. Error	≤ 30 degrees	≤ 55 degrees	(not addressed)

3.3.2.2 Surface Meteorological Performance Across the SoCAB

Figure 3-4 displays soccer plots of WRF monthly model performance across all sites in the SoCAB 4-km domain and the June-July 2019 and 2020 modeling periods. The WRF monthly surface windspeed performance across all sites achieves the most stringent bias simple conditions performance benchmark (±0.5 m/s) with a slight slow bias with the wind speed error right at the simple benchmark (2.0 m/s). The WRF monthly wind direction bias also achieves the simple performance benchmark (±10 °) with the direction error falling between the simple (30 °) and complex (55 °) benchmarks.

The WRF monthly temperature performance across all sites in the SoCAB is also quite good achieving the simple benchmark for both bias (±0.5 °C) and error (2.0 °C). The WRF humidity performance is not as good with a dry bias between -1.0 and -2.0 g/kg that falls outside the humidity bias complex benchmark (±1.0 g/kg) with humidity error achieving the simple benchmark for all months but July 2019.

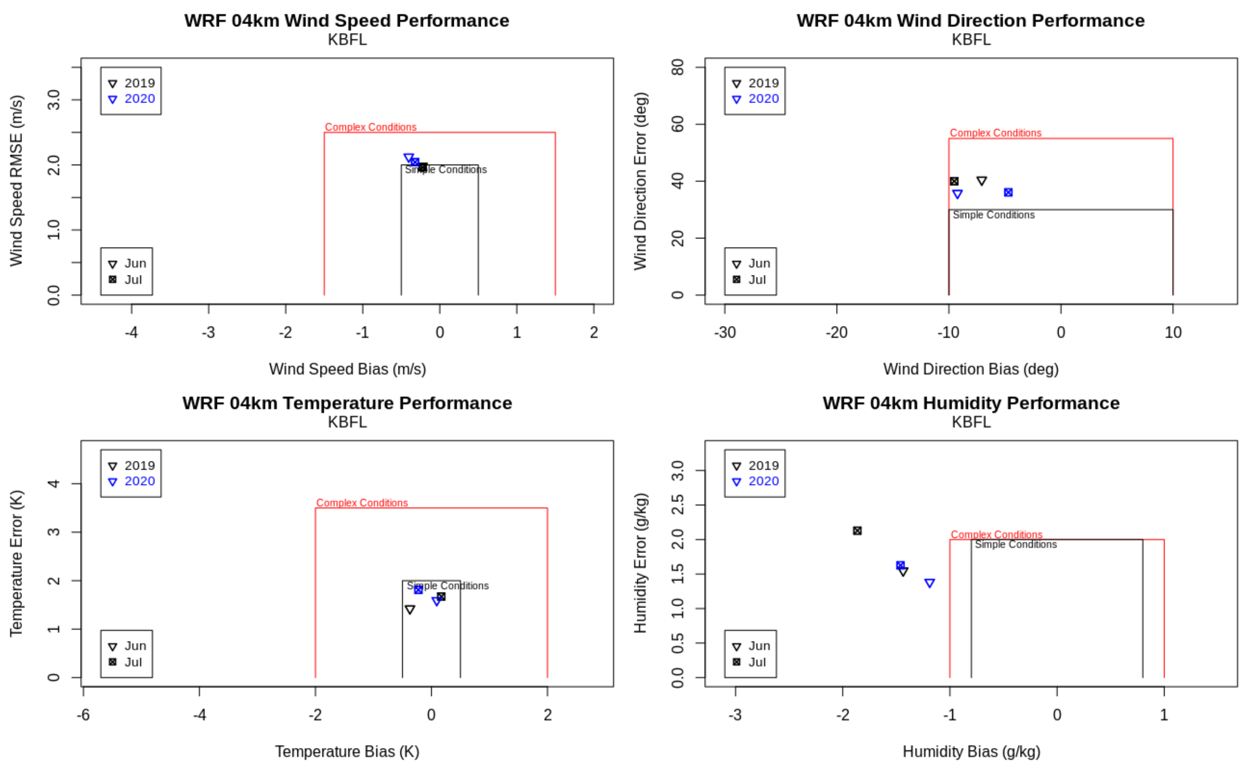

Figure 3-4. Soccer plots of wind speed, wind direction, temperature, and humidity WRF monthly model performance across all sites in the SoCAB 4-km domain for June and July 2019 and 2020.

3.3.3 Surface Meteorological Performance at Individual Sites

Soccer plots of WRF surface performance were generated at all 63 sites in the SoCAB 4-km domain, example results are presented below for five airports in the SoCAB as shown in Figure 3-5. Three of the locations are near the coast, and two are within the Inland Empire.

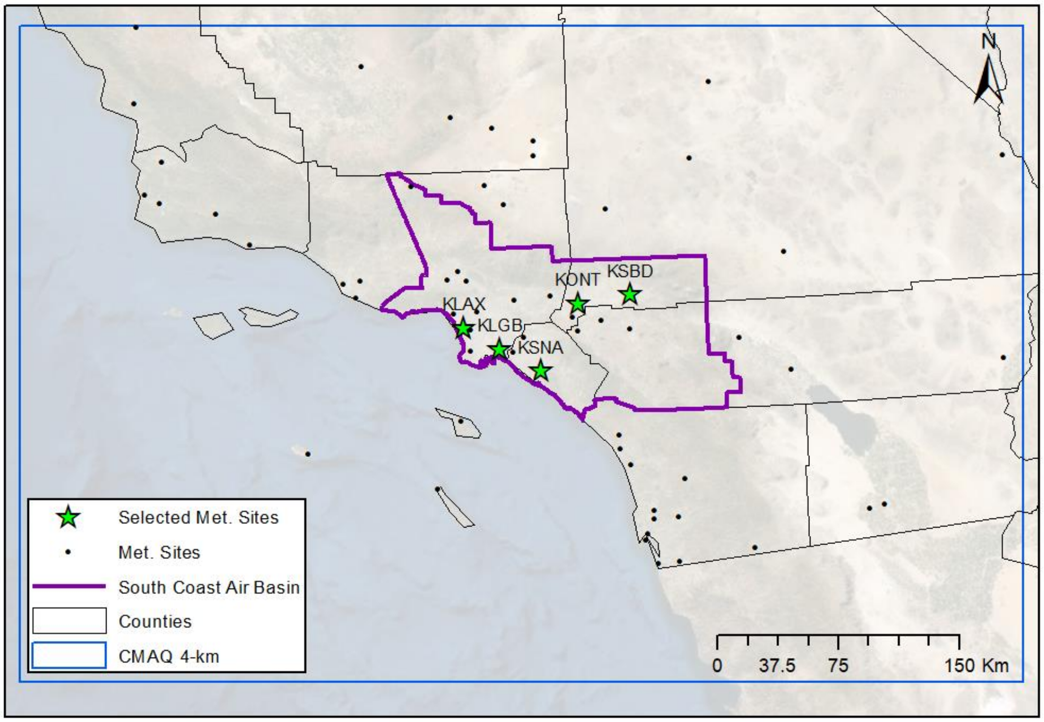

Figure 3-5. Meteorological site locations and the locations of the five example sites presented in this section.

The WRF performance at the Los Angeles International Airport (KLAX) coastal site is shown in Figure 3-6. The WRF monthly wind speed bias is approximately -1.0 m/s for all four months falling between the simple and complex benchmarks with wind speed error achieving the simple benchmark. WRF monthly wind direction bias at LAX is -10 ° in 2020 and -15 ° in 2019 with error right at the simple benchmark.

The WRF monthly temperature bias has a warm bias at KLAX that achieves the complex benchmark suggesting it may be understating the marine penetration with June performing better than July in both years. WRF monthly humidity performance at KLAX achieves the simple benchmark with a slight wet bias.

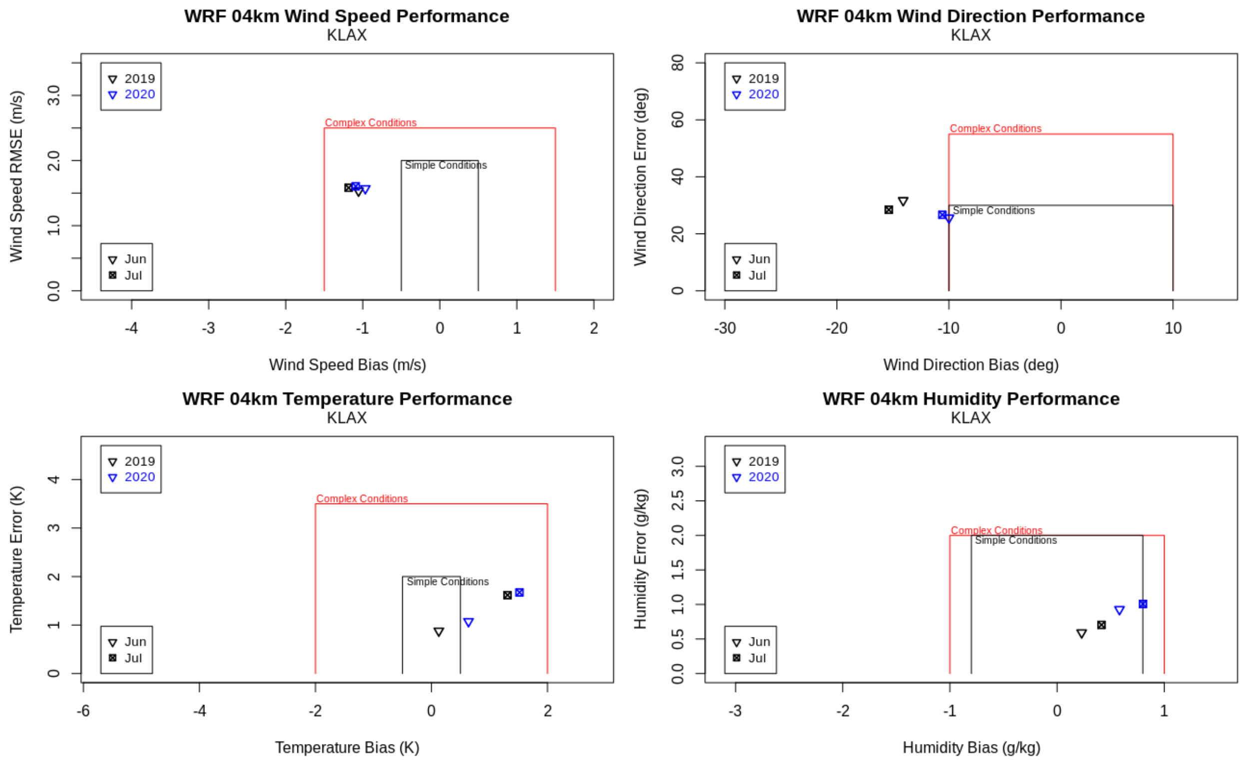

Figure 3-6. Soccer plots of wind speed, wind direction, temperature, and humidity WRF monthly model performance at the Los Angeles International Airport (KLAX).

There are similarities in the WRF model performance at the coastal Long Beach Airport (KLGB; Figure 3-7) to KLAX. The monthly wind speed and direction performance for June and July are similar for both years with wind speed achieving the bias and error simple benchmarks and wind direction achieving it in June but not July. As seen at KLAX, temperature has a warm bias at Long Beach that achieves the complex benchmark except for July 2020. Humidity performance is good at Long Beach and slightly better than at KLAX but has a slight wet bias.

The WRF monthly surface performance at the Santa Ana (John Wayne; KSNA) airport in Orange County is also fairly good achieving the simple benchmarks for all parameters but wind direction bias for all months and temperature bias in July 2020 only that just barely falls outside of the simple benchmark (Figure 3-8).

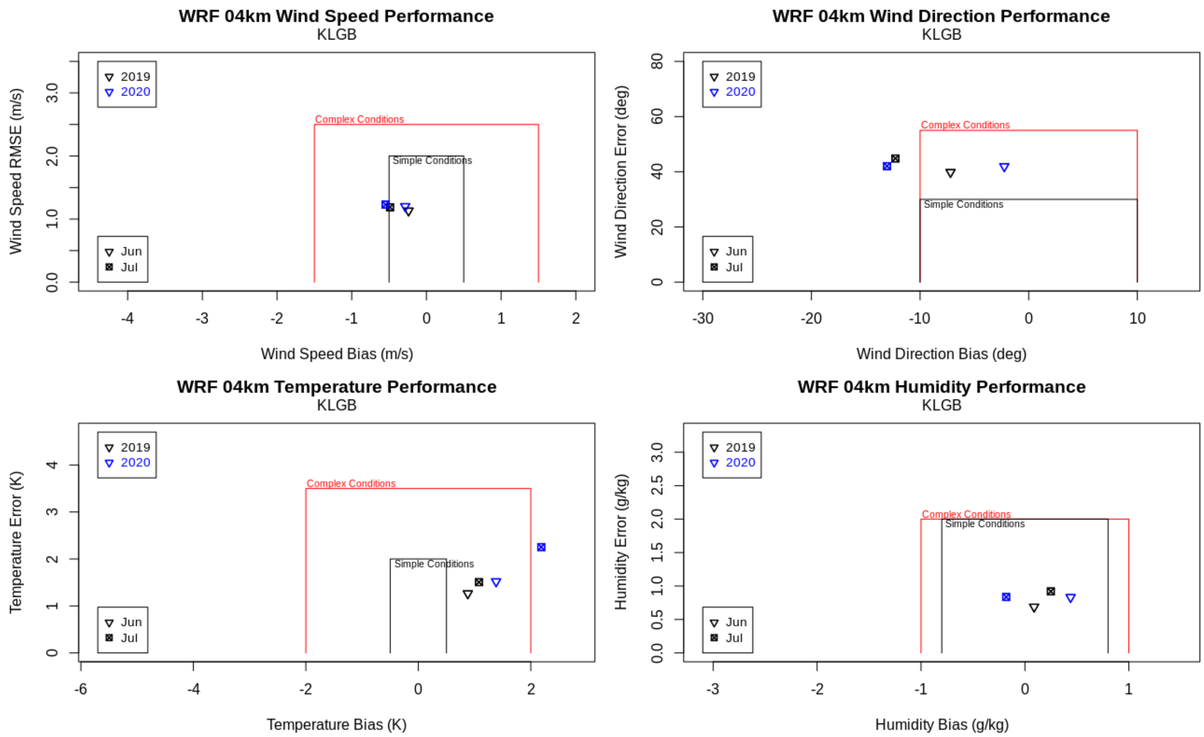

Figure 3-7. Soccer plots of wind speed, wind direction, temperature, and humidity WRF monthly model performance at the Long Beach Airport (KLGB).

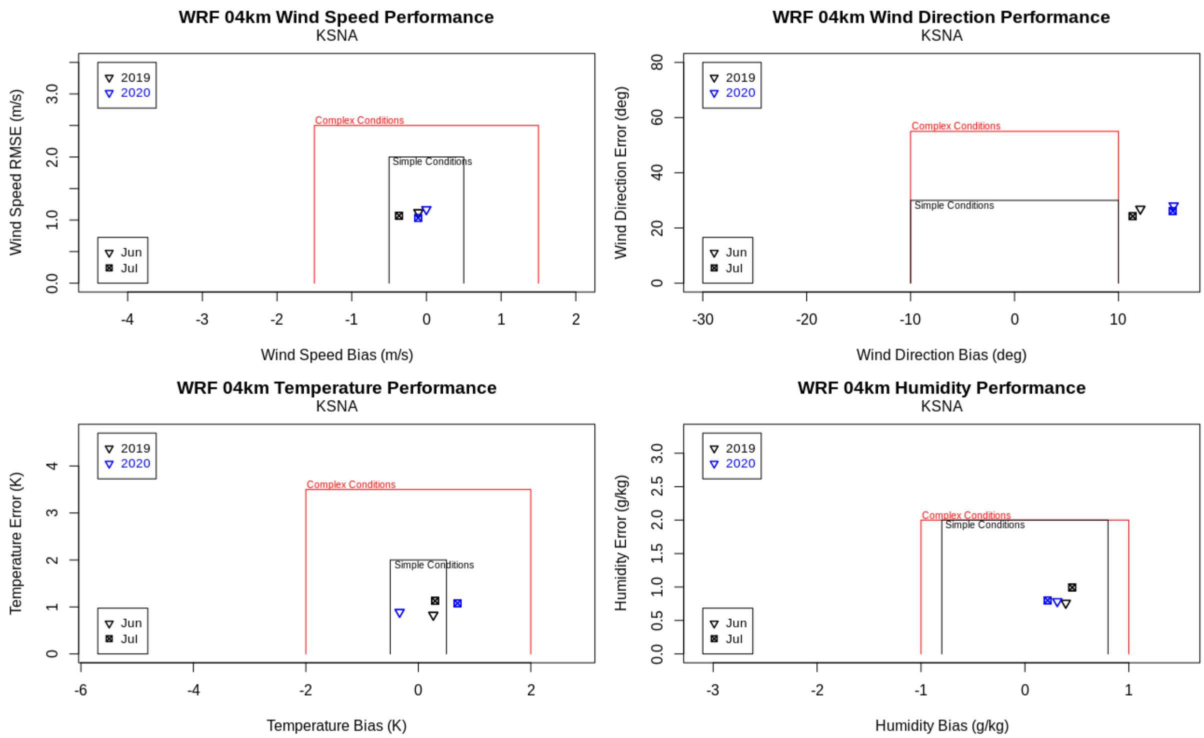

Figure 3-8. Soccer plots of wind speed, wind direction, temperature, and humidity WRF monthly model performance at the Santa Ana (John Wayne) airport (KSNA).

Figure 3-9 and Figure 3-10 display WRF monthly model performance at the two inland airports of Ontario (KONT) and San Bernardino (KSBD) that is approximately 30 miles east of Ontario. The WRF monthly wind speed and direction at these two Inland Empire airports is quite good achieving the simple benchmarks. Although the WRF monthly temperature performance for 2020 has similar performance at these two sites, with a +1.0 ° bias that falls between the simple (±0.5°) and complex (±2.0°) benchmarks, the 2019 monthly temperature performance at these two sites is different with San Bernardino having a +1.0 °C warm and Ontario having a -1.0 °C cold bias. The WRF monthly humidity performance at the two inland sites are similar for June and July in 2020 achieving the simple benchmark, but for 2019 WRF monthly humidity achieves the simple benchmark at San Bernardino but has a very large dry bias (-2.0 g/kg) at Ontario.

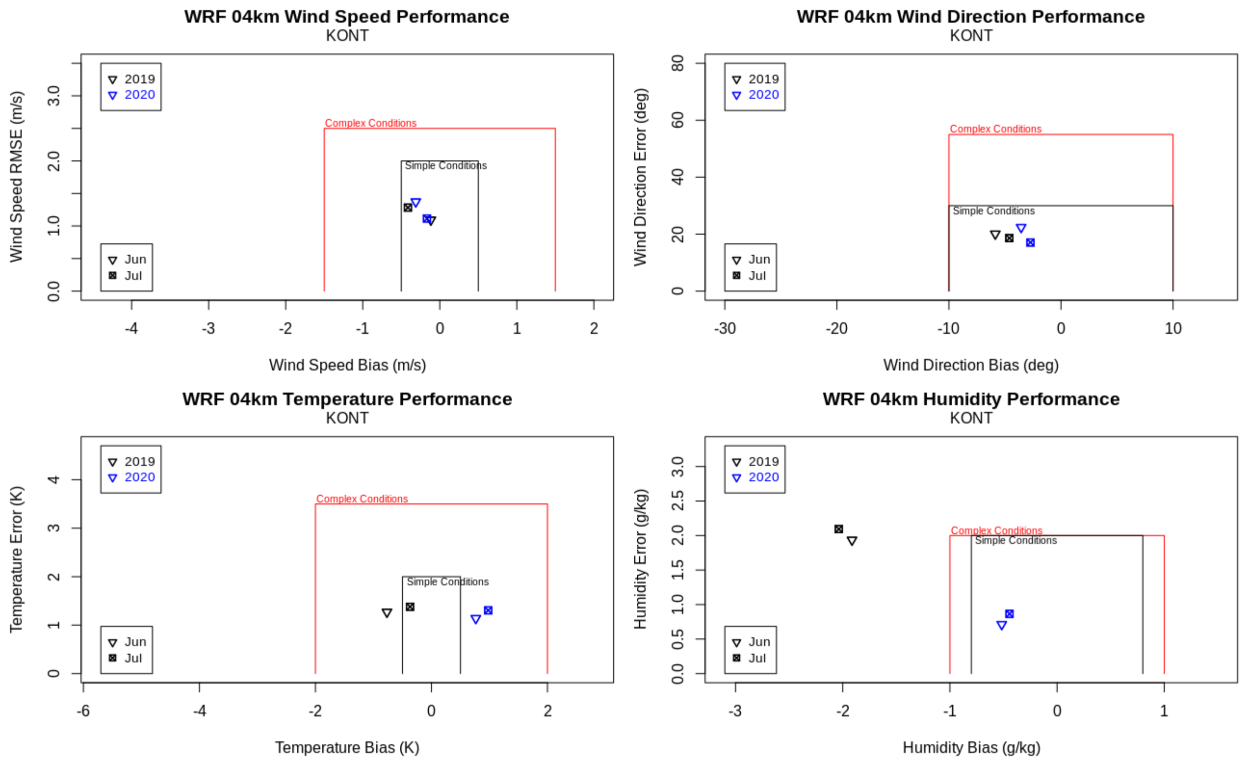

Figure 3-9. Soccer plots of wind speed, wind direction, temperature, and humidity WRF monthly model performance at the Ontario (KONT) airport.

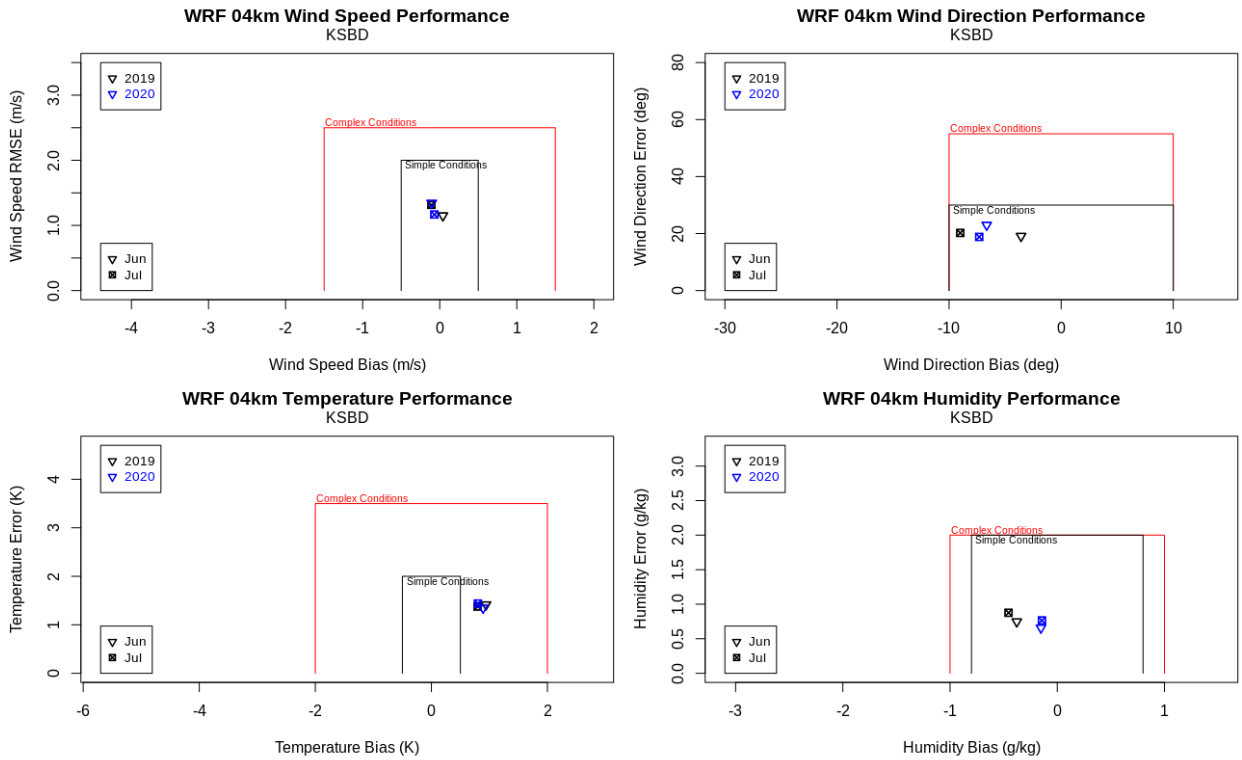

Figure 3-10. Soccer plots of wind speed, wind direction, temperature, and humidity WRF monthly model performance at the San Bernardin (KSBD) airport.

3.4 WRF Model Performance Conclusions

The WRF model performance is fairly typical for a good WRF application. The performance for T850 in San Diego and Vandenburg was quite good. When averaged across all sites in the SoCAB the WRF monthly surface meteorological performance met the most stringent simple model performance benchmarks except for temperature bias that fell between the simple and complex benchmarks. The WRF surface performance at some individual sites was not as good although it usually met the complex benchmarks and frequently met the simple benchmarks as well.

3.5 MCIP Processing

The Meteorology – Chemistry Interface Processor (MCIP[9]) was used to process the WRF output and generate CMAQ-ready meteorological inputs for the mid-May through July periods in 2019 and 2020 for the 12-km California and 4-km SoCAB modeling domains.

[9] https://www.cmascenter.org/help/documentation.cfm?model=mcip&version=4.3

4.0 PRELIMINARY CMAQ MODELING

Preliminary CMAQ modeling was performed for June-July 2020 using a top-down adjustment of 2020 NO_X emissions in the SoCAB to account for the effects of the COVID-19 shelter-in-place orders. Initial results of the preliminary CMAQ modeling were presented at the 2021 30th CRC Real World Emissions Workshop[10]. The meteorology used in the preliminary modeling was the WRF data described in the previous chapter. CMAQ version 5.2.1 was run for the mid-May through July period on just the 4-km SoCAB domain for a 2020 Business as Usual (BAU) and 2020 COVID emission scenarios that are described below. Boundary Conditions (BCs) for the CAMx 4-km SoCAB domain simulations were extracted from the Whole Atmosphere Community Climate Model (WACCM[11]) global model. A 10-day spin-up period during the end of May was used to initialize the model.

4.1 Preliminary Emissions Development

Emissions for two 2020 scenarios were developed in the preliminary COVID modeling analysis:

> 2020 BAU Case: The 2020 BAU case emission inputs for May-July were obtained for the CMAQ model by backcasting anthropogenic emissions for the 2023 year from the 2016 Air Quality Management Plan (AQMP[12]) EI to 2020 using adjustment factors from the California Air Resources Board (ARB) CEPAMS[13] website. The 2020 BAU emissions scenario represents what the anthropogenic emissions would have been in 2020 without the effects of the response to the COVID-19 pandemic.
>
> 2020 COVID Case Top-Down Approach: The 2020 COVID case was developed using a top-down approach that adjusted the 2020 BAU Case anthropogenic NO_X emissions based on differences in satellite NO_2 measurements between 2019 and 2020 accounting for NO_X emissions trends between 2019 and 2020.

The top-down 2020 COVID emissions scenario used satellite NO_2 measurements for June-July 2019 and 2020 to estimate the level of NO_X emissions reductions that occurred in response to the COVID-19 pandemic shelter-in-place orders. Figure 4-1 shows a March-August time series of the ratio of the 2020 to 2019 satellite NO_2 measurements over Los Angeles with Figure 4-2 displaying the spatial distribution of the June-July average 2020 to 2019 satellite NO_2 ratios. The NO_2 satellite observations were provided by Daniel Goldberg and accounts for meteorological variations (Goldberg et al., 2020). In early March 2020 satellite NO_2 observations were higher than 2019, but in mid-March the 2020 satellite NO_2 observations dropped to 40% below 2019 values and stayed that way through April. In May 2020, NO_2 was approximately 20% below the levels in 2019, but for June and July 2020 satellite NO_2 was approximately 30% below the values in 2019. Given that the California Air Resources Board CEPAMS emission projections for the SoCAB estimate that pre-existing regulations would result in an approximate 5% reduction in NO_X emissions in the SoCAB between 2019 and 2020 under the no COVID BAU case, we assumed the 2020 COVID Case anthropogenic NO_X emissions would be reduced by 25% from the 2020 BAU Case emissions for the top-down 2020 COVID modeling scenario.

[10] https://crcao.org/30th-crc-real-world-emissions-workshop-2/.

[11] https://www2.acom.ucar.edu/gcm/waccm. *The **WACCM** forecasts are driven by meteorological fields from the NASA GMAO GEOS-5 model. This simulation uses anthropogenic emissions from CEDS provided for CMIP6, with emissions for 2014 used for this year. Open fire emissions are from FINN-v1 (Wiedinmyer et al., Geosci. Model Devel., 2011). The results are at 0.9x1.25 degrees with 88 levels. Each file (global for 1 day) is 8 GB.*

[12] https://www.aqmd.gov/home/air-quality/clean-air-plans/air-quality-mgt-plan/final-2016-aqmp

[13] https://www.arb.ca.gov/app/emsinv/fcemssumcat/fcemssumcat2016.php

Natural Emissions: Biogenic emissions for all three scenarios were based on the MEGAN v3.1 biogenic emissions model using the May-July 2019 and 2020 12/4-km WRF meteorological data with data filling for the urban leaf area index (LAI) inputs.

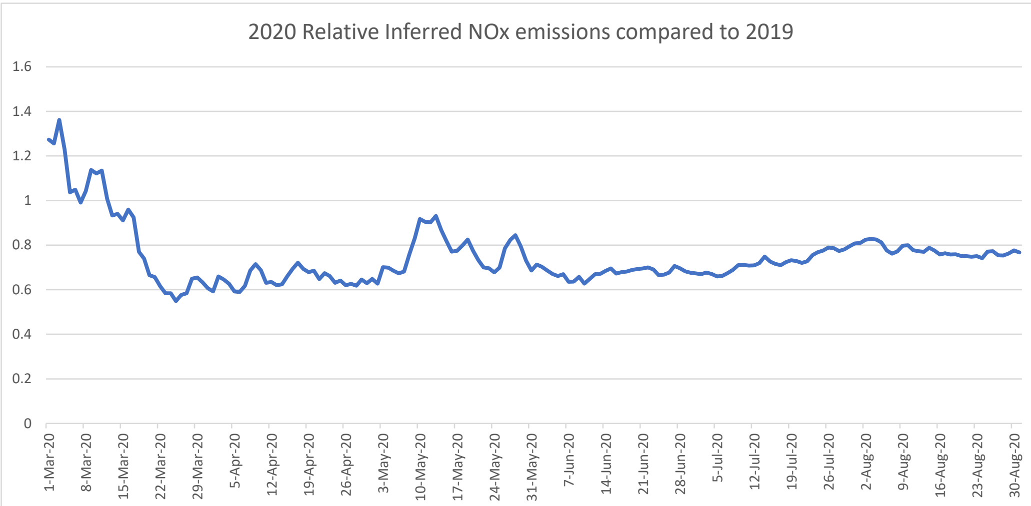

Figure 4-1. Time series of ratio of 2020 to 2019 meteorology-adjusted satellite NO_2 measurements over Los Angeles (Source: Goldberg et al., 2020).

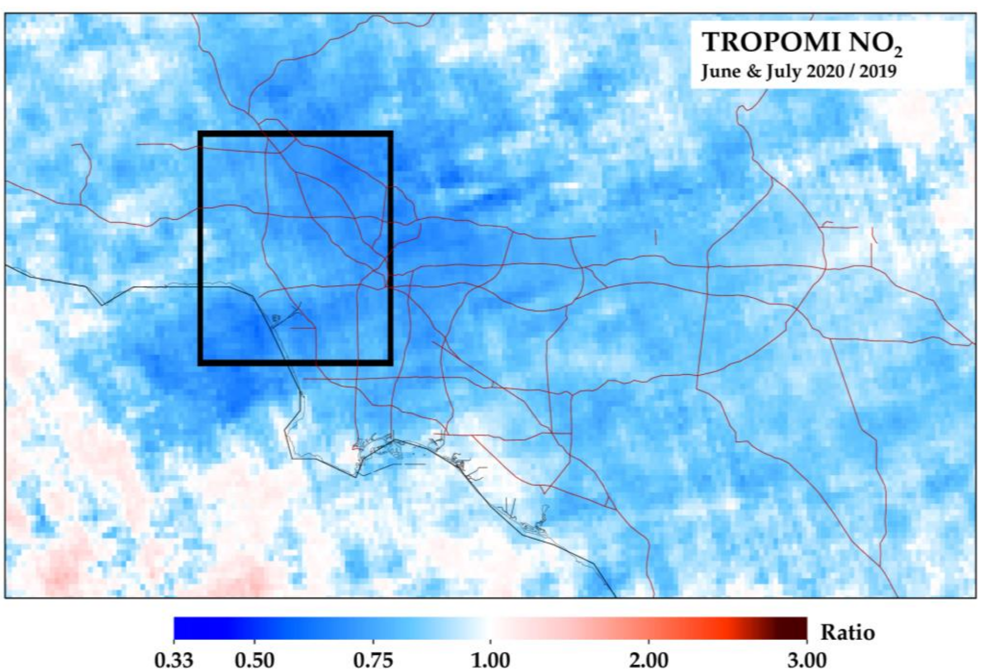

Figure 4-2. Ratio of two-month average meteorology-adjusted satellite NO_2 measurements for 2020 and 2019 and June-July and location data used to define Los Angeles used in Figure 4-1.

4.2 Preliminary CMAQ Modeling Results

Figures 4-3 and 4-4 display spatial maps of the maximum daily average 8-hour (MDA8) ozone concentrations for the 2020 COVID scenario and differences in MDA8 ozone concentrations between the 2020 COVID and 2020 BAU scenarios for 6 example days from the June-July 2020 modeling period.

On June 2nd, there is a peak MDA8 ozone of 97 ppb in the 2020 COVID scenario that occurs near Redlands in western San Bernardino County with MDA8 ozone in excess of 76 ppb stretching westward from Redlands into eastern and northern (Santa Clarita) Los Angeles County as well as another high ozone location in southern Kern County (Figure 4-3, top left). At the location of the 97 ppb MDA8 ozone peak near Redlands, the 2020 COVID scenario has ozone reductions of 4-5 ppb compared to the 2020 BAU scenario. However, from approximately Upland in western San Bernardino County westward into Los Angeles County where MDA8 ozone is 76 ppb or higher there are increases in MDA8 ozone concentrations due to the 25% anthropogenic NO_X emissions reductions in the preliminary 2020 COVID scenario. The maximum MDA8 ozone increase (12.7 ppb) in central Los Angeles County in the 2020 COVID scenario is over double the maximum ozone reduction (5.6 ppb).

On June 19th, the peak MDA8 ozone concentration of 87 ppb in the 2020 COVID also occurs near Redlands (Figure 4-3, middle left) and the level of ozone increase and decrease due to the NO_X emission reductions are less than seen on June 2nd. The area of ozone increase due to the NO_X emission reductions stretches from approximately Pasadena to Fontana with a peak ozone increase of 5.5 ppb that is comparable to the peak ozone decrease of -4.4 ppb (Figure 4-3, middle right).

Although June 22nd had a much higher MDA8 ozone peak (102 ppb) than June 19th (87 ppb) the level of ozone increases and decreases due to the NO_X emission reductions are similar (Figure 4-3, bottom).

On July 6th, the 2020 COVID case has a peak MDA8 ozone of 98 ppb at Upland in far western San Bernardino County that is 2-4 ppb lower than the 2020 BAU case (Figure 4-4, top left). The 2020 COVID scenario has higher ozone concentrations than the 2020 BAU scenario in southern Los Angeles County that stretches offshore and up the coast (Figure 4-4, top right) with the maximum ozone increase (4.1 ppb) being comparable to the maximum ozone decrease (-4.6 ppb).

On July 20th, the 2020 COVID case MDA8 ozone peak of 87 ppb occurs near Pasadena in central Los Angeles County (Figure 4-4, middle left), which is also where the largest ozone increase occurs (7.4 ppb) due to the NO_X emission reductions (Figure 4-4, middle right).

Similarly, on July 29 the 2020 COVID ozone peak of 98 ppb occurs near Upland where the 2020 COVID scenario has higher ozone than the 2020 BAU scenario due to the NO_X emission reductions (Figure 4-4, bottom). The maximum ozone increase in the 2020 COVID scenario is 7.5 ppb occurs near Glendora in eastern Los Angeles County.

The 25% NO_X emission reductions in the 2020 COVID case compared to the 2020 BAU case consistently results in ozone increase in Los Angeles County that sometimes spreads into far western San Bernardino and Riverside Counties with much wider areas of ozone reductions in the eastern portion of the SoCAB.

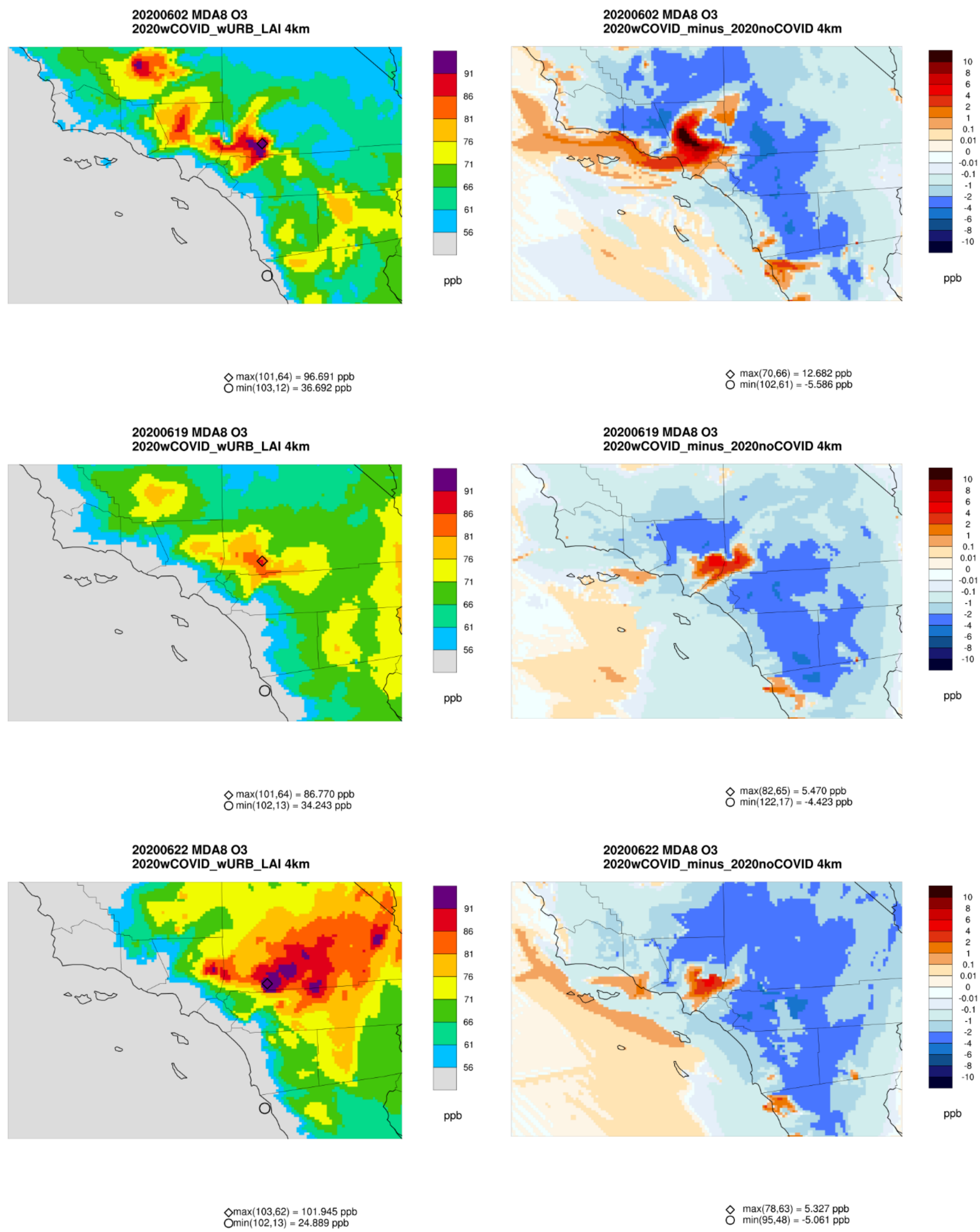

Figure 4-3. MDA8 ozone concentrations in the 4-km SoCAB domain for the 2020 COVID actual emissions scenario (left) and the differences in MDA8 ozone between the 2020 COVID and 2020 BAU (2020 COVID – 2020 BAU) scenarios (right) on June 2 (top), 19 (middle) and 22 (bottom), 2020.

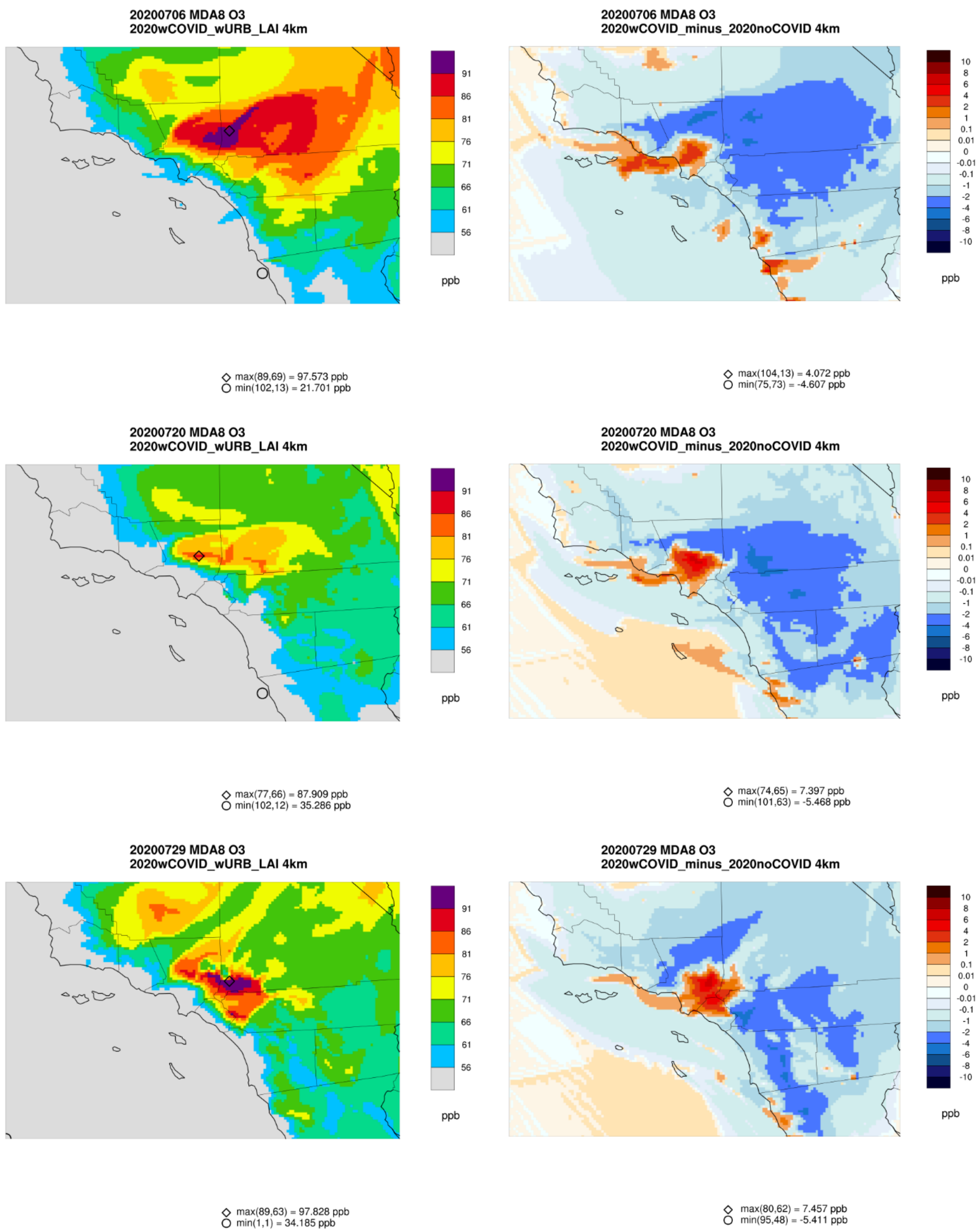

Figure 4-4. MDA8 ozone concentrations in the 4-km SoCAB domain for the 2020 COVID actual emissions scenario (left) and the differences in MDA8 ozone between the 2020 COVID and 2020 BAU (2020 COVID – 2020 BAU) scenarios (right) on July 6 (top), 20 (middle) and 29 (bottom), 2020.

5.0 EMISSIONS DEVELOPMENT

The preliminary CMAQ modeling discussed in the previous Chapter primarily used emission inventories from the 2016 Air Quality Management Plan (2016 AQMP[14]) with top-down adjustments of the effects of the shelter-in-place COVID pandemic response that reduced anthropogenic NO_X emissions based on satellite NO_2 observations. For the updated CMAQ modeling, the primary source of emissions is the 2020 emissions inventory (EI) obtained from the California Air Resources Board (ARB).[15] A primary reason for using these alternative emissions is the availability of pre-merged emissions (i.e., by individual source sector) that enables utilization of source-sector-specific bottom-up adjustments to account for the effect of COVID on the 2020 BAU emissions. An additional benefit is that the ARB inventory was prepared for 2020, which is the primary model year for the study and makes back-casting of the 2023 inventory from the 2016 AQMP unnecessary. The pre-merged emissions sectors are listed below. Emissions were developed for CMAQ for three emission scenarios:

- 2019 Base Case.
- 2020 Business as Usual (BAU) Case.
- 2020 COVID Case.

5.1 2019 Base Case

2019 Base Case emission inputs for mid-May through July were obtained by scaling the ARB 2020 EI. We inspected 2019 and 2020 CEPAMS[16] summertime grown and controlled emissions for the South Coast Air Basin (SoCAB) by source sector and found that the only sector with year-over-year changes of greater than ±5% difference as well as an emissions contribution of greater than 3% for any pollutant was the on-road mobile source category. Therefore, for the 2019 Base Case we kept all sectors besides on-road mobile at the same emissions rate as in 2020 BAU scenario and adjusted the on-road mobile source sector only. The adjustment factors used for the on-road mobile category were derived from CEPAMs and are: NO_X = 1.11, TOG = 1.07, and CO = 1.10. These factors were applied uniformly over the 4-km domain to the on-road mobile source emissions for each hour.

5.2 2020 BAU Case

2020 BAU emissions for mid-May through July were taken directly from the ARB 2020 EI without any scaling adjustment since these emissions were compiled without accounting for the COVID pandemic so do not include the COVID response effects on emissions. The pre-merged categories in the ARB 2020 EI are as follows:

- Aircraft
- Area Source (including Non-Road Mobile)
- Consumer Products
- On-Road Mobile
- Point Sources
- Fertilizer
- Livestock
- 2nd Livestock (Lvst, a2p)
- Ocean Going Vessels (OGV) Area
- OGV Point (In-line)
- OGV military

[14] https://www.aqmd.gov/home/air-quality/clean-air-plans/air-quality-mgt-plan/final-2016-aqmp
[15] Jeremy Avise, personal communication
[16] https://www.arb.ca.gov/app/emsinv/fcemssumcat/fcemssumcat2016.php

- Paved Road Dust
- Residential Wood Combustion
- Unpaved Road Dust

Figure 5-1 displays the anthropogenic emissions contributions by source sector for the 2020 ARB inventory summed over the four SoCAB counties for NO_X and total organic gases (TOG). Any sector with less than 1% contribution to the total is not displayed. The period average is June 1 – July 31, 2020. On-Road Mobile has the highest contribution for NO_X (37%) with Area Sources (including Non-Road Mobile) having a comparable amount (36%) and then Point Sources (15%). For TOG, Area Sources have by far the largest contributions (76%) followed by Consumer Products (8%).

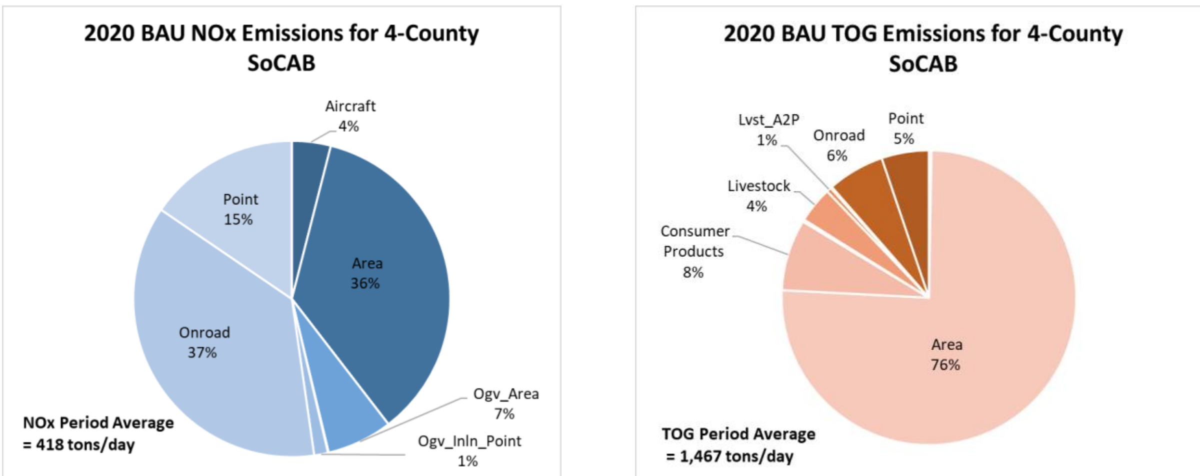

Figure 5-1. Emissions contributions by Source Sector for NOx and total organic gases (TOG) for the 4-Counties in the SoCAB from ARB emissions inventory.

5.3 2020 COVID Case

The preliminary CMAQ modeling discussed in Chapter 4 used a top-down approach to adjust the 2020 BAU Case NO_X emissions based on differences in satellite NO_2 measurements between 2019 and 2020 accounting for NO_X emissions trends between 2019 and 2020. The NO_X adjustment scaling factor was 0.756 and was applied uniformly to the 2016 AQMP 2020 merged model-ready emissions that includes all anthropogenic and natural emissions sectors. For the updated CMAQ modeling, a bottom-up approach was employed with source-sector-specific adjustment factors based on changes in source sector-specific activity data between 2019 and 2020 to account for the effects the response to the COVID pandemic had on emissions.

We developed adjustment factors to scale the BAU 2020 ARB emission inventory to actual activity and emission levels for the June-July 2020 period in the SoCAB region, to the extent feasible. The spatial and geographical specificity of the COVID-19 adjustment factors was determined by the extent to which applicable data was readily available for specific counties and months of interest. In certain instances, readily available data was limited to annualized and/or statewide activity.

The adjustment factors were developed for source categories listed above and shown in Table 5-1. Adjustment factors were applied to criteria air pollutants to adjust June and July 2020 emissions for all counties in the SoCAB 4-km modeling domain. Adjustment factors for each source category in Table 5-1 were cross-referenced to emission inventory source classification codes (SCC) to adjust the SCC-level ARB 2020 emission inventory. COVID-adjusted SCC-level emissions were then aggregated to the sector-level and sector-level COVID adjustment factors were estimated for application to model-ready emissions based on the ratio of COVID-adjusted to COVID-unadjusted sector-level emissions. Table 5-1 provides detailed information on the basis and temporal and geographical coverage of the adjustment factors. Consumer product VOC emissions were estimated to go up 11% due to implementation of the 2020 COVID shelter-in-place orders due to COVID, which makes sense given people are at home more often under the 2020 COVID case than 2020 BAU case. Construction activity is down 5% that is consistent with the essential services coming back by June-July 2020. However, passenger rail activity is down approximately 50% due to COVID with freight rail down 20% and Los Angeles airport activity down 30%. Ocean Going Vessel (OGV) activity is down 6% to 73% depending on the type of OGV with the largest reduction is for OGV passenger ships (e.g., cruise ships). Commercial heating/cooking is down ~10% and residential cooking/heating is up ~10% due to COVID.

Based mainly on reductions in gasoline and diesel sales between 2019 and 2020, the source sector that produced the largest emission reductions in June-July 2020 due to the COVID shelter-in-place orders was on-road mobile sources with a ~20% reduction.

Table 5-1. Bottom-up COVID adjustment factors by sector.

Source Category [a]	Region	Pollutant	Metric	Temporal	Adjustment Factor	Adjustment Factor Basis	Data Source
Consumer Products	Nationwide	All	Product sales, product production and household expenditures data	Episode Period (June - July)	1.105	Ratio of 2020 to 2019 production and household expenditures for the month of June and July	NielsenIQ Reporting: https://nielseniq.com/global/en/insights/analysis/2021/which-pandemic-inspired-purchasing-shifts-are-here-to-stay/ Media Reports: https://www.nature.com/articles/d41586-021-00251-4 https://www.perioimplantadvisory.com/clinical-tips/article/14206274/the-dangers-of-hand-sanitizer-use-and-misuse Industry Report: https://www.cleaninginstitute.org/covid19report, Consumer Expenditure Governement Report: https://www.bls.gov/news.release/cesan.nr0.htm
Construction Equipment	California-wide	All	All Employees: Construction in California	Episode Period (June - July)	0.952	Ratio of total employees in 2020 to 2019 for the month June and July	https://fred.stlouisfed.org/series/CACONS
Passenger Rail	Los Angeles County	All	Total Passenger Miles	Episode Period (June - July)	0.497	Ratio of total passenger miles in 2020 to 2019 for the month June and July	https://isotp.metro.net/MetroRidership/Index.aspx
Freight Rail	Nationwide	All	Total Train Miles	Episode Period (June - July)	0.802	Ratio of total train miles in 2020 to 2019 for the month June and July	https://safetydata.fra.dot.gov/OfficeofSafety/publicsite/Query/rrstab.aspx
Aircraft	Los Angeles County	All	Total Operation	Episode Period (June - July)	0.702		https://aspm.faa.gov/opsnet/sys/main.asp

Source Category [a]	Region	Pollutant	Metric	Temporal	Adjustment Factor	Adjustment Factor Basis	Data Source
	San Bernardino County				0.780	Ratio of total operations in 2020 to 2019 for the month of June and July	
	Riverside County				0.803		
	Orange County				0.853		
	SoCAB	All	Total Operation	Episode Period (June - July)	0.739		
Ocean Going Vessels (OGV) - Container Ships	SoCAB	All	Twenty-foot Equivalent Unit (TEU)	Episode Period (June - July)	0.976	Ratio of total TEU in 2020 to 2019 (Port of Los Angles (LA) and Long Beach (LB)) for the months of June and July	Port of LA: https://www.portoflosangeles.org/business/statistics/facts-and-figures Port of LB: https://polb.com/business/port-statistics/#tonnage-summary
OGV - Tankers	California-wide	All	Crude Oil Imports	Episode Period (June - July)	0.698	Total crude import ratio in California from 2020 to 2019 for the months of June and July	2020: https://www.energy.ca.gov/data-reports/energy-almanac/californias-petroleum-market/foreign-sources-crude-oil-imports/2020 2019: https://www.energy.ca.gov/data-reports/energy-almanac/californias-petroleum-market/foreign-sources-crude-oil-imports/2019-0
OGV - Auto Carriers/Roll On-Roll off Vessels	SoCAB	All	Automobiles (Units)	Annual	0.814	Ratio of annual automobile units (import and export) in 2020 to 2019 for the Port of LA	https://www.portoflosangeles.org/business/statistics/automobile-statistics
OGV - Bulk Cargo, Refrigerated Cargo and General Cargo	SoCAB	All	Metric Revenue Tons	Annual	0.941	Ratio of annual Toonage in 2020 to 2019 for the Port of LA and Port of LB	POLA: https://www.portoflosangeles.org/business/statistics/facts-and-figures POLB: https://polb.com/business/port-statistics/#tonnage-summary

Source Category [a]	Region	Pollutant	Metric	Temporal	Adjustment Factor	Adjustment Factor Basis	Data Source
OGV - Passenger Ships	SoCAB	All	Cruise Ship Calls	Annual	0.274	Ratio of annual cruise ship calls in 2020 to 2019 for the Port of LA	https://www.portoflosangeles.org/business/statistics/automobile-statistics
Cargo Handling Equipment (Port and Railyard)	SoCAB	All	Container Volume (TEU)	Episode Period (June - July)	0.976	Ratio of total TEU in 2020 to 2019 (Port of LA and LB) for the months of June and July	Port of LA: https://www.portoflosangeles.org/business/statistics/facts-and-figures Port of LB: https://polb.com/business/port-statistics/#tonnage-summary
Commercial Cooking and Heating	Los Angeles County	All	Google Mobility Trend (Average of Rail and Recreation, Grocery and Pharmacy and Workplace sectors)	2020 percent change from baseline activity	0.893	2020 percent change from baseline activity	https://www.gstatic.com/covid19/mobility/2020-05-09_US_California_Mobility_Report_en.pdf
	San Bernardino County				0.950		
	Orange County				0.910		
	Riverside County				0.940		
	SoCAB				0.910		
Residential Cooking and Heating	Los Angeles County	All	Google Mobility Trend (Residential)	2020 percent change from baseline activity	1.140	2020 percent change from baseline activity	https://www.gstatic.com/covid19/mobility/2020-05-09_US_California_Mobility_Report_en.pdf
	San Bernardino County				1.100		
	Orange County				1.140		
	Riverside County				1.110		
Refinery	California-wide	All	Weekly West Coast (PADD 5[17]) Gross Inputs into Refineries	Episode Period (June - July)	0.708	Based on ratio of average daily input in 2020 to 2019 for the months of June and July	https://www.eia.gov/dnav/pet/pet_sum_sndw_dcus_r50_w.htm
	Los Angeles County	All excep	NO_x[18] emissions	Episode Period (June - July)	0.802	Based on ratio of emissions in 2020 to 2019	https://ampd.epa.gov/ampd/

[17] PADD: Petroleum Administration for Defense Districts

Source Category [a]	Region	Pollutant	Metric	Temporal	Adjustment Factor	Adjustment Factor Basis	Data Source
Electric Generation Unit (EGU)	Orange County	t SO_2[18]			2.415	for the months of June and July	
	Riverside County				1.014		
	San Bernardino County				1.004		
	Los Angeles County	SO_2[18]	SO_2[18] emissions	Episode Period (June - July)	0.960		
	Orange County				2.822		
	Riverside County				1.036		
	San Bernardino County				1.011		
On-road	SoCAB	NO_x[18]	Emissions and Vehicle Miles Traveled (VMT)	Summer Day	0.794	1) Estimated June-July 2020 VMT with COVID-19 impacts based on the product of EMFAC 2019 average summer day VMT and the ratio of 2020 to 2019 EIA fuel sales volumes for June-July. 2) Estimated 2020 EMFAC emissions per mile by fuel type for each vehicle classification. 3) Estimated 2020 COVID emissions based on the product of #1 and #2 above. 4) EMFAC includes annualized COVID adjustments for calendar year 2020. We estimated a 2020 COVID unadjusted emission inventory by interpolating EMFAC 2019	EMFAC2021 v1.0.1: https://arb.ca.gov/emfac/emissions-inventory/b8cfe2a8a4b5424be91e8e14748e8fde1de999c1 EIA Gasoline: https://www.eia.gov/dnav/pet/hist/LeafHandler.ashx?n=PET&s=A103650061&f=M EIA Diesel : https://www.eia.gov/dnav/pet/pet_cons_refoth_c_SCA_EPD2DXL0_mgalpd_m.htm
		$PM_{2.5}$[18]			0.787		
		PM_{10}[18]			0.784		
		TOG[18]			0.776		
		CO[18]			0.776		
		SO_2[18]			0.776		
		NH_3			0.776		

[18] SO_2: sulfur dioxide; NOx: nitrogen dioxide; PM2.5: particulate matter (PM) 2.5; PM10: particulate matter 10; TOG: total organic gas; CO: carbon dioxide; NH3: ammonia

Source Category [a]	Region	Pollutant	Metric	Temporal	Adjustment Factor	Adjustment Factor Basis	Data Source
						and 2021 emissions, which are assumed not to be impacted by COVID in EMFAC. 5) The on-road adjustment factor was estimated based on the product of #3 and #4 above.	

5.4 SoCAB Anthropogenic Summary

Figure 5-2 summarizes the emissions changes between 2019 Base, 2020 BAU and 2020 COVID Cases for the four SoCAB counties and NO_X and TOG in the upper and lower panels, respectively. Total anthropogenic NO_X and TOG emissions are reduced by, respectively, -3.6% and -0.4% between the 2019 Base and 2020 BAU cases. The 2020 COVID case has -12.9% less NO_X and -0.9% less TOG emissions than the 2020 BAU case. Approximately 60% of the COVID caused NO_X emissions reductions are from on-road mobile with another 16% reduction from the area sources (that includes non-road mobile), 14% from all OGV sectors and 9% from aircraft. Although the total net change in TOG emissions between the 2020 BAU and 2020 COVID scenarios is approximately -1%, it is due to an increase in TOG emissions of +1% from consumer products that is offset by a decrease in TOG emissions of -2% from all other source sectors (most notably on-road mobile).

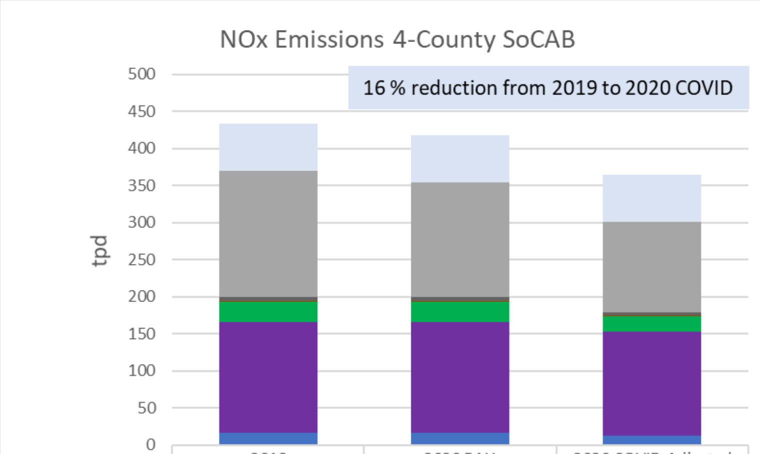

	2019	2020 BAU	2020 COVID-Adjusted
point	64.6	64.6	63.3
onroad	169.4	154.0	122.2
Ogv_Inln_point	5.9	5.9	4.7
Ogv_Inln_area	0.3	0.3	0.3
Ogv_Area	28.0	28.0	21.5
area	148.9	148.9	140.5
aircraft	16.6	16.6	12.0

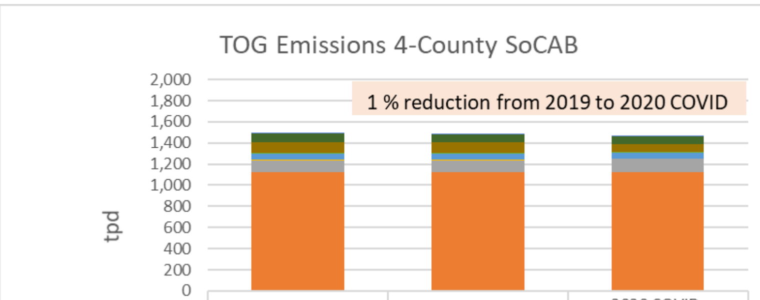

	2019	2020 BAU	2020 COVID-Adjusted
Rwc	0.1	0.1	0.1
point	76.9	76.9	75.3
onroad	98.9	92.4	71.7
Ogv_Inln_point	0.4	0.4	0.3
Ogv_Inln_area	0.1	0.1	0.1
Ogv_Area	2.3	2.3	1.9
Lvst_a2p	7.5	7.5	7.5
Livestock	58.5	58.5	58.5
Fert	3.7	3.7	3.7
consumer_products	115.8	115.8	127.9
area	1,117.5	1,117.5	1,116.1
aircraft	4.0	4.0	2.9

Figure 5-2. NOx and TOG emissions summary by source sector for the 2019 Base, 2020 BAU and 2020 COVID adjusted emission scenarios (tons per day).

5.5 Biogenic and Fire Emissions

Biogenic emissions were based on the Model Of Emissions Of Gases And Aerosols From Nature (MEGAN) v3.1 biogenic emissions model with ARB's adjusted urban leaf area index (LAI) using the mid-May through July 2019 and 2020 12/4-km WRF meteorological data.

Fire emissions are based on the Fire INventory from NCAR (FINN[19]). Although 2020 was the worst wildfire year on record for California,[20] the most intense fires occurred in August and September outside of our modeling period. Of note were the remnants of a tropical storm producing dry lightning in mid-August that sparked over 650 wildfires, mainly in northern California. Appendix A provides monthly average FINN fire emissions for June and July 2019 and 2020.

5.6 Mexico Emissions

The ARB 2020 EI was developed for California and does not include emissions from Mexico. The SoCAB 4-km modeling domain includes a portion of Mexico and we used the same Mexico emissions as were used in the preliminary CMAQ modeling (i.e., from the 2016 AQMP). No modifications were made to the emissions from Mexico for the 2019 Base or 2020 COVID/BAU scenarios.

5.7 SoCAB 4-km Domain Emissions Processing

Table 5-2 reports the CMAQ modeling domain parameters including map projection specifications and the grid definition. Figure 5-3 displays the 12-km California and 4-km SoCAB modeling domains. The 2020 ARB emissions were "windowed" to the SoCAB 4-km modeling domain extent and reconfigured ("stitched") so that each daily file spanned a 25-hour period that started at 0-hr in Universal Time Coordinate (UTC) prior to applying 2019 and 2020 COVID effect adjustments. All non-point source sectors were merged so that they could be run with CMAQ version 5.2.1 (which allows for layer collapsing which newer versions of CMAQ do not). In addition, since the SoCAB 4-km domain extends into Mexico, Mexico emissions were also merged into the final gridded file for each day as well as the 2019 and 2020 year-specific natural emissions from MEGAN/FINN that were described above.

For 2019 emissions, as well as the on-road mobile adjustment described above, we also performed a day of the week (dow) adjustment and July 4 holiday adjustment to correctly match 2020 dow to 2019 dow to account for different emissions patterns throughout the week, in particular differences in weekday versus weekend traffic patterns and resultant emissions.

Table 5-2. CMAQ modeling domain parameters

Projection: Lambert Conformal Conic *Datum: Sphere EMEP* *False Easting: 0.0000* *False Northing: 0.0000* *Central Meridian: -120.5000* *Standard Parallel 1: 30.0000* *Standard Parallel 2: 60.0000* *Latitude Of Origin: 37.0000* *Units: Meter*	Grid definitions: 12 km grid: SW corner (origin): -684, -564 km nx x ny: 107 x 97 4 km grid: SW corner (origin): -84, -552 km nx x ny: 156 x102

[19] https://www2.acom.ucar.edu/modeling/finn-fire-inventory-ncar
[20] https://en.wikipedia.org/wiki/2020_California_wildfires

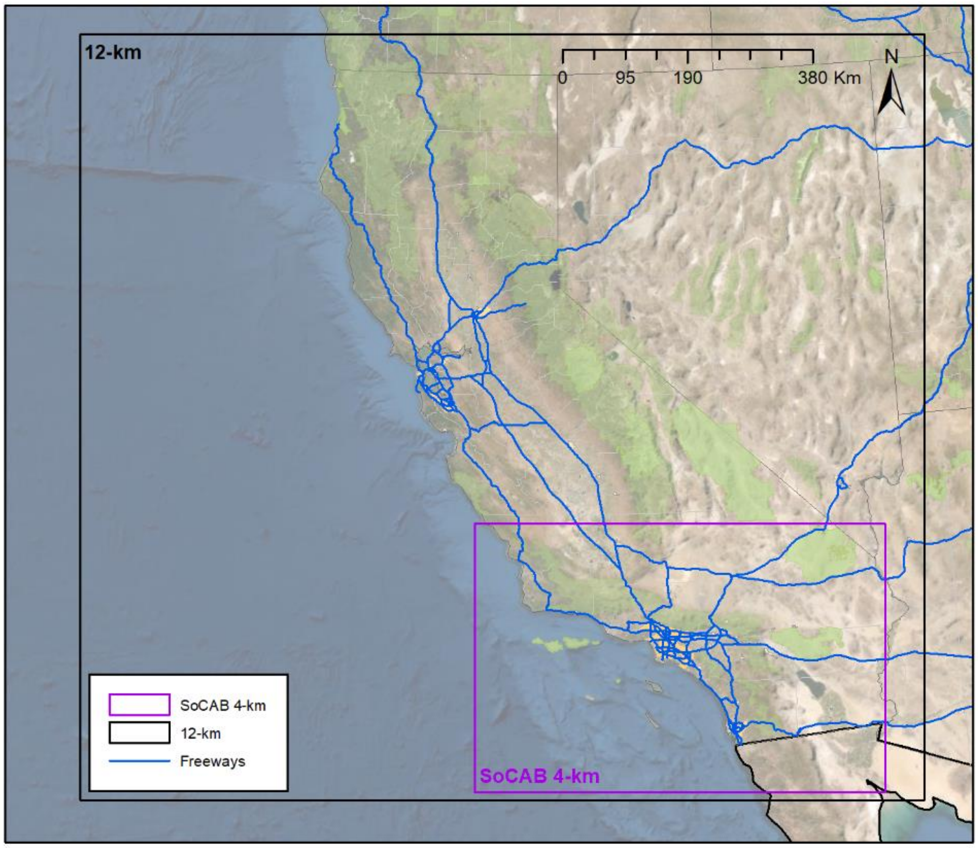

Figure 5-3. 12-km and 4-km CMAQ modeling domains.

5.8 Emissions Processing for 12-km CMAQ simulation

The emissions processing steps for the 12-km CMAQ simulations and the 2019 and 2020 emissions scenarios involved several steps as follows:

1. Acquisition of the California domain (12-km in Figure 5-3) model-ready 2020 baseline total and biogenic inventories at 4-km grid resolution from the California Air Resources Board[21].
2. Aggregate 4-km total and biogenic emissions to 12-km resolution and subtract biogenic emissions from the total emissions to obtain 12-km 2020 anthropogenic-only emissions.
3. Reconfigured (i.e., "stitched") files so that each daily file spanned a 25-hour period that started at 0-hr in Universal Time Coordinate (UTC) as required by the CMAQ model.
4. For 2019, adjusted 2020 anthropogenic emissions to 2019 using CEPAMS[22] derived backcast factors based on CA state-wide factors for all anthropogenic sources (2019 to 2020 emissions backcast factors for NO_X = 1.05, CO = 1.03, TOG = 0.9997). Other pollutants were left unadjusted. Also performed a day of the week (dow) adjustment for 2019. These factors differ from the SoCAB counties factors because the domain is larger, and it is a total anthropogenic inventory and not sector-specific as used in the SoCAB domain.
5. Run MEGAN3.1 biogenic emissions model using 2019 and 2020 WRF 12-km hourly gridded meteorological data to generate day-specific hourly 12-km biogenic emission inputs.
6. Merge 2019 and 2020 anthropogenic emissions with 2019 and 2020 MEGAN biogenic emissions.

[21] Jeremy Avise, personal communication

[22] https://www.arb.ca.gov/app/emsinv/fcemssumcat/fcemssumcat2016.php

5.9 Example of Model-Ready Emission

5.9.1 Spatial Distribution

This section presents examples of model-ready emissions on the SoCAB 4-km domain in moles/sec per 4-km grid cell. Figure 5-4 displays model-ready nitrogen oxide ($NO_X \approx NO + NO_2$) emissions for an example timestep (0:00 UTC or 5 PM PDT, June 10, 2020) for the 2020 BAU case and 2020 COVID case in the upper two panels. For NO_X, the conversion factor for moles/sec to tons/day is 4.38. The lower two panels in Figure 5-4 display the difference and ratio of emissions for the two 2020 scenarios in the left and right figures, respectively. Note that differences between the two scenarios are barely discernable in the top two panels of total NO_X emissions. The lower left panel shows the highest absolute reductions of NO_X emissions between the 2020 BAU and 2020 COVID emission scenarios occur over Los Angeles, San Diego and along the highways that extend from Los Angeles. The greatest reduction is 0.123 moles/sec (i.e., 0.54 tons/day per 4-km grid cell). The lower right panel shows relative reductions over a larger number of grid cells including approximately an 8% reduction over the Pacific due to the reductions in OGV NO_X emissions, and a range of reductions due to the different source sector combinations that range from approximately 24% to zero percent. In Mexico, there are no differences between the scenarios since those emissions were kept at 2020 BAU levels. Appendix A provides additional model-ready plots by source sector to better understand the spatial variations of emissions sectors throughout the SoCAB 4-km domain.

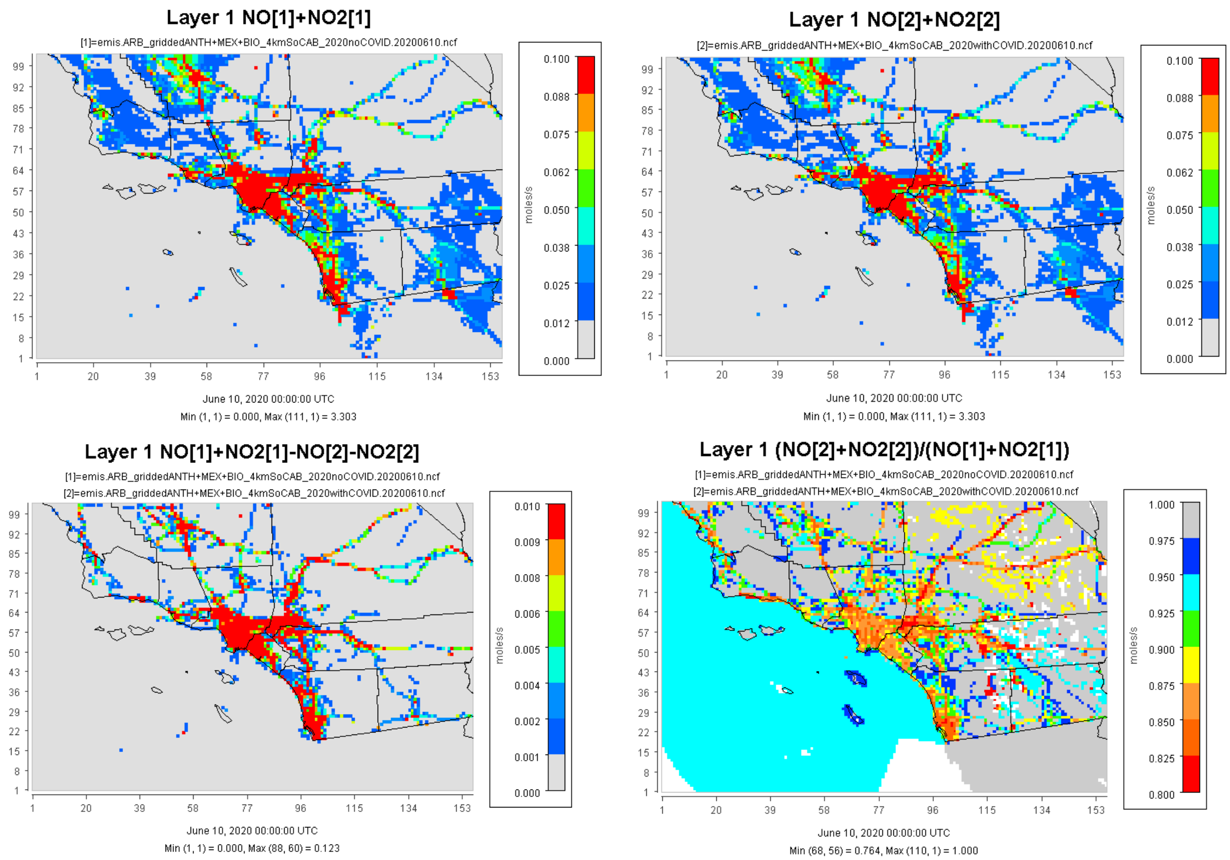

Figure 5-4. NO$_X$ emissions comparison for 2020 BAU (top right) and 2020 COVID (top left) and their differences (2020 BAU – 2020 COVID, bottom left) and ratios (2020 COVID/2020 BAU, bottom right).

Figure 5-5 displays model-ready SAPRC chemical mechanism lumped Alkane 1 (ALK1) emissions for the same timestep (0:00 UTC, May 24, 2020) for the 2020 BAU case and 2020 COVID case in the upper two panels. ALK1 is a lumped species in the SAPRC chemical mechanism for short-chain alkane VOC species and its spatial distribution is fairly representative of the spatial distribution of TOG emissions. The lower two panels display the difference and ratio of emissions for the two 2020 scenarios in the left and right figures, respectively. The lower left panel shows the highest absolute decreases in ALK1 emissions are largest in the urban areas over Los Angeles and San Diego that have highest density of on-road mobile source emissions. The lower right panel shows a mix of reductions and increases over a broader area with the range of reductions due to the different source sectors across the domain approximately ±15% with the largest ALK1 reductions along the roadways and increases away from the roadways due to increases in consumer product TOG emissions.

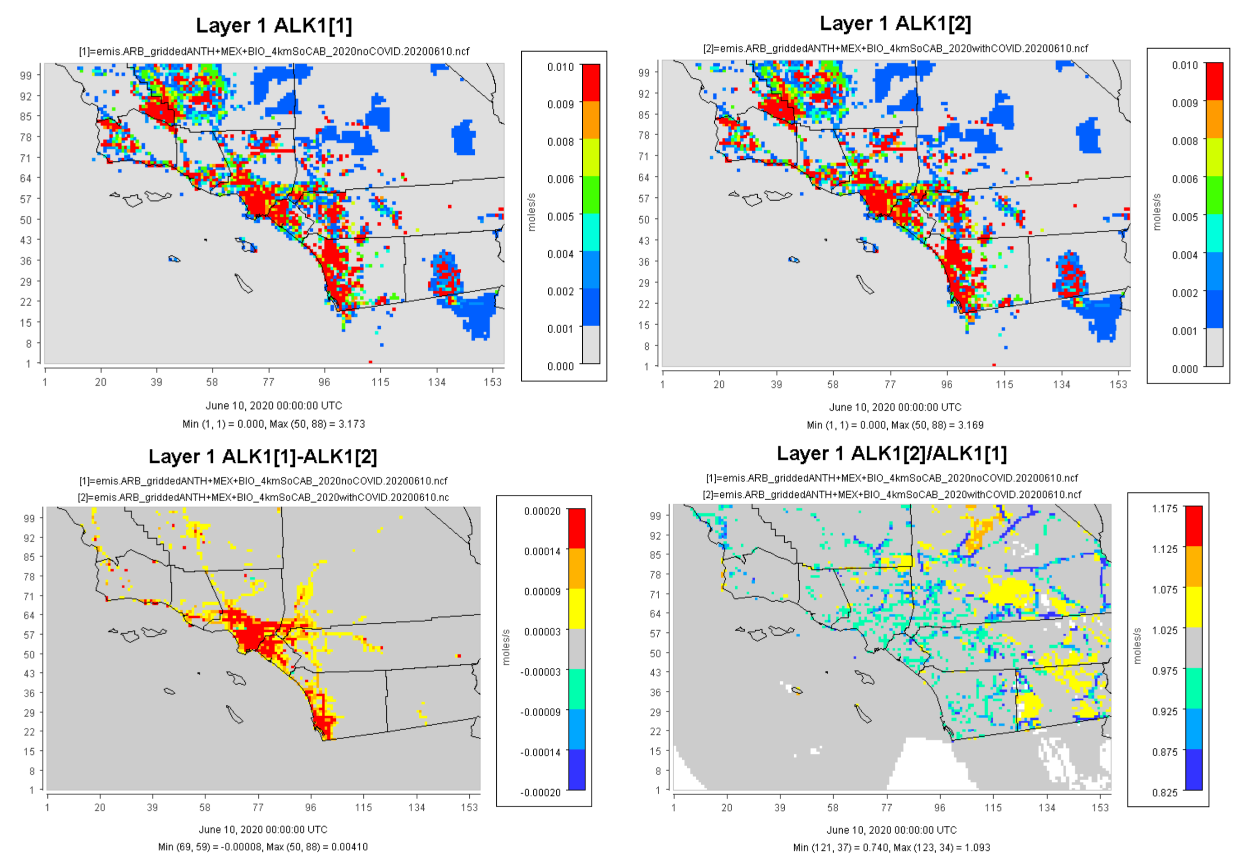

Figure 5-5. Short-Chain Alkane (ALK1) emissions for the 2020 BAU (top left) and 2020 COVID (bottom right) emissions scenarios and their differences(2020 BAU – 2020 COVID, bottom left) and ratios (2020COVID/2020BAU, bottom right).

5.9.2 Temporal Distribution

Figure 5-6 presents the diurnal distribution of on-road mobile NO_X emissions for an example Wednesday on June 10 and the following Sunday on June 14, 2020. The plots represent the average NO_X emission rates across the 4-km grid cells in the SoCAB 4-km modeling domain. The morning and afternoon commute periods are clearly present on Wednesday but are not seen on Sunday. Note that a different scale is used on the y-axis for the Wednesday and Sunday diurnal emissions plots. The Wednesday peak emissions rate are greater than 0.0053 moles/sec at 1400 UTC (7 AM PDT) and 2200-2400 UTC (3 – 5 PM PDT). On Sunday peak hourly 4-km grid cell average NO_X emissions rate is approximately 0.0030 moles/sec. For NOx, the conversion factor for moles/sec to tons/day (tpd) is 4.38. The number of grid cells in the SoCAB 4-km domain is 156 x 102 (=15,912), therefore the domain-wide total NO_X emissions rate at the peak hour on Wednesday, June 10 is approximately 370 tpd and on Sunday, June 14 it is approximately 210 tpd. The overnight minimum emissions rates are approximately 105 tpd and 63 tpd for Wednesday and Sunday, respectively.

2020 BAU Onroad: (**Wednesda**y, June 10, 2020) SoCAB 4-km domain-wide average NO_X emission rate.

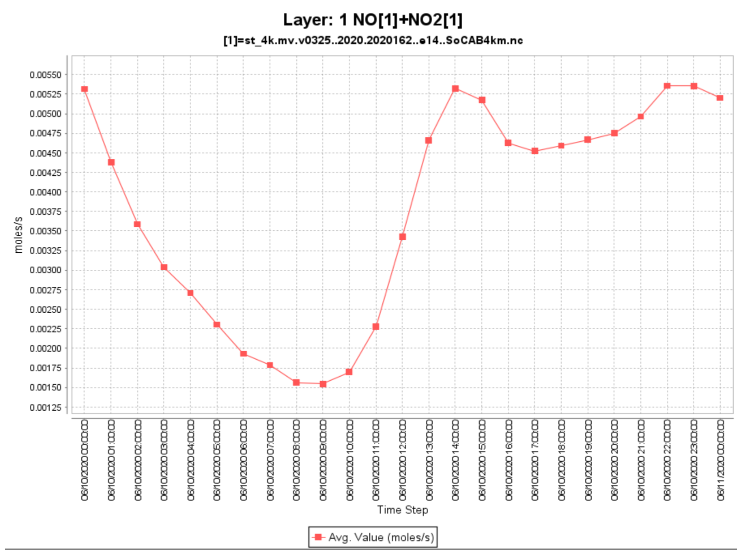

2020 BAU Onroad: (**Sunday**, June 14, 2020) SoCAB 4-km domain-wide average NO_X emission rate.

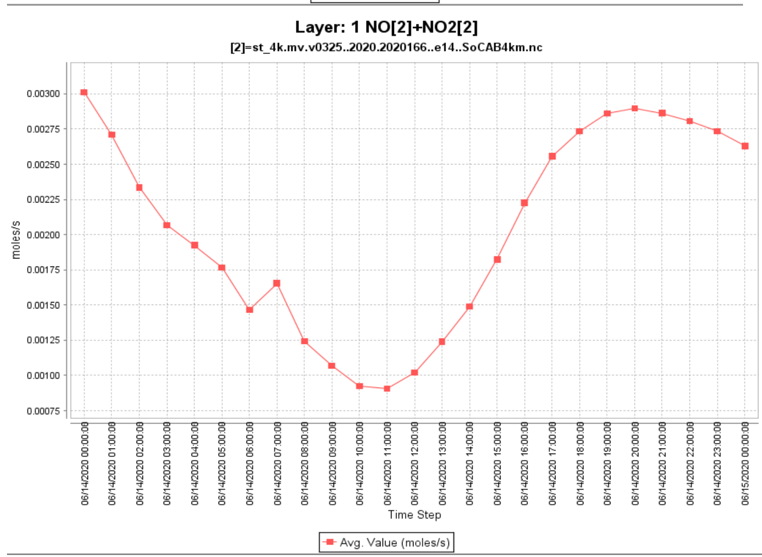

Figure 5-6. Diurnal profiles of SoCAB domain-wide 4-km grid cell average emissions for the on-road mobile category and the 2020 BAU scenario. Upper panel is for a Wednesday and lower panel is for a Sunday.

Figure 5-7 presents an example of average diurnal hourly emissions of the merged total NO_X emissions (i.e., all gridded emissions sectors) for the 2020 BAU and 2020 COVID cases for Wednesday June 10, 2020. The morning and afternoon commute periods seen in the diurnal hourly emissions for the on-road mobile source sector in Figure 5-6 are not apparent when looking at total NO_X emissions as it is subsumed in the merged emissions by other contributing emission source sectors. However, a clear daytime/nighttime pattern is observable. Note that the peak emissions rate, which occurs at 2100 UTC (i.e., 2 PM PDT) in the 2020 BAU case, is reduced in the 2020 COVID case. The emissions rates are 0.018 moles/sec compared to 0.0165 moles/sec which equates to domain-wide total emissions of 1,255 tpd compared to 1,150 tpd for 2020 BAU and 2020 COVID, respectively (an 8.3% reduction). Note also that the overnight minimums are comparable (~ 0.005 moles/sec; 348 tons/day) since the on-road contribution, which has the largest COVID reduction, is a smaller fraction during those hours.

2020 BAU: Merged gridded Emissions (Wednesday, June 10, 2020).

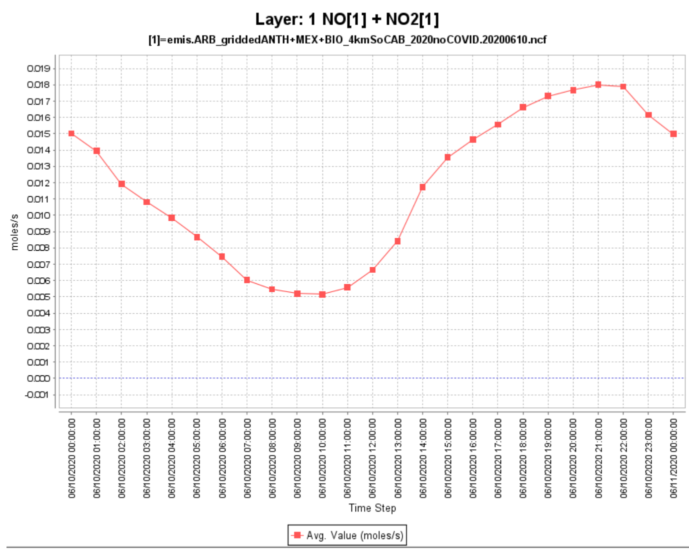

2020 COVID: Merged gridded Emissions (Wednesday, June 10, 2020).

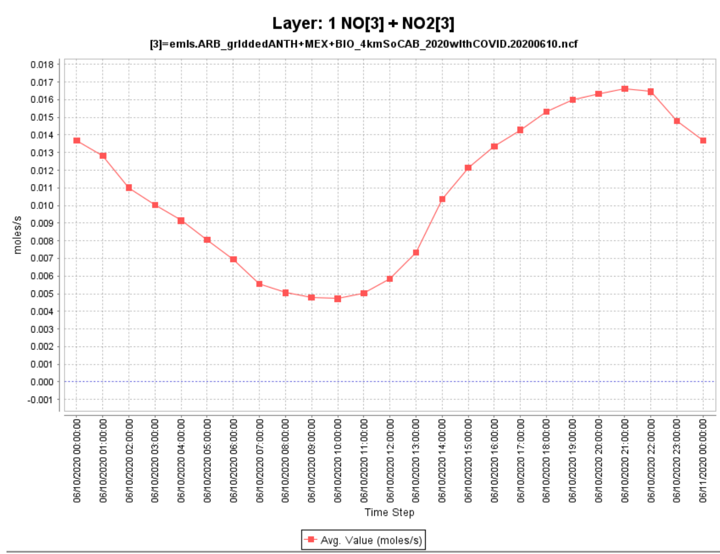

Figure 5-7. Diurnal Profile plots of SoCAB domain-wide average 4-km grid cell total NO_X emissions for the merged gridded emissions for Wednesday June 10, 2020. Upper panel is for the 2020 BAU case and lower panel is the 2020 COVID case.

6.0 CMAQ MODEL CONFIGURATION

CMAQ version 5.2.1 was run from June 1 through July 31 (with a 10-day spin-up in May) for the 12-km California domain and the 2019 Base Case and 2020 BAU emission scenarios and the 4-km SoCAB domain for the 2019 Base Case and 2020 BAU and COVID emission scenarios.

6.1 12-km CMAQ Simulations

For the preliminary CMAQ modeling that was described in Chapter 4.0 that used the top-down approach for implementing the COVID effects on emissions, boundary conditions (BCs) for the SoCAB 4-km CMAQ simulation were taken from the Whole Atmosphere Community Climate Model (WACCM[23]) global chemical transport model simulation which has a horizontal grid resolution of sizes 1.25 degrees in the x-direction and 0.95 degrees in the y-direction (~100-km). EPA ozone modeling guidance[24] suggests that for regional and urban model applications, which typically have less than or equal to 12-km grid cells, "*it may be worthwhile to apply the regional scale model at a coarser grid resolution (e.g., 36 km) to downscale global model estimates to the regional model. The coarser simulation results provide a better transition from the global simulation to the nested urban or urban/regional area of interest both at the boundaries near the surface and in the free troposphere"* (EPA, 2018). Therefore, for this study's final CMAQ simulations using the bottom-up adjustment of the 2020 BAU emissions to generate the COVID effects on emissions, 2019 Base Case and 2020 BAU Case 12-km CMAQ simulations were performed whose three-dimensional hourly concentration output were processed by the CMAQ BCON processor to generate hourly BCs for the 4-km SoCAB domain CMAQ simulations. Similarly, the CMAQ ICON initial conditions processor was used to process the CMAQ 12-km output to generate initial conditions for the CMAQ 4-km simulations. We use the same 2020 12-km CMAQ BAU simulation for BCs for both 2020 BAU and 2020 COVID CMAQ 4-km SoCAB domain simulations.

For the CMAQ 2019 and 2020 12-km domain simulations, we used output from 2019 and 2020 WAACM simulations for the BCs, respectively. The WACCM out data are mapped to CMAQ SAPRC07 mechanism species and processed through the mozart2camx downscaling tool[25] to extract lateral and vertically varying initial and boundary condition inputs. We performed 2019 and 2020 CMAQ simulations for 12-km extent shown in Figure 5-3. The emission processing for these simulations were discussed previously in Chapter 5.

6.2 4-km SoCAB Domain CMAQ Simulations

CMAQ simulations were performed for the SoCAB 4-km extent shown in Figure 5-3. For both 12-km and 4-km model simulations we used the same science options in CMAQ as shown in Table 6-1 and 6-2. These science options are defined while compiling the CMAQ Chemical Transport Model (CCTM) build and are selected in the CCTM run script. The model was run on a Linux multi-processor machine with 24 processors (6 NCOLS x 4 NROWS) for simulation period starting from May 21st until July 31st that includes 10 spin-up days (May 21st - 31st) before the June-July modeling period of interest. A CMAQ runscript with additional settings is included in Appendix D. The science module options are the same as the SCAQMD's 2016 AQMP options to the extent that they are reported in the AQMP

[23] https://www2.acom.ucar.edu/gcm/waccm. *The **WACCM** forecasts are driven by meteorological fields from the NASA GMAO GEOS-5 model. This simulation uses anthropogenic emissions from CEDS provided for CMIP6, with emissions for 2014 used for this year. Open fire emissions are from FINN-v1 (Wiedinmyer et al., Geosci. Model Devel., 2011). The results are at 0.9x1.25 degrees with 88 levels. Each file (global for 1 day) is 8 GB.*

[24] *https://www.epa.gov/sites/default/files/2020-10/documents/o3-pm-rh-modeling_guidance-2018.pdf*

[25] https://www.camx.com/download/support-software

documentation[26] although different versions of CMAQ were utilized (i.e., 2016 AQMP used CMAQ v5.0.2 whereas this study uses CMAQ v5.2.1).

Table 6-1. CMAQ v5.2.1 Chemical Transport Model (CCTM) science options used in this study.

Science Module	Option
Horizontal advection	Yamo
Vertical advection	wrf
Horizontal Diffusion	Multiscale
Vertical Diffusion	Acm2
Deposition Velocity	M3dry
Photolysis	Inline
Chemistry Mechanism	saprc07tc_ae6_aq
Aerosol Chemistry	Aero6
Cloud Chemistry	Acm_ae6
Gas Phase Chemistry Solver	Euler backward solver
Potential vorticity from free troposphere	Pv_O3

Table 6-2. CCTM Runscript Options

Science option	Option (Y or N)
Inline windblown dust	N
Lightning NOx	N
KZMIN (minimum Kz option)	Y
Ammonia bidirectional flux	N
Mercury bidirectional flux	N
Surface HONO interaction	Y
Vdiff aerosol gravitational sedimentation	Y
Inline biogenic	N
Inline plume rise for elevated point sources	Y

[26] https://www.aqmd.gov/docs/default-source/clean-air-plans/air-quality-management-plans/2016-air-quality-management-plan/final-2016-aqmp/appendix-v.pdf?sfvrsn=10

7.0 OPERATIONAL MODEL PERFORMANCE EVALUATION

The Atmospheric Model Evaluation Tool (AMET[27]) was used to conduct an operational evaluation of the CMAQ 2019 and 2020 4-km SoCAB domain simulations using concurrent observed ozone and NO_X concentrations. Model performance statistics of bias, error and correlation were calculated at each monitoring site in the SoCAB as well as across the monitoring networks. Spatial maps of site-specific performance statistics were generated. Time series and scatter plots of predicted and observed ozone and NO_X concentrations were also generated and analyzed. Model performance statistics are compared against commonly used performance goals and criteria.

7.1 Model Performance Goals and Criteria

Emery et. al., (2016) provide a set of statistics and benchmarks to assist in the assessment of a photochemical grid model (PGM) base year base case simulations. Of the possible error and bias statistical metrics, they deemed that normalized mean bias (NMB) and error (NME) statistics have the best characteristics historically to appropriate judge model performance. Different goals and criteria thresholds are provided for different pollutants. For this study, only the ozone goals and criteria are relevant as goals and criteria for ozone precursor performance metrics were not included in Emery et. al. (2016). Table 7-1 presents the normalized mean bias, normalized mean error and correlation goals and criteria thresholds for hourly and MDA8 ozone. Goal thresholds represent the statistical values that about one-third (i.e., the 33rd percentile) of top performing past applications have achieved and are considered the best a PGM can be expected to achieve. The less restrictive criteria are around the 67th percentile and indicate statistical values that about two-thirds of past applications have met. Additional relevant recommendations include: (1) a 40-ppb cutoff for hourly ozone NMB and NME, but no cutoff for correlation (r); (2) no cutoff for any statistics reported for MDA8 ozone; (3) Temporal scales for ozone statistics should not exceed 1 month; spatial scales should range from urban to less than or equal to 1,000 km. The comparison of CMAQ model performance against the performance goals and criteria help put the CMAQ 2019 and 2020 SoCAB model performance into context with past ozone model performance.

Table 7-1. Photochemical grid model ozone performance goals and criteria for Normalized Mean Bias (NMB) and Error (NME) and correlation (r) statistics (Emery et al., 2016).

	NMB		NME		r	
	Goal	Criteria	Goal	Criteria	Goal	Criteria
1-hr or MDA8 Ozone	<±5%	<±15%	<15%	<25%	>0.75	>0.50

[27] https://www.cmascenter.org/amet/

Table 7-2. Statistical measures for model performance evaluate in this study. Excerpted from Emery et. al., (2016).

Normalized mean bias (NMB)	$\frac{\sum (P_j - O_j)}{\sum O_j} \times 100$	$-100\% \leq \text{NMB} \leq +\infty$
Normalized mean error (NME)	$\frac{\sum \lvert P_j - O_j \rvert}{\sum O_j} \times 100$	$0\% \leq \text{NME} \leq +\infty$
Correlation coefficient (r)	$\frac{\sum [(P_j - \bar{P}) \times (O_j - \bar{O})]}{\sqrt{\sum (P_j - \bar{P})^2 \times \sum (O_j - \bar{O})^2}}$	Unitless, $-1 \leq r \leq +1$ $r = 1$ is perfect correlation $r = 0$ is totally uncorrelated

Note. Subscript j represents the pairing of N observations O and predictions P by site and time. Overbars signify means over site and/or time.

7.2 Atmospheric Model Evaluation Tool (AMET) Results

This section presents the AMET results for the three CMAQ simulations and June and July separately, as well as a sensitivity test to assess the potential impact from wildfires.

7.2.1 MDA8 Ozone Spatial Statistics

Figure 7-1 and 7-2 present spatial plots of site-specific normalized mean bias (NMB) and normalized mean error (NME) statistical performance metrics for the 2020 COVID and 2019 Base Case CMAQ simulations, respectively. The left panels are for June and the right panels are for July. The upper panels are NMB and the lower panels are NME. For June, the majority of SoCAB monitors meet the NMB ozone performance criteria (shaded grey) and all sites meet the NME criteria. For July, there is an underestimation bias at many monitors in the SoCAB in both 2020 and 2019. Outside of the SoCAB, CMAQ tends to overestimate ozone for both months and both years.

June 2020 **July 2020**

NMB

(Goal = ±5%; Criteria = ±15%)

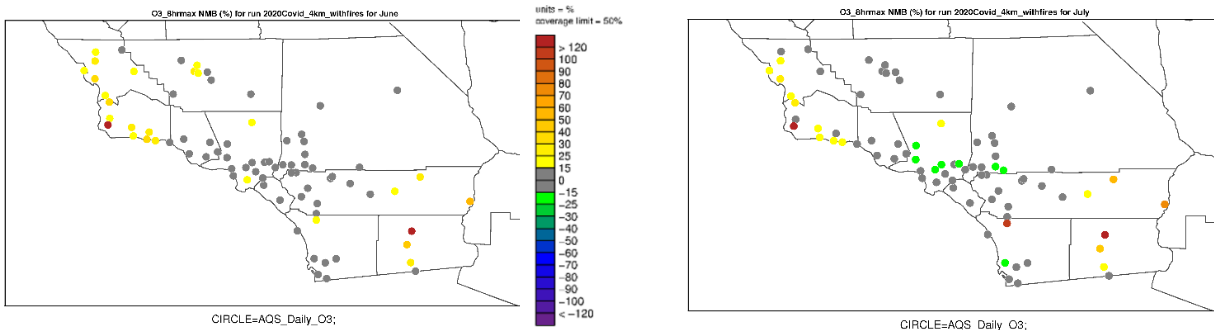

NME

(Goal = 15%; Criteria = 25%)

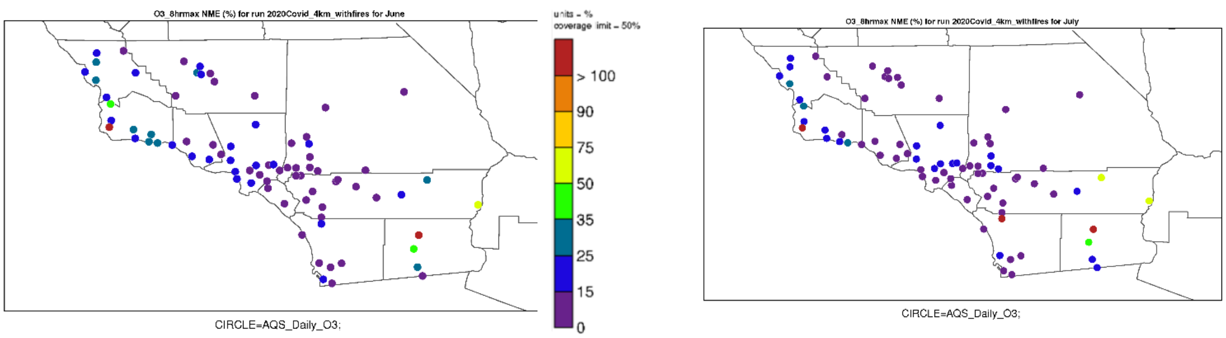

Figure 7-1. Spatial maps of June (left) and July (right) monthly site-specific NMB (top) and NME (bottom) statistics for MDA8 ozone and the 2020 COVID CMAQ simulation.

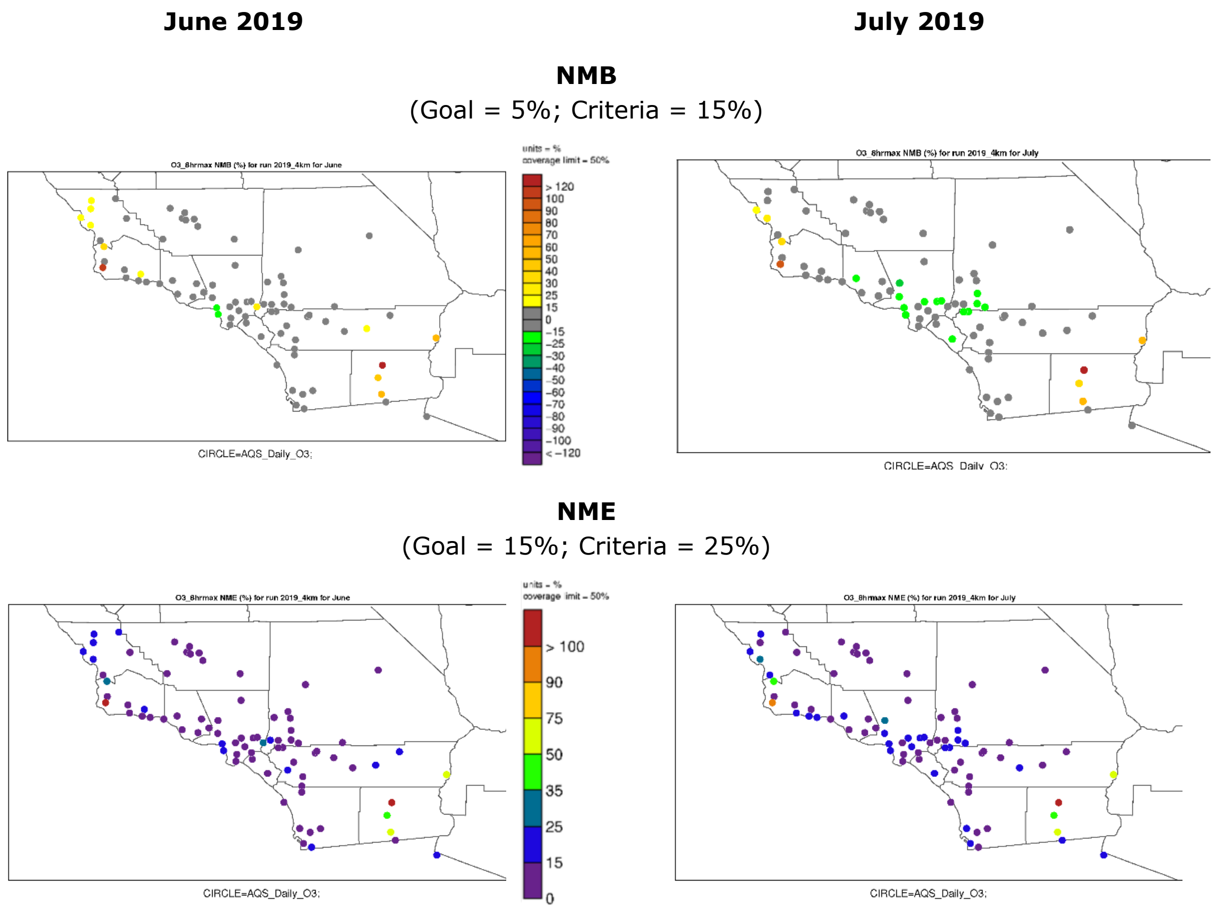

Figure 7-2. Spatial maps of June (left) and July (right) monthly site-specific NMB (top) and NME (bottom) statistics for MDA8 ozone and the 2020 COVID CMAQ simulation.

7.2.2 MDA8 Ozone Scatter Plots

Figure 7-3 presents scatter plots of predicted and observed MDA8 ozone concentrations for sites in the 4-km SoCAB domain with statistics by month for the 2020 BAU, 2020 COVID and 2019 Base cases, in the upper, middle, and lower panels, respectively. The NME statistics are quite similar for all 6 cases and range from 15.9% to 17.3% so falls between the ozone goal (15%) and criteria (25%) but is much closer to the goal than criteria. The NMB has a larger range between the 6 cases from -4.3% to +10.2% with the July NMB values achieving the ozone performance goal (±5%), while June NMB values fall between the performance goal and criteria. The 2020 BAU and 2020 COVID statistics are very similar, with marginally improved statistics for 2020 COVID compared to 2020 BAU, which is encouraging as the 2020 COVID scenario represents actual emissions that occurred in 2020. All cases exhibit CMAQ under-predictions at the higher range of observed MDA8 ozone (i.e., greater than 80 ppb) that is more prominent in July than June as well as over-predictions of the observed low MDA8 ozone values. Section 8.1 explores the performance at higher MDA8 ozone in more detail. In general, the model performance is well within the criteria threshold for both NMB and NME and close or achieving the goal threshold.

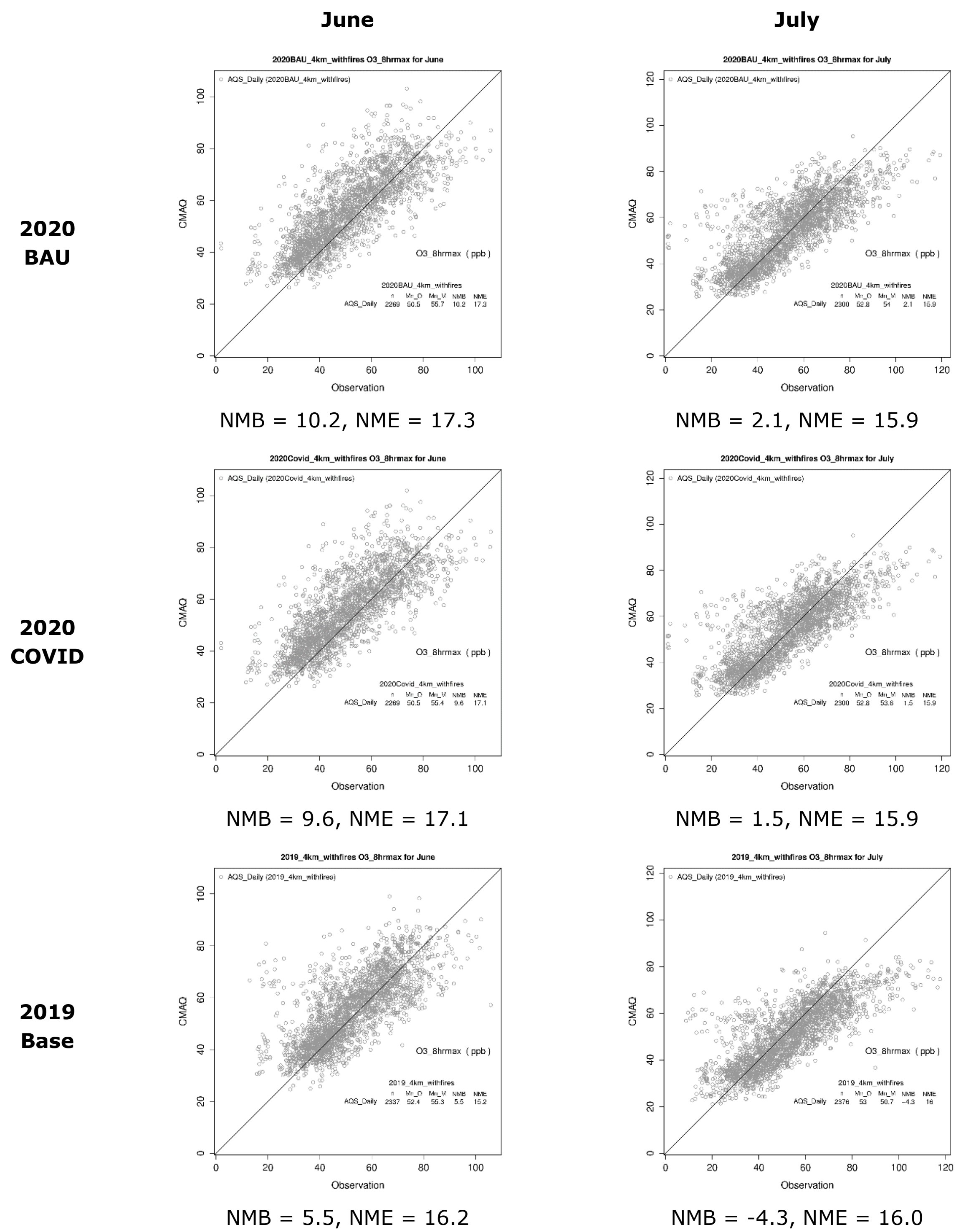

Figure 7-3. Scatter plots of MDA8 ozone for June (left) and July (right) and the 2020 BAU, 2020 COVID, and 2019 Base emission scenarios.

7.2.3 MDA8 Ozone Time Series Plots

This section presents time series plots that compare modeled versus observed MDA8 ozone for June and July 2020 and a selected set of monitors that span the basin and include sites with the highest current ozone design values. These monitors are highlighted in Figure 7-4 that also list their corresponding AQS numbers. The full list of SoCAB ozone monitors from the SCAQMD 2021 Annual Network plan is provided in Appendix B. The 2019 timeseries plots for the same selected sites are provided in Appendix C.

Selected Sites	AQS Number
LAX	06-037-5005
Los Angeles Main	06-037-1103
Azusa	06-037-0002
Glendora	06-037-0016
Pomona	06-037-1701
Upland	06-071-1004
Fontana	06-071-2002
Crestline	06-071-0005
San Bernardino	06-071-9004
Redlands	06-071-4003

Figure 7-4. Ozone monitors in the SoCAB. Circled monitors are the selected monitors.

Figure 7-5 through 7-9 present time series of predicted and observed MDA8 ozone concentrations from June 1 through July 31 for the 2020 BAU and 2020 COVID scenarios. The upper panels present MDA8 ozone and the lower panels present the difference between observed and modeled values MDA8 ozone values (i.e., the bias). For most sites and days, the modeled 2020 BAU and 2020 COVID MDA8 ozone are very closely aligned, which shows that the modeled ozone was not that sensitive to the COVID emissions adjustments (i.e., ~13% NO_X reduction between scenarios). Where differences are discernable, 2020 COVID ozone is generally higher than 2020 BAU for the Los Angeles county monitors (i.e., 06-037-xxxx) as well as Upland and Fontana in western San Bernardino County. And MDA8 ozone in the 2020 COVID case was generally slightly lower than the 2020 BAU case at the other San Bernardino County locations further east. Differences between the 2020 BAU and 2020 COVID scenarios are explored in Chapter 8.0. Model performance is generally fair, but as seen in the previous section there is an underprediction in July. The highest observed MDA8 ozone concentrations generally occurred around July 10 when CMAQ did not capture the magnitude of the observed ozone and was approximately 20 ppb lower.

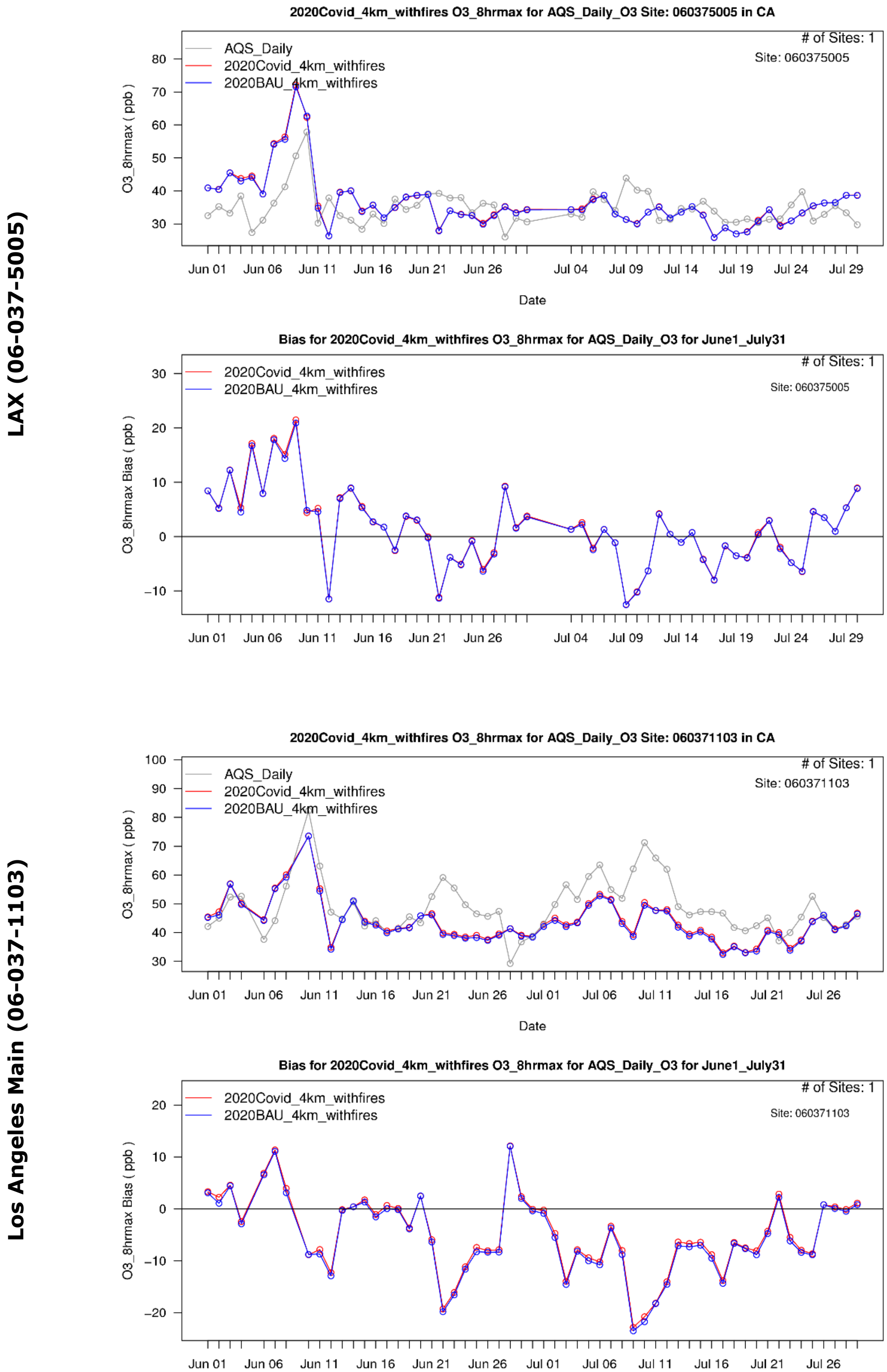

Figure 7-5. LAX and Los Angeles Main 2020 MDA8 ozone time series plots.

Azusa (06-037-0002)

Glendora (06-037-0016)

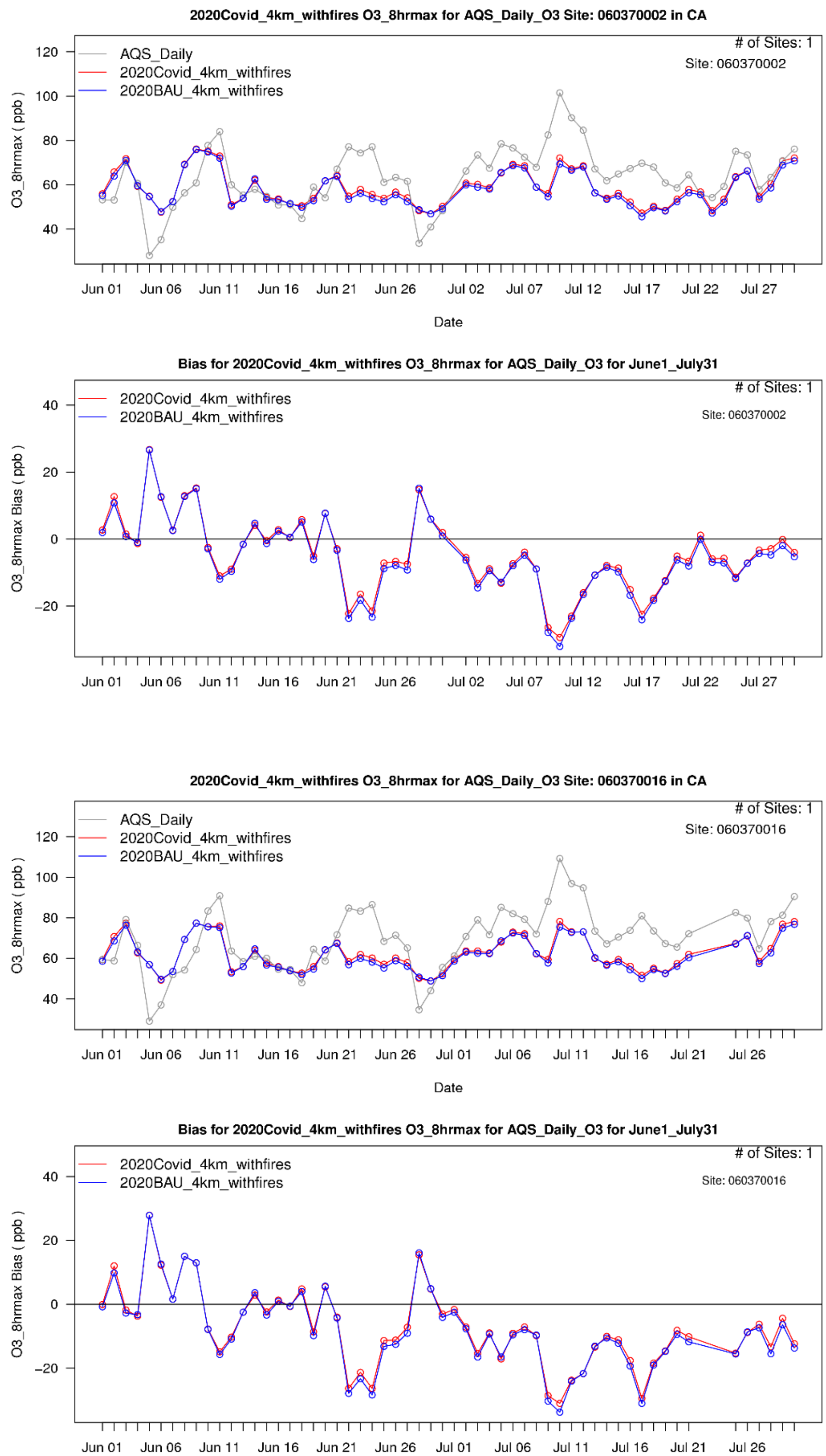

Figure 7-6. Azusa and Glendora 2020 MDA8 ozone time series plots.

Pomona (06-037-1701)

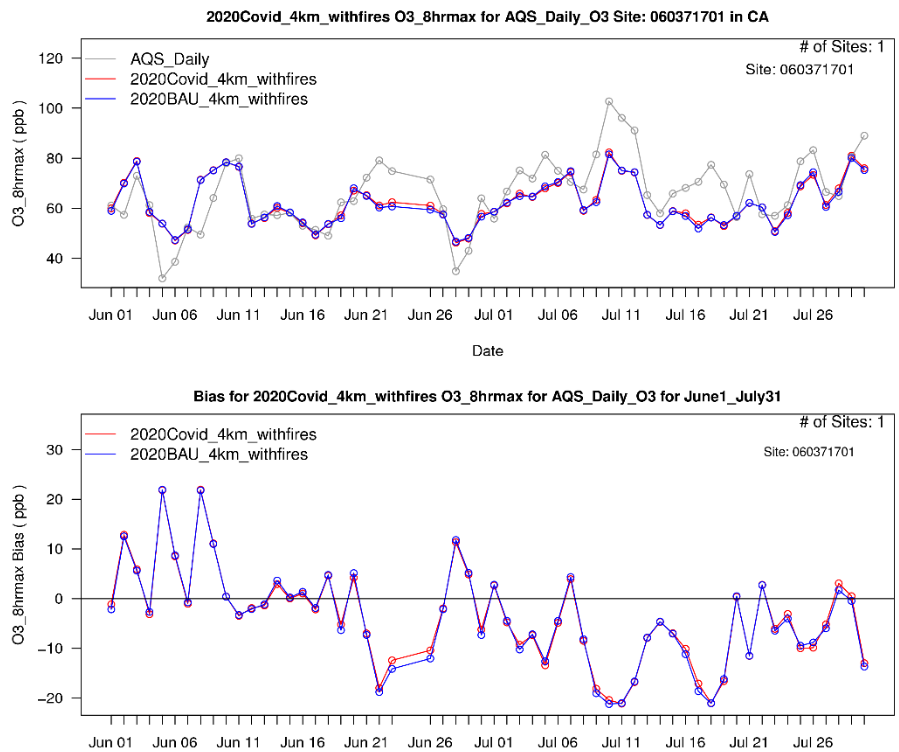

Uplands (06-071-1004)

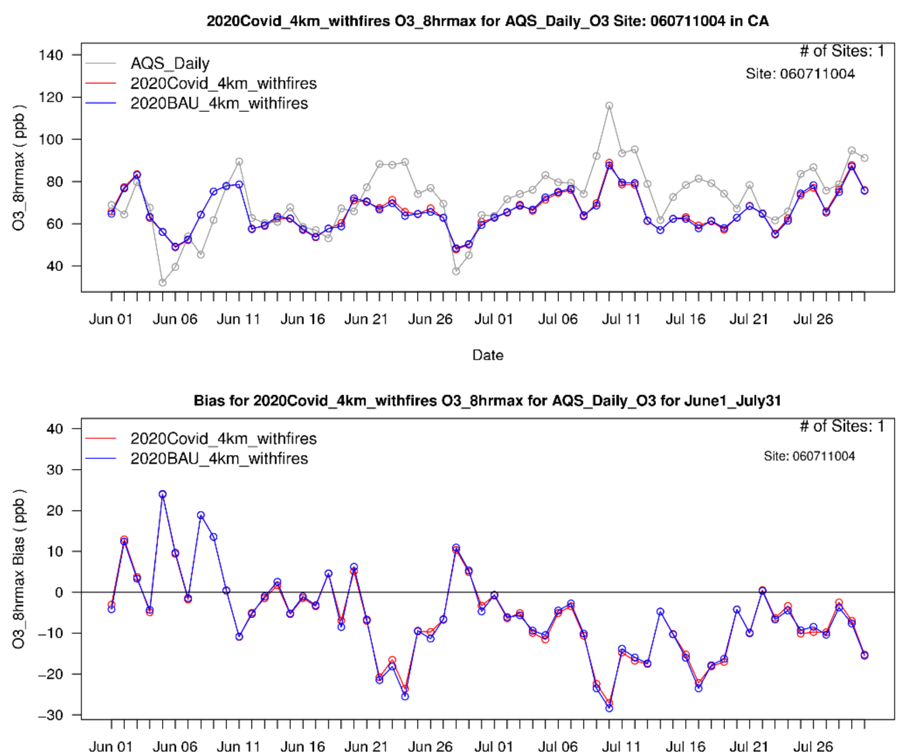

Figure 7-7. Pomona and Uplands 2020 MDA8 ozone time series plots.

Fontana (06-071-2002)

Crestline (06-071-0005)

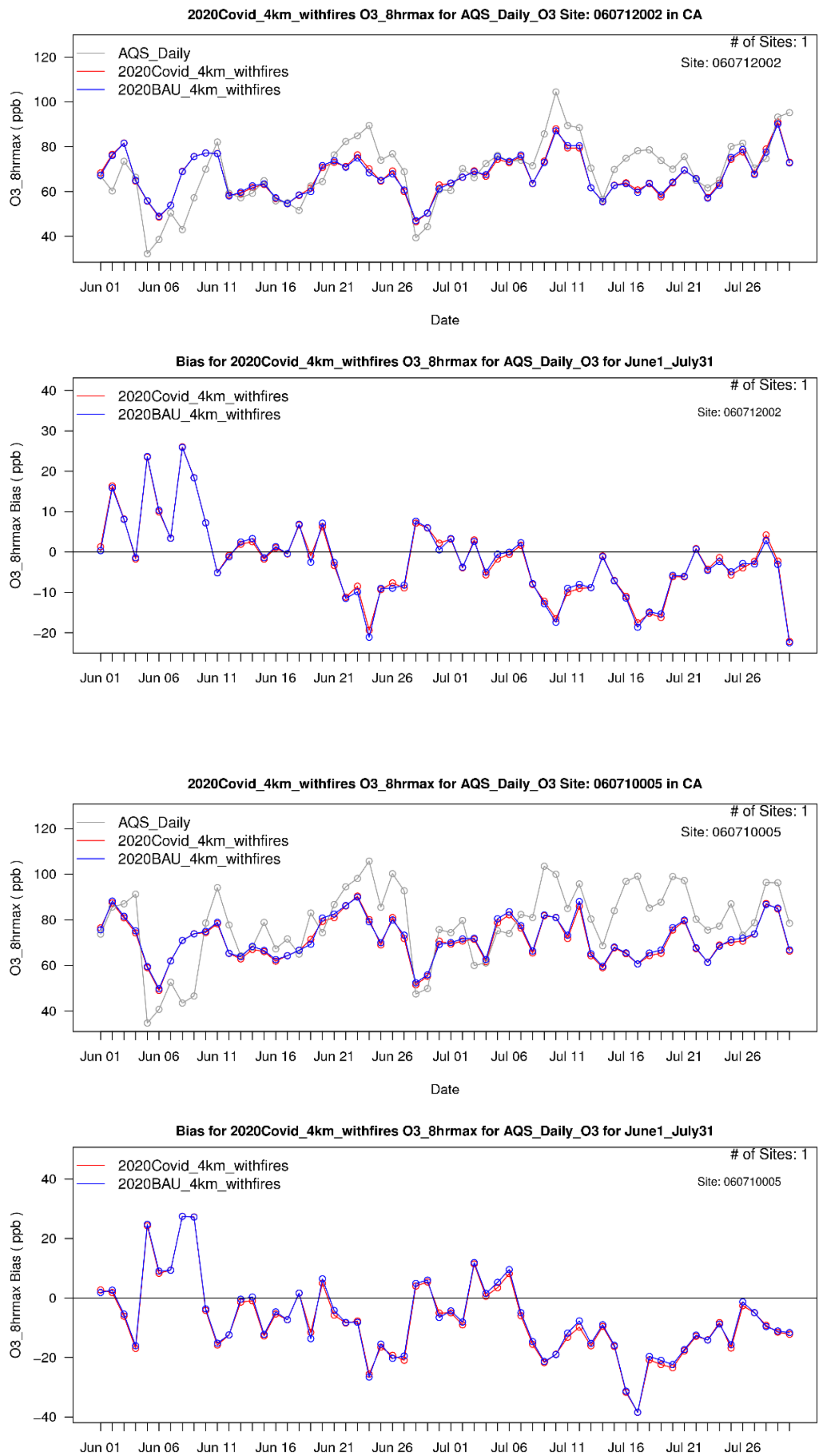

Figure 7-8. Fontana and San Bernardino 2020 MDA8 ozone time series plots.

San Bernardino (06-071-9004)

Redlands (06-071-4003)

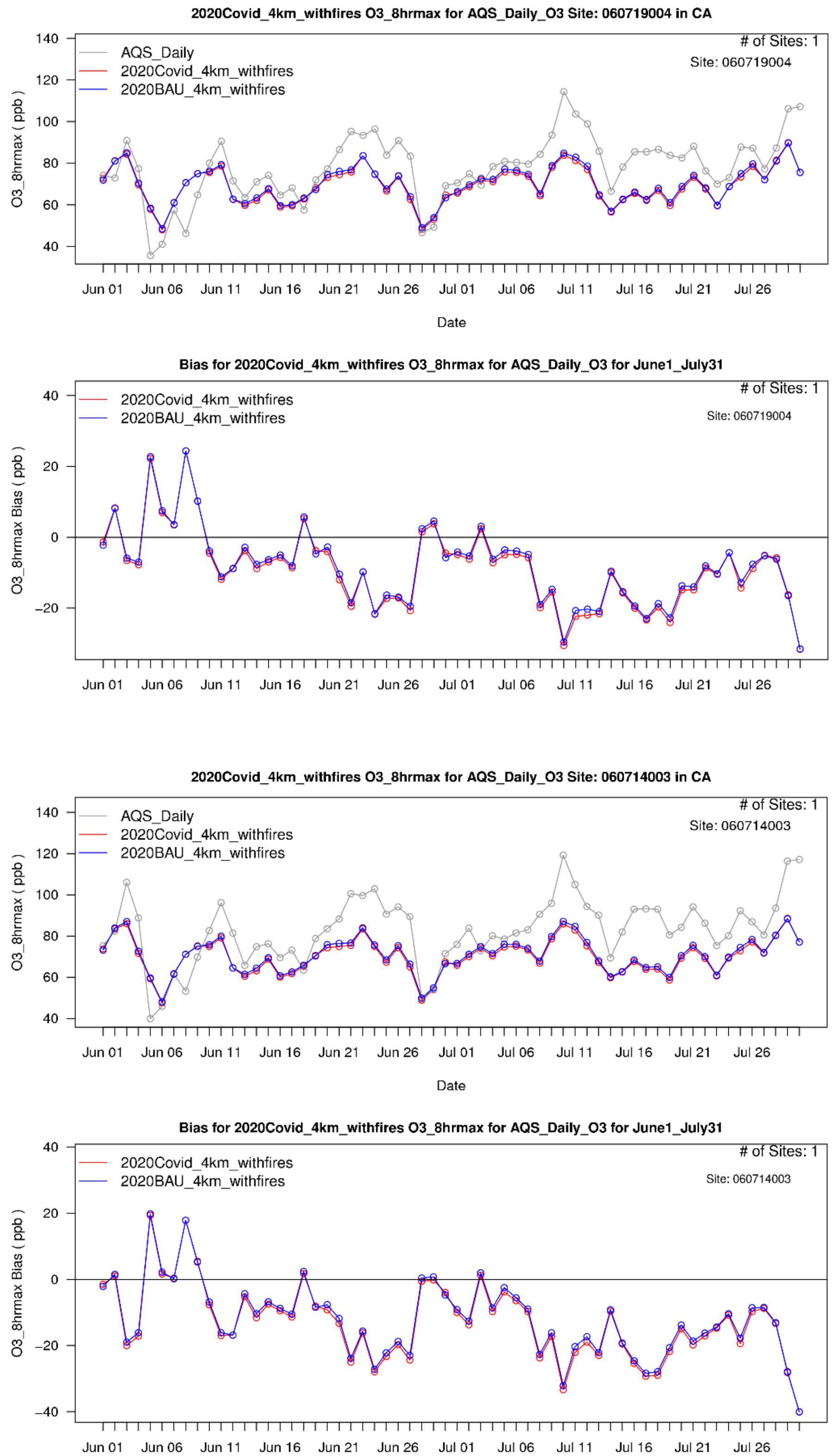

Figure 7-9. San Bernardino and Redlands 2020 MDA8 ozone time series plots

7.2.4 MDA8 Ozone Statistics By-Site

This section presents MDA8 ozone performance statistics by site for the selected sites and compares the 2020 COVID and 2020 BAU scenarios. Figure 7-10 displays monthly averaged MDA8 ozone for observations and the CMAQ predicted 2020 COVID and 2020 BAU scenarios for June and July, in the upper and lower panels respectively. For June, monthly average MDA8 is within 5 ppb for all sites except Redlands. For July, however, there is a large negative bias for all sites except LAX. In general, 2020 COVID MDA8 is slightly lower than 2020 BAU MDA8 at the sites LAX through Glendora, 2020 COVID MDA8 is very similar to 2020 BAU MDA8 at Pomona to Fontana and 2020 COVID MDA8 is slightly higher that 2020 BAU MDA8 at Crestline to Redlands. This is indicative of the changing ozone formation regimes across the basin with ozone formation being more VOC sensitive near the coast and in Los Angeles County transitioning to more NO_X sensitive as you go further east.

June

July

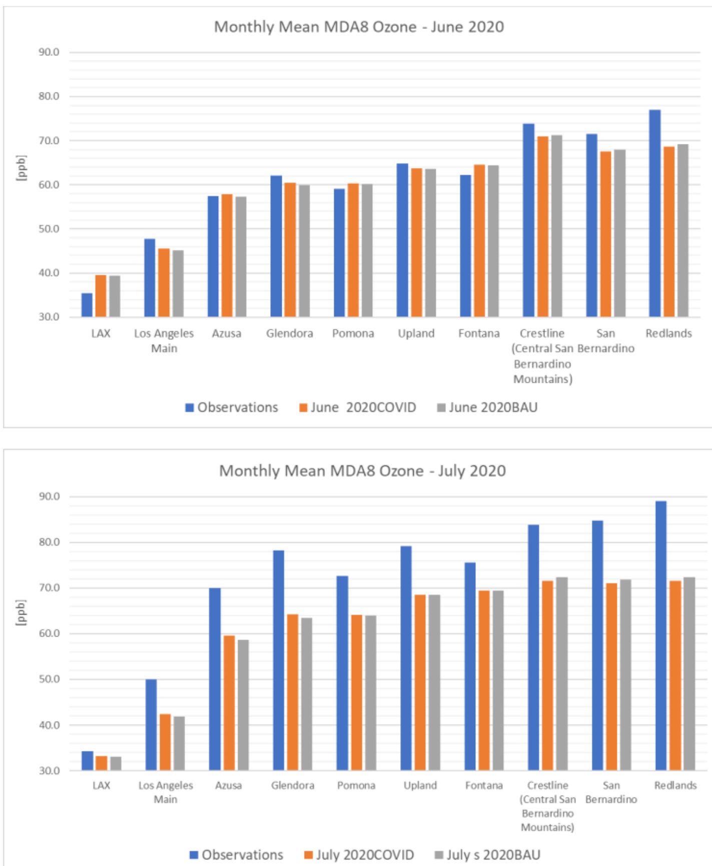

Figure 7-10. Monthly averaged observed and CMAQ predicted 2020 COVID and BAU scenario MDA8 ozone at selected sites for June(top) and July (bottom).

Table 7-3 presents the monthly NMB, NME and correlation (COR or r) statistics for the selected sites, the 2019 Base Case, 2020 COVID and 2020 BAU scenarios and June and July. The NMB, NME and COR statistics are color coded as to whether they achieve the performance goals (green), fall between the performance goals and performance criteria (blue) or fall outside of the performance criteria (red). In June, all the ozone performance statistics achieve the ozone performance criterion with the exception of LAX and Pomona in 2019. Most sites also achieve the bias and error performance goal in June as well. Ozone performance is not as good in July with CMAQ exhibiting an ozone underestimation bias in both years that fails to achieve the performance criteria at approximately half of the sites.

Performance statistics are similar between the two 2020 scenarios indicating that the bottom-up COVID-19 adjustment of emissions had a noticeable but not an appreciable effect on ozone model performance. Marginal improvements or degradation can be seen for different metrics and different locations.

Table 7-3. Comparison of 2020 COVID and 2020 BAU Performance Statistics for Select Sites for June (green achieves performance goal; blue falls between performance goal and criterion; red falls outside of performance criterion)..

	2019 BAU			2020 COVID			2020 BAU		
Monitor	NMB	NME	COR	NMB	NME	COR	NMB	NME	COR
				June					
LAX	-17.3	17.9	0.5	11.7	20.0	0.6	11.2	19.7	0.6
Los Angeles Main	1.3	11.4	0.7	-4.5	12.3	0.7	-5.3	12.5	0.7
Azusa	-0.6	14.1	0.7	0.9	14.3	0.6	-0.2	14.8	0.5
Glendora	-1.3	14.2	0.7	-2.5	15.0	0.6	-3.5	15.9	0.5
Pomona	25.1	27.2	0.6	2.2	11.3	0.7	1.9	11.9	0.7
Upland	2.8	15.6	0.5	-1.7	12.9	0.7	-1.9	13.4	0.7
Fontana	0.4	12.5	0.5	3.7	12.2	0.7	3.5	12.4	0.7
Crestline	-5.7	12.8	0.6	-3.9	14.5	0.8	-3.6	14.5	0.8
San Bernardino	-4.5	13.7	0.5	-5.6	13.6	0.8	-5.0	13.3	0.8
Redlands	-4.9	12.9	0.5	-10.8	14.9	0.8	-10.0	14.4	0.8
				July					
LAX	-21.8	22.2	0.1	-3.2	11.4	0.1	-3.5	11.4	0.1
Los Angeles Main	-11.8	13.2	0.5	-15.1	15.8	0.7	-16.1	16.7	0.7
Azusa	-16.2	17.0	0.6	-14.9	15.0	0.7	-16.3	16.3	0.7
Glendora	-16.2	17.1	0.7	-17.8	17.8	0.7	-18.9	18.9	0.7
Pomona	5.9	11.0	0.7	-11.7	12.9	0.8	-11.9	13.1	0.8
Upland	-11.7	12.9	0.7	-13.3	13.4	0.8	-13.4	13.4	0.8
Fontana	-12.6	13.1	0.7	-8.2	9.3	0.8	-8.1	9.2	0.8
Crestline	-18.9	18.9	0.8	-14.5	16.4	0.5	-13.7	15.9	0.4
San Bernardino	-17.9	17.9	0.8	-16.2	16.4	0.7	-15.3	15.6	0.7
Redlands	-23.9	23.9	0.8	-19.6	19.7	0.7	-18.6	18.7	0.7

7.2.5 NO_X Performance Evaluation

A limited NO_X model performance evaluation of spatial statistics by month for NMB and NME is presented here. A rigorous NO_X performance analysis is recommended for future work, that avoids the pitfalls detailed by Dickerson et al. (2019) related to the fact that most commercial NOx analyzers do not measure true NO_X and when used as a basis for evaluating modeled NO_X may involve errors of a factor of two or more. Dickerson et al. (2019) report that the primary issue with commercial monitors is that they "*suffer substantial interferences from other reactive species. These interfering species include nitrous acid (HONO), nitric acid (HNO_3), nitric acid anhydride (N_2O_5), organic nitrogen peroxides, alkyl nitrates (RONO2), nitryl chloride (ClNO2) and other important air pollutants. These instruments more nearly measure NOy than NOx; in the US, a good approximation is NOy = NOx + HONO + HNO3 + 2XN2O5 + PANs + RONO2, where PANs represent the family of peroxyacetyl nitrates and RONO2 represents the family of alkyl nitrates … Commercial "NOx" instruments are in common use because the interferences do not cause a problem when such monitors are deployed to demonstrate attainment with NO_2 standards – they provide an upper bound on NO_2 and NO_X concentrations. So while these monitors can be useful, they generate numbers with variable, and often severe, high bias*".

A potential solution is to follow the example of Toro et al. (2021) who recognize the issue of artifacts in ambient NOx measurements but note that this is "*most pronounced at times and locations with higher fractions of aged NOy species compared to NO_X. To bound this measurement uncertainty, we compared measured NO_X both to modeled NO_X and to modeled NOy. In addition, we focus analysis on morning hours (4–9 AM LST) when fresh NO_X emissions are expected to dominate NOy, thus limiting the impact of measurement artifacts."* Other researchers, namely Tong et al. (2015) and Fujita et al. (2013), also focus their analysis of AQS NOx concentrations on the early morning hours of 6 – 9 am.

Figure 7-11 and Figure 7-12 present spatial statistics plots by month for NO_X concentrations of NMB and NME for 2020 COVID, and 2019 Base scenarios, respectively. The left panels are for June and the right panels are for July. The upper panels are NMB, and the lower panels are NME. For both months and years, most of the SoCAB monitors have a negative bias which tends to be consistently between -50% to –100% at the San Bernardino monitors. Outside of the SoCAB, the bias is more variable and of mixed sign. The underestimation of the observed NO_X may be due in part to the measurement issues discussed above. NME is generally greater than 35% throughout the domain for both months and years.

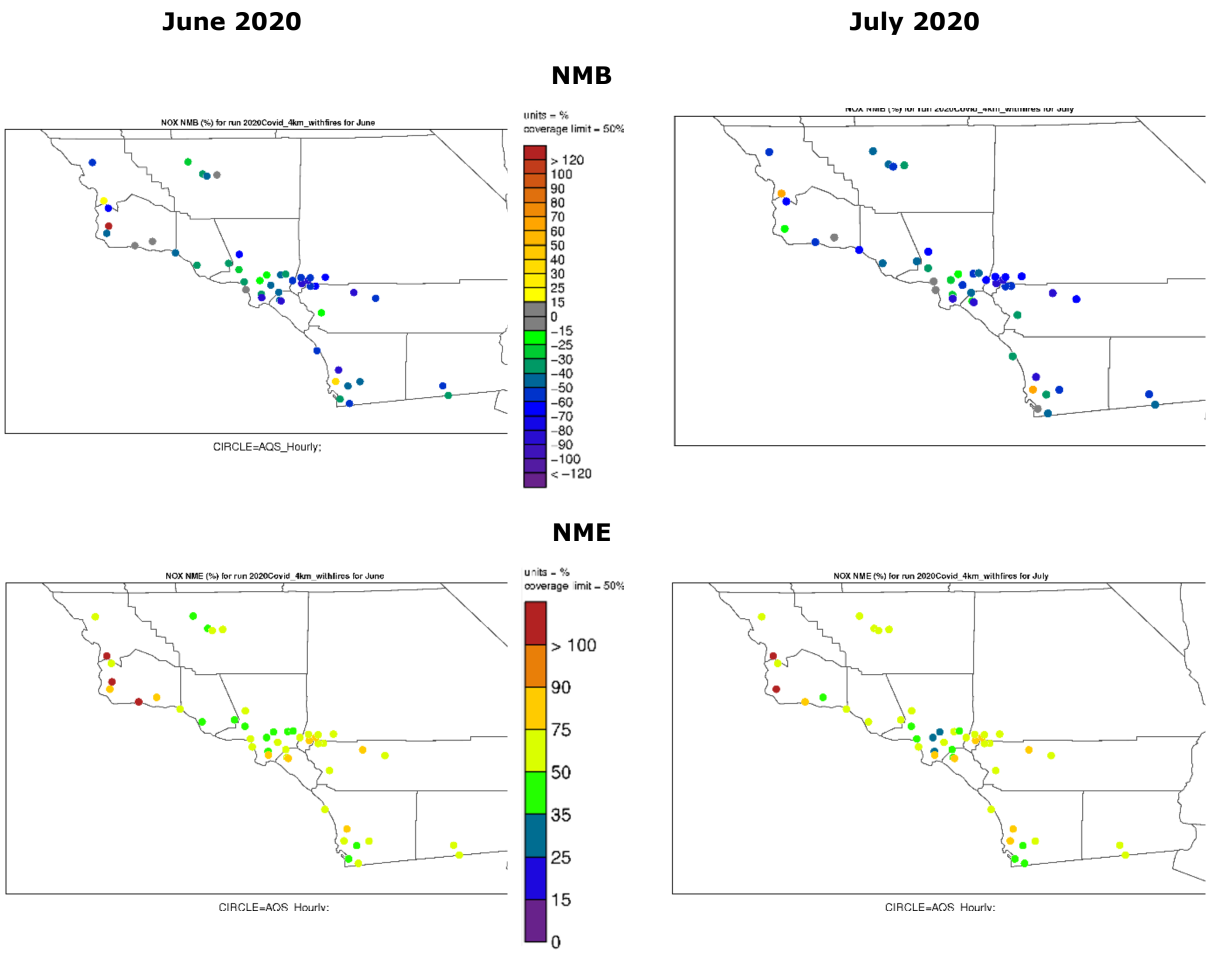

Figure 7-11. Site-specific NMB and NME plots for NO_X for June (left) and July (right) and the 2020 COVID scenario.

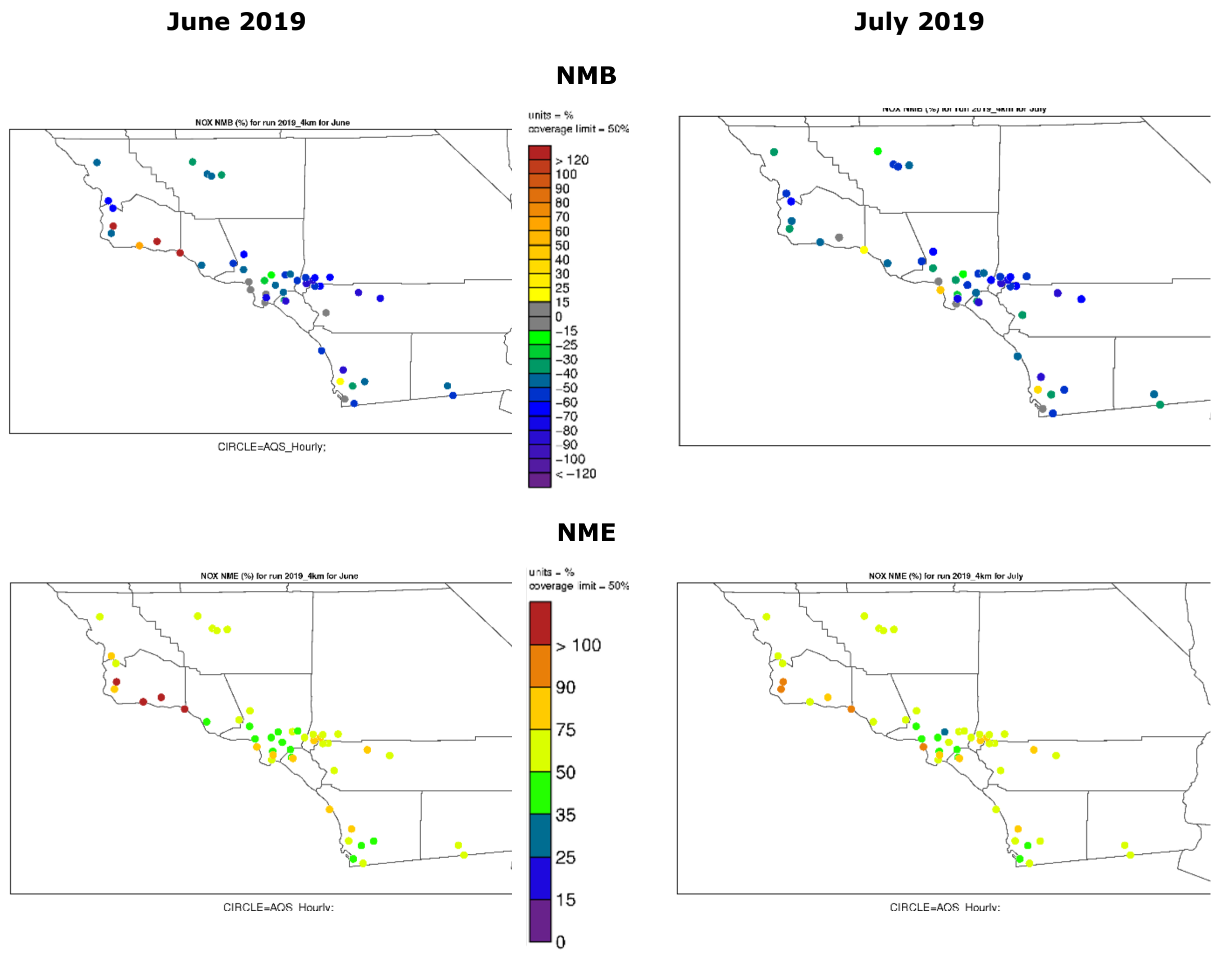

Figure 7-12. Site-specific NMB and NME plots for NO_X and June (left) and July (right) and the 2019 Base Case scenario.

7.2.6 Wildfire Sensitivity Evaluation

To assess whether fire emissions played a significant role in ozone formation during our modeling period we performed “zero-out” simulations for June-July 2019 and 2020 where CMAQ was run without fire emissions. Since fires are episodic by nature, potential fire impacts may be restricted to a small number of days and may not be apparent in analysis that averages over a longer period. Regardless, we first consider fire impacts at the selected sites on a monthly basis to determine whether sites were substantially impacted by fires and whether model performance changes substantially for the scenarios, secondly, we consider potential episodic impacts.

Figure 7-13 shows negligible differences in monthly average MDA8 at all the selected sites for both June in the upper panel and July in the lower panel. The largest difference is 0.39 ppb at Glendora in July.

June

July

Figure 7-13. Monthly averaged MDA8 ozone at select sites. Comparison of 2020 COVID and 2020 COVID without fire emissions scenarios for select sites. Upper panel is June and lower panel is July.

Table 7-4 reports the NMB, NME and correlation statistics for the selected sites for the 2020 COVID and 2020 COVID w/o fires scenarios for June and July. The NMB is generally very similar for the two scenarios. For June there is generally a +0.1% increase in bias for the 2020 COVID case compared to the 2020 COVID w/o fires case, which may improve or degrade the performance depending on whether the model is over or underpredicting at that monitor. For July, the increase in bias for the 2020 COVID case relative to the 2020 COVID w/o fires case, may be as much as +0.5 %. This is also a very small change and we conclude that fires played a minimal role in monthly ozone production during June and July 2020

Table 7-4. Comparison of 2020 COVID and 2020 COVID without Fires Performance Statistics for Select Sites for June.

			2020 COVID				2020 COVID w/o Fires			
Monitor	**Num_Obs**	**Obs_mean**	**Mod_mean**	**NMB**	**NME**	**COR**	**Mod_mean**	**NMB**	**NME**	**COR**
June										
LAX	30.0	35.4	39.6	11.7	20.0	0.6	39.5	11.5	19.8	0.6
Los Angeles Main	28.0	47.7	45.6	-4.5	12.3	0.7	45.5	-4.6	12.4	0.7
Azusa	30.0	57.4	57.9	0.9	14.3	0.6	57.8	0.8	14.3	0.6
Glendora	30.0	62.1	60.5	-2.5	15.0	0.6	60.5	-2.6	15.1	0.6
Pomona	28.0	59.1	60.4	2.2	11.3	0.7	60.3	2.1	11.3	0.7
Upland	30.0	64.8	63.7	-1.7	12.9	0.7	63.7	-1.7	12.9	0.7
Fontana	30.0	62.3	64.6	3.7	12.2	0.7	64.5	3.6	12.2	0.7
Crestline	30.0	73.9	71.0	-3.9	14.5	0.8	70.9	-4.0	14.6	0.8
San Bernardino	30.0	71.5	67.5	-5.6	13.6	0.8	67.5	-5.6	13.7	0.8
Redlands	30.0	76.9	68.6	-10.8	14.9	0.8	68.5	-10.9	15.0	0.8
July										
LAX	27.0	34.3	33.2	-3.2	11.4	0.1	33.2	-3.1	11.3	0.1
Los Angeles Main	29.0	49.9	42.4	-15.1	15.8	0.7	42.3	-15.3	16.0	0.7
Azusa	29.0	70.0	59.6	-14.9	15.0	0.7	59.3	-15.4	15.5	0.6
Glendora	27.0	78.2	64.3	-17.8	17.8	0.7	63.9	-18.3	18.3	0.6
Pomona	30.0	72.6	64.1	-11.7	12.9	0.8	63.8	-12.1	13.3	0.7
Upland	30.0	79.1	68.6	-13.3	13.4	0.8	68.3	-13.7	13.7	0.8
Fontana	30.0	75.6	69.4	-8.2	9.3	0.8	69.2	-8.4	9.5	0.8
Crestline	30.0	83.8	71.6	-14.5	16.4	0.5	71.5	-14.7	16.6	0.4
San Bernardino	30.0	84.8	71.1	-16.2	16.4	0.7	71.0	-16.2	16.4	0.7
Redlands	30.0	88.9	71.5	-19.6	19.7	0.7	71.5	-19.6	19.7	0.7

Figure 7-14 presents the period maximum MDA8 ozone fire impacts and corresponding FINN fire emissions. The maximum days were identified by inspecting the spatial plots for the entire period. The 2019 period maximum fire impact occurred on July 29 and the spatial maximum impact was 2.8 ppb. In 2020 the maximum fire impact occurred on June 10 and was 8.75 ppb. These fires were short-lived and had no detectable ozone impact after 2 days. In general, the months of June and July in 2019 and 2020 throughout the SoCAB were not substantially impacted by fire emissions.

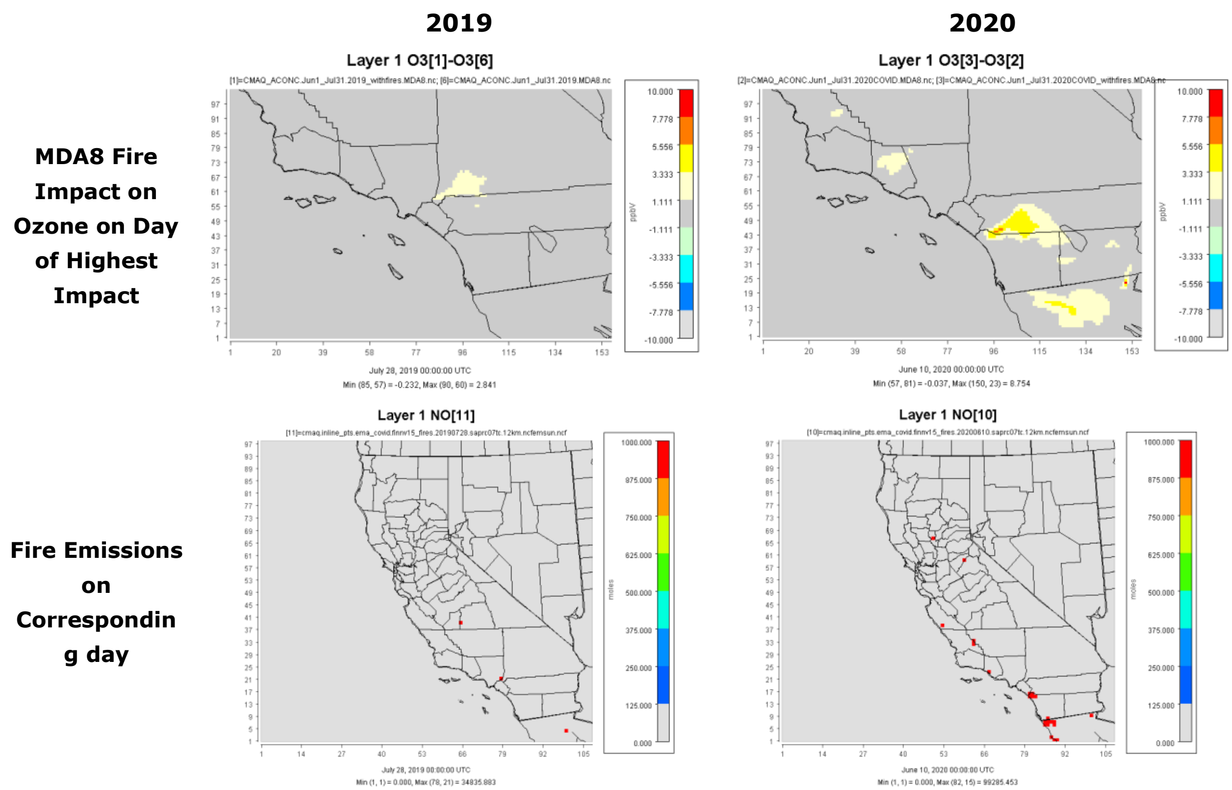

Figure 7-14. Maximum fire impacts over the June-July modeling periods and the 2019 Base and 2020 COVID cases.

7.2.7 MPE Conclusions

Ozone model performance is generally within typical thresholds based on historical PGM applications. The upper range of MDA8 ozone has a negative bias as is typical in these applications and that underestimation bias is generally larger in July than June for both years. A detailed NO_X performance evaluation was beyond the scope of this work but is recommended for future work. The model performance is deemed sufficient for this analysis, but the results should be interpreted with consideration of model biases. Additional effort to improve model performance may be warranted if this modeling platform is to be used in additional applications.

8.0 DYNAMIC MODEL PERFORMANCE EVALUATION

This project has two main goals: (1) to examine the effects the COVID-19 emissions reductions had on ozone air quality in the SoCAB; and (2) to assess whether the CMAQ model that is used to define future year ozone attainment control strategies can reproduce the observed ozone response to the sudden emissions reductions due to the response to the COVID-19 pandemic. The first goal is primarily accomplished by comparing the two 2020 modeled scenarios (i.e., 2020 COVID and 2020 BAU). The second goal is accomplished by considering the two scenarios that occurred (i.e., 2019 Base and 2020 COVID) and comparing the modeled and observed ozone responses.

The evaluation of whether a photochemical model can reproduce the observed ozone changes in response to emission changes as in the second goal listed above is termed a Dynamic Evaluation and is one of the four types of model evaluations listed in EPA's photochemical modeling guidance (EPA, 2018):

- Operational Evaluation evaluates how well the model reproduces observed concentrations for the base year simulation (discussed in Chapter 7).
- Diagnostic Evaluation evaluates the model's sensitivity to key inputs, parameters or other assumption (e.g., the without fire sensitivity test discussed in Chapter 7).
- Dynamic Evaluation evaluates whether a model can reproduce the observed changes in concentrations to changes in emissions, such as over time or comparing weekday and weekend ozone changes.
- Probabilistic Evaluation evaluates a model for an ensemble of simulations.

Most Dynamic Evaluations compare the observed and modeled response to a large change in emissions (e.g., over a decade or after a large regional emissions control strategy, such as the NO_X SIP Call). When looking at smaller changes in emissions it is important to try and disentangle the effects of the emissions change from the effects of meteorology, which we attempt to do in the discussion below.

8.1 Dynamic Model Performance Evaluation

A dynamic evaluation was conducted to evaluate whether the CMAQ model and procedures used to make ozone projections in the SoCAB AQMPs can reproduce the observed changes in ozone due to the changes in emissions between 2019 and 2020 due to the COVID pandemic response. The dynamic model performance evaluation compares the CMAQ ozone results from the 2020 COVID case with those from the 2019 Base case with the changes in observed ozone between 2019 and 2020.

8.1.1 Ozone Dynamic Evaluation Procedures

For this analysis, we followed EPA modeling guidance (EPA, 2018[28]) for an ozone model attainment demonstration since that is the procedure used to make ozone projections using the CMAQ model in the SoCAB AQMPs. In this evaluation of the AQMP future year ozone projection procedures, the 2020 COVID-19 emission reductions are used to represent a future-year emissions scenario and 2019 Base Case represents the base year. Typically, a future year for a model attainment demonstration may be five or more years in the future (or a decade or more for the SoCAB extreme ozone NAA). For example, the attainment year for the SoCAB under the 2008 and 2015 ozone NAAQS are, respectively, 2032 and 2037. The abrupt emissions reductions due to COVID-19 restrictions mimic a potential

[28] https://www.epa.gov/sites/default/files/2020-10/documents/o3-pm-rh-modeling_guidance-2018.pdf

future-year scenario that has the unique attribute of also having observed changes in ozone in addition to the modeled projections. In a model attainment demonstration, emissions are reduced in the future year compared to the base year, but the meteorology remains the same since the future year meteorology is unknown. For this analysis, the meteorology is different between 2019 and 2020 although the June-July 2019 and 2020 modeling periods were selected to try to obtain periods in different years with as similar meteorology as possible (as discussed in Chapter 2). The primary meteorological parameters we evaluated were the T850 mb and surface temperatures at the KONT site (i.e., Ontario), which were found to be similar between the years in the selected months of June and July. Other meteorological factors, in particular, winds, cloud cover and the strength and depth of the marine layer, may have been different between the two years and may impact the analysis at some locations as discussed in more detail below.

EPA recommends using model estimates in a relative rather than absolute sense to reduce potential model bias effects for making future year ozone projections (EPA, 2018). Fractional changes in air pollutant concentrations between the model future year and model base year are calculated, these ratios are called relative response factors (RRFs). The RRFs are multiplied by base year observed ozone concentrations to predict future year ozone concentrations. The base year observations are the average of three-years of ozone design values (DVB) and the future year ozone design value (DVF) projection formula is as follows:

$$DVF_i = RRF_i \times DVB_i$$

Where DVF_i is the estimated design value for the future year in which attainment is required at monitoring site i; RRF_i is the relative response factor at monitoring site i; and DVB_i is the base design value at monitoring site i.

For the Dynamic Evaluation, RRFs are calculated the same way as use for making future year ozone design value projections only instead of using PGM modeling results for a base and future year emissions scenario that use the same meteorological inputs, we use the modeling results for the 2019 Base Case and 2020 COVID Case emission scenarios that have different meteorological conditions. Observation-based RRFs are also calculated using the 2019 and 2020 ozone observations in a consistent fashion to how the modeled RRFs are calculated and the CMAQ-based RRFs are compared with the observation-based RRFs to determine whether the CMAQ model predicts the same ozone response to the COVID-19 emissions reductions as was observed.

There are additional important considerations for the RRF calculations regarding which days to use in the RRF calculation. EPA guidance has evolved over the years in this regard, and we follow the current EPA recommendation which is to calculate RRFs based on the 10 highest modeled days in the base year modeling near the monitor location. As discussed by EPA (EPA, 2018), basing the calculation on a set of high days rather than all days reflects the fact that design values are based on the three-year average 4th high observed MDA8 ozone values. EPA recommends "*selecting a set of modeled days that are likely to encompass a range of values that are somewhat higher than and somewhat lower than the 4th high value… this balances the desire to have enough days in the RRF to generate a robust calculation, but not so many days that the RRF does not represent days with concentrations near the observed design values"* (EPA, 2018). EPA adds an additional specification that MDA8 values be greater than or equal to 60 ppb for that day and in cases for which the base model simulation does not have 10 days with MDA8 values greater than or equal to 60 ppb at a site, then EPA recommends using all days where MDA8 is greater than or equal to 60 ppb, if there are at least 5 days that meet the minimum threshold criteria. For the SoCAB, most sites easily meet the MDA8 greater than or equal to 60 ppb criteria for the top 10 modeled MDA8 ozone days, but there are a few sites near the coast that do not meet this criterion. For simplicity, and since this is not a formal attainment demonstration, we follow the EPA's top 10 days recommendation but do not eliminate ozone projections at the few sites that have MDA8 greater than or equal to 60 ppb for less than 5 days for the sake of completeness. In addition, EPA recommends averaging model results over a 3 x 3 array of grid cells that surround the monitor. However, we use the single grid cell where the monitor is located for the modeled RRF for consistency with the observed RRF as that is the only choice for the RRF based on observations. However, we also provide spatial gridded plots of modeled RRFs for the entire SoCAB and sharp gradients near a monitor will be visible in these plots.

For the 2019 Base Case and 2020 COVID Case CMAQ modeling results, we identify the 10 days with highest modeled MDA8 ozone concentrations at each monitoring site i9n each year and calculate the average modeled MDA8 ozone concentration for those days. We then calculate the average observed MDA8 using the same set of days, (so the meteorology will be the same) to derive 4 averaged MDA8 values (i.e., 2019 and 2020, modeled and observed). The modeled and observed RRFs are calculated as the ratio of averaged MDA8s across those days for the 2019 Base to 2020 COVID cases modeling results. We do this for each SoCAB grid cell that contains a monitor to obtain a modeled/observed pair of RRFs at each monitoring site. In addition, for all model grid cells we calculate modeled RRFs over the entire SoCAB grid cells. In general, the top 10 days may be different at each grid cell but there is probably some overlap in selected days in adjacent and nearby grid cells and sites.

8.1.2 Operational Ozone Model Evaluation for Days used in the Dynamic Evaluation

The model performance for the days used in the RRFs (i.e., the top 10 modeled days at each site) was also examined. Figure 8-1 presents a scatter plot of observed versus modeled MDA8 each day in the set of top 10 days at each monitoring site for 2019 and 2020 with model performance statistics for selected sites shown in Table 8-1. Across all sites the model performance is similar between the two years and has a similar underestimation bias that almost achieves (-6.3 %) or does achieve (-4.0 % in 2020) the ozone performance goal for bias (±5%) with error achieving the performance goal in both years (15 %). However, the model underestimates the highest observed MDA8 ozone concentrations. In 2019, the range of observed MDA8 ozone is approximately 40 to 110 ppb and the range of modeled MDA8 is approximately 40 to 90 ppb. In 2020, the range of observed MDA8 is approximately 30 to 120 ppb, and the range of modeled MDA8 is approximately 40 to 90 ppb.

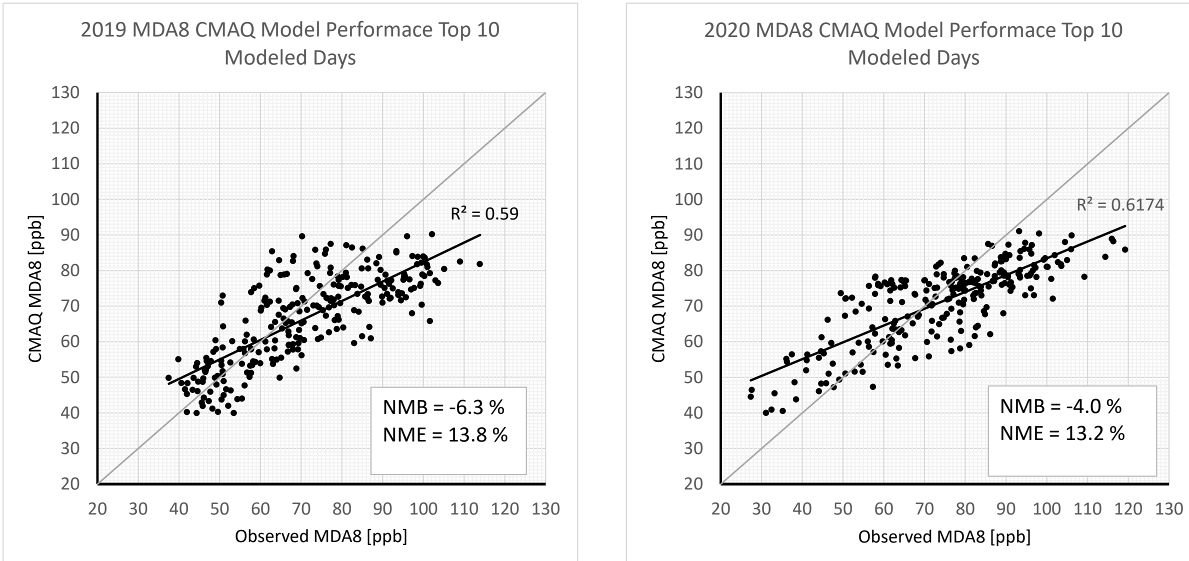

Figure 8-1. Model performance scatter plots for the top 10 modeled MDA8 days at SoCAB monitoring sites.

Although there is similar ozone model performance in 2019 and 2020 for the top 10 modeled MDA8 ozone days when examining across all sites in the SoCAB, there are differences when analyzed at individual sites (Table 8-1). For example, at LAX CMAQ is underestimating the observed ozone in 2019 (-12%) and greatly overestimating the observed ozone in 2020 (+30%). At Pomona there is a large overestimation bias in 2019 (+19%) and a smaller underestimation bias in 2020 (-6%). And Redlands has large underestimations in both years (-16% and -18%). Except for those three sites, all other sites achieve the ozone performance criteria for bias and error with many sites also achieving the error performance goal and one site (Los Angeles Main) achieving the bias performance goal in both years.

Table 8-1. Normalized Mean Bias (NMB) and Error (NME) for the 10 highest modeled MDA8 ozone days in 2019 and 2020 used in calculating the predicted and observed RRFs. Color shading indicates whether the model performance statistics achieve the ozone performance goal (green), fall between the performance goal and criterion (yellow) or fail to achieve the performance criterion (red).

		2019		2020	
Selected Sites	**AQS Number**	**NMB (%)**	**NME (%)**	**NMB (%)**	**NME (%)**
LAX	06-037-5005	-11.8	13.3	30.3	30.3
Los Angeles Main	06-037-1103	2.2	10.2	-2.1	10.8
Azusa	06-037-0002	-10.8	11.5	-5.4	13.2
Glendora	06-037-0016	-12.0	12.4	-13.1	16.0
Pomona	06-037-1701	19.4	20.3	-6.4	11.7
Upland	06-071-1004	-6.0	12.8	-8.2	12.1
Fontana	06-071-2002	-7.0	10.3	-1.3	10.1
Crestline	06-071-0005	-12.3	15.5	-10.2	12.3
San Bernardino	06-071-9004	-12.7	16.6	-12.7	14.4
Redlands	06-071-4003	-15.7	19.0	-17.6	17.8

8.1.3 Dynamic Evaluation Results

Figure 8-2 is a spatial plot that compares gridded CMAQ RRFs with observed RRFs at the monitoring sites across the SoCAB. Over most of the SoCAB both the modeled and observed RRFs are consistent and estimate that ozone increases between 2019 BAU and 2020 COVID cases with the exception of the following:

- The furthest east monitors in the SoCAB (Banning Airport and Morongo) where both the modeled and observed RRFs estimate ozone is reduced;
- Crestline and Perris where the model estimates essentially no change in the RRFs (i.e., between -0.99 and 1.01) and the observed RRF indicates a slight reduction;
- Sites near the coast (i.e., West LA, LAX and Compton) where the model estimates ozone increases (RRF > 1.1), while the observed RRF have ozone decreases (RRF < 0.98); and
- At the Glendora monitor where the observed RRF indicates no change and the model estimates a 5-10 % ozone increase and at the Fontana monitor where observed RRF indicates a decrease of 2-5 % and the model estimates an increase of 2-5 %.

Across a vast majority of the monitoring sites, however, the modeled and observed RRFs agree that the ozone projection procedure estimates that ozone increases between the 2019 Base and 2020 COVID scenarios. The only locations where this is clearly not true are three sites in western Los Angeles County near the coast where observed RRFs are less than one and the modeled RRFs are greater than 1.15. At these three sites, CMAQ responds inversely to the changes in emissions between 2020 Base and 2020 COVID-19 compared to observations. Some potential reasons for this are discussed below. Besides these three sites, there is broad agreement between CMAQ and the observed responses to the 2020 COVID reductions as shown in the scatter plot in Figure 8-2 which compares the observed and modeled RRFs but excludes the RRFs for the three coastal sites discussed above. In fact, when the three coastal sites are excluded the average modeled and observed RRF across the other sites are identical estimating an average 7% increase in ozone between 2019 and 2020 (i.e., average RRF = 1.07). This suggests that CMAQ is broadly able to replicate the observed ozone increase between 2019 Base and 2020 COVID that includes the COVID-19 response emissions reductions within the framework of EPA's recommended ozone projection procedure used in a modeled attainment demonstration, although in general the model response is generally weaker than the observed response and responses at individual sites may vary. An obvious difference in modeled/observed RRFs is seen in the far right side of the scatter plot in Figure 8-2 that is Pomona where the observed ozone increase (RRF =1.32) is much greater than the modeled ozone increase (1.04).

A possible reason for the CMAQ and observed RRF disagreement at the three sites near the coast in western Los Angeles County is the inability of the model to reproduce the observed ozone at these sites. LAX was one of the selected sites for the operational model performance in Table 8-1 where CMAQ exhibited an extreme ozone overestimation in 2020 (+30%) and modest underestimation in 2019 (-12%). Reasons for the poor performance at LAX potentially include meteorology and/or Boundary Conditions (BCs). Specifically, the representation of the coastal marine layer in the WRF fields and the BCs from the WACCM global chemistry model. The marine layer is important throughout this region and in the western portion of the SoCAB can inhibit ozone formation by trapping fresh NO_X emissions within a shallow surface marine layer producing more VOC-sensitive ozone formation conditions. The WRF evaluation noted a warm bias at LAX that may indicate an underestimation of the marine layer encroachment inland. A meteorological analysis of the highest 10 ozone days (which varies by site) focused on an evaluation of the marine layer is recommended but beyond the current scope of work. Inspection of the LAX ozone MDA8 timeseries plots for 2020 in Section 7.2.3 and 2019 in Appendix A reveals that most of the top 10 highest modeled days at this site occurred in early June for both years and shows a very different model bias during these days which likely plays a role in the discrepancy at this site and similar mechanisms may impact the other two nearby sites. Note that these sites are of lesser importance in term of ozone attainment since they have much lower ozone concentrations compared to sites further east in Los Angeles county and in San Bernardino county. These western Los Angeles County sites are also more highly influenced by the WACCM BCs than more inland sites and are less affected by the emissions within the SoCAB, including the effects of the COVID-19 emission reductions.

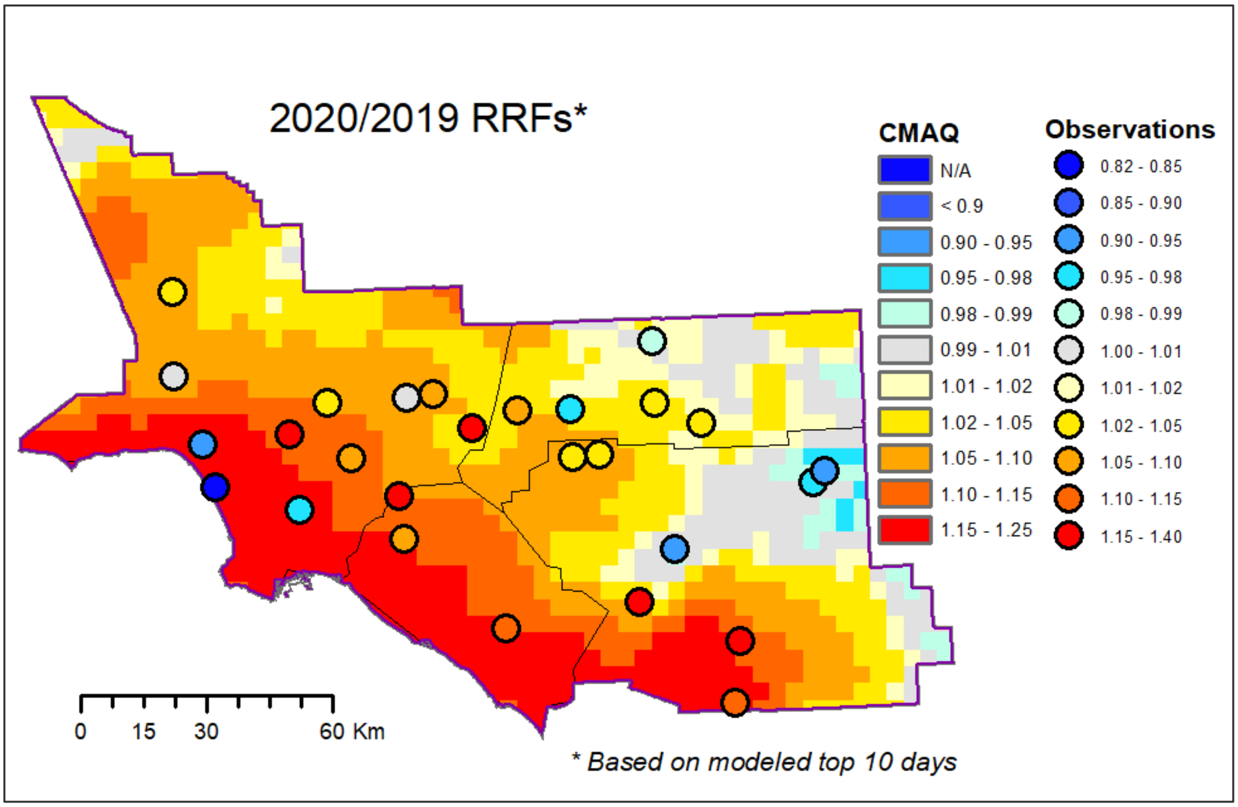

Figure 8-2. Comparison of CMAQ versus observed RRFs based on an average across the top 10 modeled MDA8 ozone days for the 2019 Base and 2020 COVID Cases.

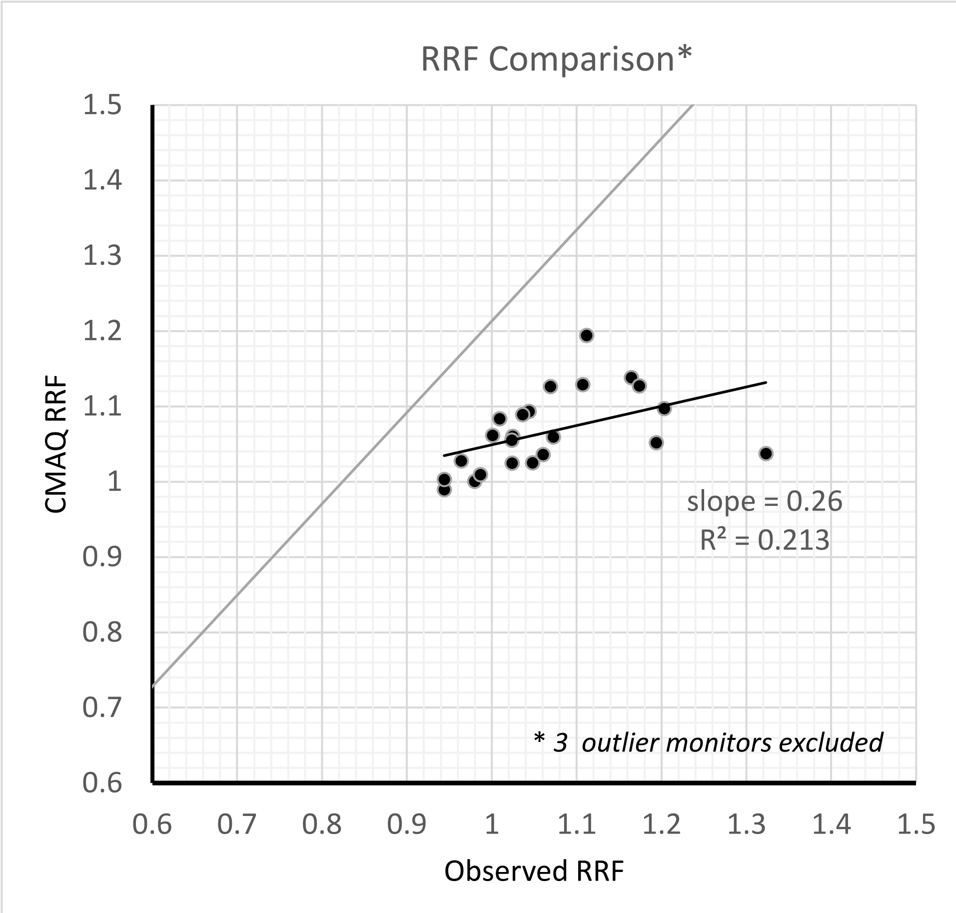

Figure 8-3. Scatter plot of observed and modeled RRFs based on the average of the top 10 modeled MDA8 ozone days in the 2019 Base and 2020 COVID Cases.

8.2 Emissions Reduction Versus Meteorological Impacts on Ozone

Note that the analysis in Figure 8-2 and 8-3 has year-specific meteorology for the two years in the RRF calculations. Although the modeling periods of June-July 2019 and 2020 were selected to try to obtain modeling episodes in two different years with as similar meteorological conditions as possible, there will be differences between the June-July 2019 and 2020 meteorology and the extent to which those meteorological differences affect the modeled and observed RRF signal confounds the analysis of the ozone formation signal between 2019 and 2020 in response to the emission changes.

We attempt to disentangle meteorological impacts of the modeled and observed ozone signal between 2019 and 2020 from COVID-19 emissions reduction impacts by comparing two different CMAQ derived RRFs. The first CMAQ derived RRF is the same as previous (i.e., 2020 COVID/2019 Base) that has 2019 and 2020-specific meteorology as well as COVID-19 emissions reductions in both the modeled and observed RRF ozone signal. The second CMAQ derived RRFs are 2020 COVID/2020 BAU which have emissions reduction only and the same meteorology for both cases but is only available for the modeled RRF ozone signal. Note that the 2020 BAU NO_X emissions are slightly lower than the 2019 base emissions (-4%), but those emissions reduction are much less than the 2020 COVID-19 reductions compared to the 2019 base (-17%). Therefore, a comparison of the modeled RRFs with: (1) emissions and meteorological changes, versus; (2) emissions changes only may provide insight into the magnitude of meteorological impacts on the ozone changes compared to COVID-19 emissions reduction impacts. Figure 8-4 compares the two modeled RRF fields over the SoCAB. RRF deviations from one (i.e., colors away from the grey bin) for the static meteorological case (i.e., 2020 meteorology in right figure) compared to the dynamic meteorological case (i.e., 2019 and 2020 meteorology changes in left figure) are much smaller which suggest that the COVID-19 emissions reductions play a much smaller role than meteorology. In addition, the spatial pattern is quite different between the two figures. The right panel in Figure 8-4 has a spatial pattern like the MDA8 difference in Section 8.2 (as expected) with regions of VOC-sensitive (yellow) and NO_X-sensitive (blue) ozone formation chemical regimes clearly delineated.

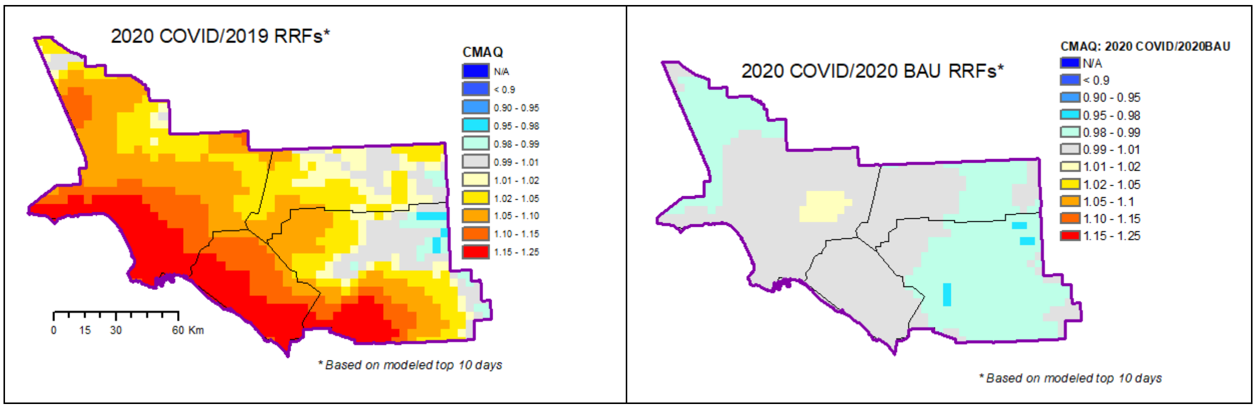

Figure 8-4. CMAQ RRFs for 2020 COVID/2019 Base (left) and 2020 COVID/2020 BAU (right).

8.3 Spatial Plots of Modeled MDA8 Ozone Model Results to COVID Emissions Reductions

This section presents CMAQ-predicted differences between the 2020 COVID and the 2020 BAU scenarios to assess what effects the COVID-19 emissions reductions had on modeled ozone concentrations.

The upper left panel of Figure 8-5 shows June 1 – July 31 period-average MDA8 ozone for the 2020 COVID scenario. The maximum MDA8 is 74.7 ppb in the southwest corner of San Bernardino county. Two-month average MDA8 ozone greater than 70 ppb also extends a little into eastern Los Angeles county to approximately Azusa. Average MDA8 along the coastline is approximately 40 ppb. The upper right panel is the period-average of the difference between the 2020 COVID and 2020 BAU scenarios. Grey represents differences within ±0.143 ppb, cool shades represent ozone decreases which occur over most of the 4-km domain with the largest decrease is -1.3 ppb that occurs near Fontana in western San Bernardino County. The southeast quadrant of Los Angeles county shows average MDA8 ozone increases of up to 0.8 ppb at Azusa, which indicates that this region is more VOC sensitive as the emission reductions are primarily NO_X related. These modest changes are consistent with the timeseries plots in the model performance analysis section. The ozone response to the NO_X reductions (i.e., approximately -13%) clearly delineates the average extent of the modeled VOC-sensitive versus NOx-sensitive chemical regimes within the SoCAB.

The middle left panel of Figure 8-5 presents the June 1 – July 31 period-maximum MDA8 ozone for the 2020 COVID scenario with a domain-wide maximum of 119 ppb that again occurs near Fontana. Note the different scale for this plot compared to the period-average ozone plot (Figure 8-4, top left). Modeled maximum MDA8 ozone concentrations of greater than 90 ppb are estimated across almost all of San Bernardino County and into western Los Angeles and Kern Counties a few southern excursions into Riverside County. However, along the coast the episode maximum MDA8 ozone is much lower in the 60-75 ppb. The lower left panel of Figure 8-5 presents the June 1 – July 31 period-minimum MDA8 ozone for the 2020 COVID scenario. The lowest period-minimum MDA8 is over the Pacific Ocean and is approximately 20 ppb, the lowest onshore values are along the coast and are approximately 30 ppb. Further inland, the spatial maximum of the period-wide minimum is 56 ppb. Note the different scale for this plot compared to the period-average and period-maximum plots.

The middle and bottom right panels in Figure 8-5 are the period-maximum and minimum of the differences in MDA8 ozone concentrations between the 2020 COVID and 2020 BAU scenarios, respectively. The maximum MDA8 ozone increase is 3.2 ppb in Los Angeles County between the downtown Los Angeles Main Street and Pasadena monitoring sites. Maximum increases of over 2 ppb occur over a sizable region in Los Angeles county and a small region of southwestern San Bernardino county. The colored area in Figure 8-5, middle right is the area where the largest NO_X disbenefits (i.e., VOC-sensitive areas where NO_X emissions reductions result in ozone increases) are estimated to occur. The areas of maximum ozone decrease due to the COVID caused emission reductions (Figure 8-1, bottom right) is much more widespread than the areas of maximum ozone increase. The maximum ozone decrease is 2.5 ppb and occurs near Fontana in western San Bernardino County.

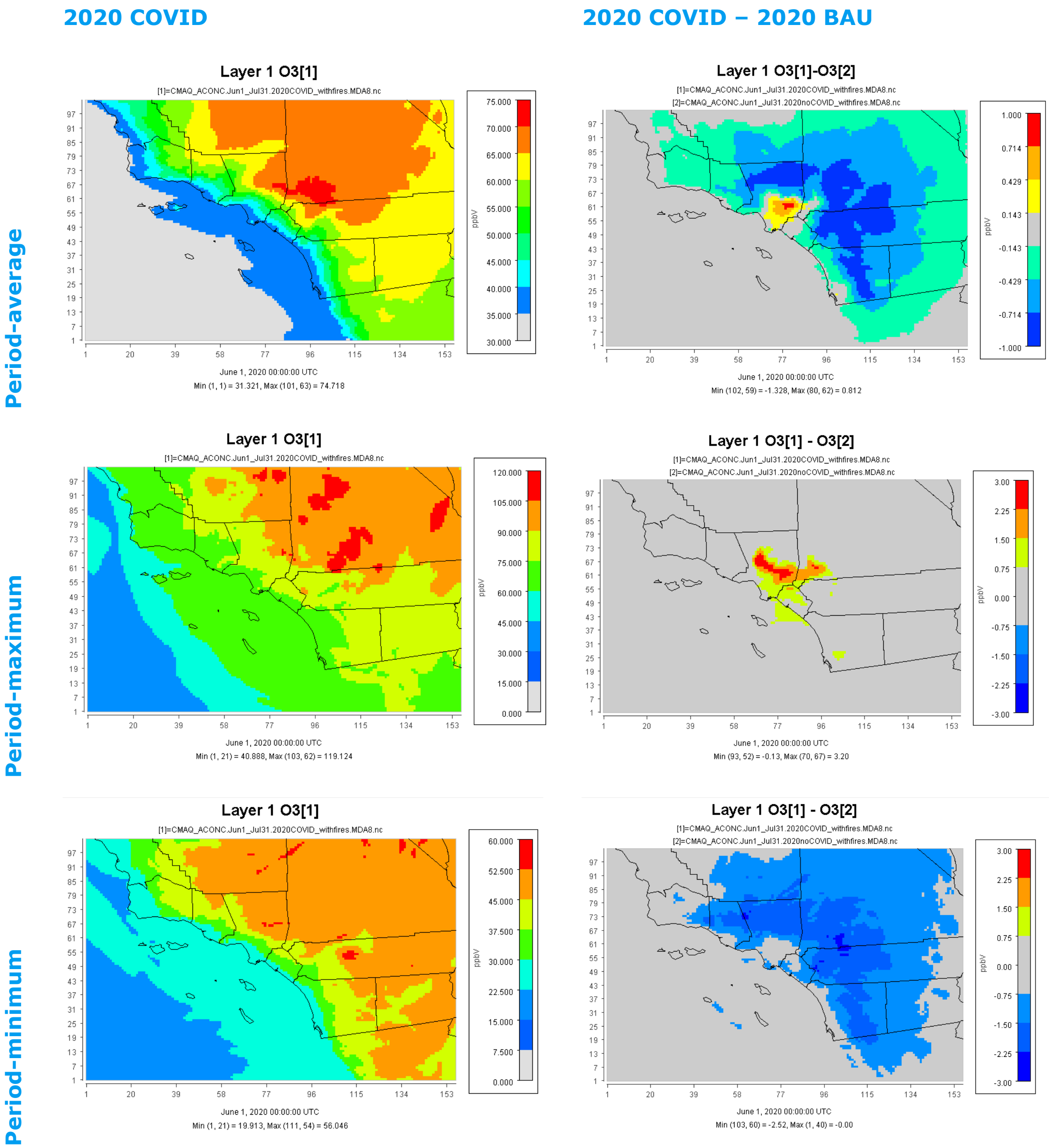

Figure 8-5. 2020 COVID case CMAQ estimated June 1 – July 31 period average, period maximum, and period minimum MDA8 ozone spatial maps (right panels). Right panels are 2020 COVID minus 2020 BAU differences.

Figure 8-6 provides a closer look at the ozone response to the COVID caused emission reductions throughout the SoCAB for the period average MDA8 ozone concentrations (2020 COVID minus 2020 BAU), as well as a map that identifies the ozone monitors throughout the basin. Figure 8-6 presents the CMAQ predicted period average MDA8 ozone difference and period maximum and minimum differences for the SoCAB monitors. Monitors that have higher ozone on average in the 2020 COVID case than the 2020 BAU case are highlighted in red, and those with lower ozone are highlighted in blue. The area of modeled episode average ozone increases due to the COVID NO_X emissions reductions stretches from just east of West Los Angeles in the west to Fontana in the east and from northern Orange County in the south to San Fernando Valley in the north (Figure 8-6, top). While the area of episode average ozone decreases due to the COVID inspired NO_X emissions reductions occur over a larger area that includes Santa Clarita Valley, San Bernardino County east of Fontana, most of Riverside County and southern Orange County. Although the area of ozone decreases is greater than the area of ozone increases, a vast majority of the population resides in the area of ozone increases. However, many of the monitoring sites with the highest MDA8 ozone concentrations reside in the western part of the SoCAB area of episode-average ozone decreases (e.g., Crestline, San Bernardino and Redlands). This results in a conundrum with the current SoCAB NO_X-focused emission reduction ozone attainment control plan that increases ozone concentrations in highly populated areas in the intervening years on path toward ozone attainment a decade or more in the future.

Looking at the maximum ozone increases due to the COVID caused emission reductions at the monitoring sites (Table 8-2, column 4), all monitors have higher ozone for at least one day in the June1 -July 31 period with an ozone increase indicating that the NO_X disbenefits are not just limited to the SoCAB central urban areas on all days. The maximum ozone increase at any monitor is at Glendora (2.77 ppb) with Azusa (2.72 ppb) a close second and Pomona third (2.08 ppb), all three sites are in western Los Angeles County that is an area where ozone formation is usually more VOC-sensitive so that the NO_X emission reductions result in modeled ozone increases most days of the modeling period. Surprisingly, the monitoring site with the fourth highest ozone increase is Crestline at Lake Gregory far downwind up in the San Bernardino Mountains that is a site where ozone formation is usually more NO_X-sensitive, at least for one day during the episode ozone formation at Crestline is more VOC-sensitive.

For the period minimum differences (Figure 8-2, column 5), all monitors have lower ozone for at least one day in the June1 -July 31 period. The largest ozone decreases with reductions of over -2 ppb occur at sites that tend to be the furthest downwind: Banning Airport (-2.3 ppb), Lake Elsinore (-2.2 ppb), Morongo (-2.2 ppb) and Crestline (-2.1 ppb). Even at monitoring sites within central Los Angeles County where ozone formation is more VOC-sensitive, there is at least one day during the June-July 2020 episode that ozone is reduced due to the NO_X controls. In some cases the ozone decrease is not significant (e.g., -0.05 ppb in downtown Los Angeles Main Street) or very small (e.g., -0.2 to -0.3 ppb at Pasadena and LAX). However, at the sites in western Los Angeles County that saw the largest ozone increases exceeding 2 ppb on any day due to the NO_X emissions reductions on another day see ozone decreases approaching -1 ppb (e.g., -0.6 ppb at Azusa, -0.8 ppb at Glendora and -1.1 ppb at Pomona).

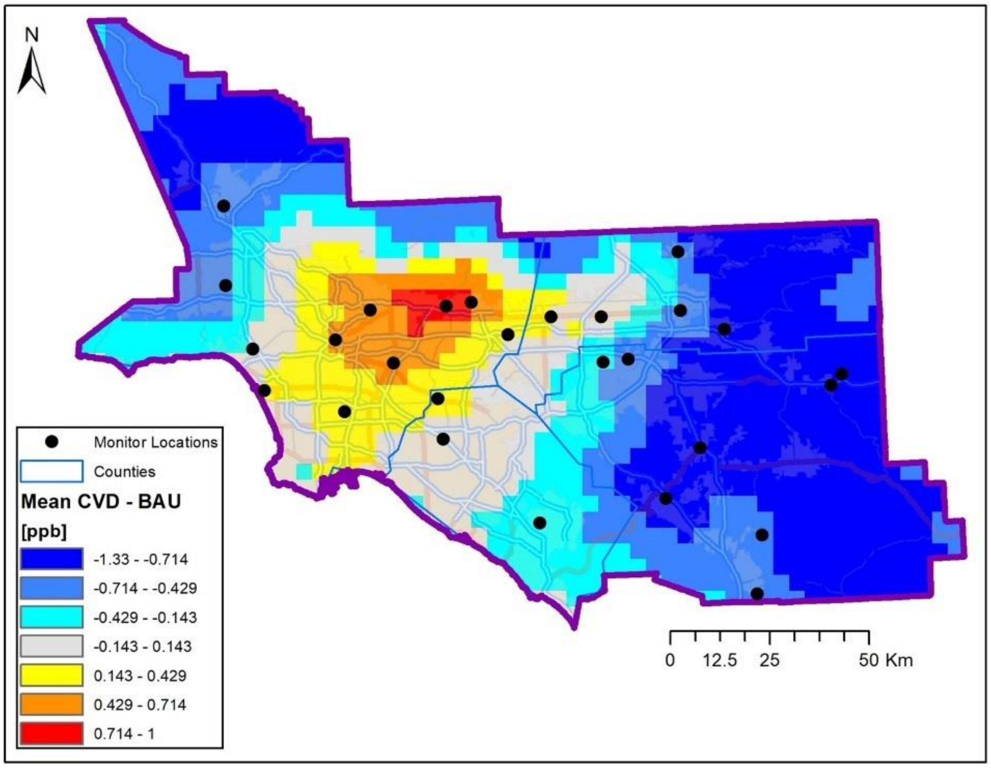

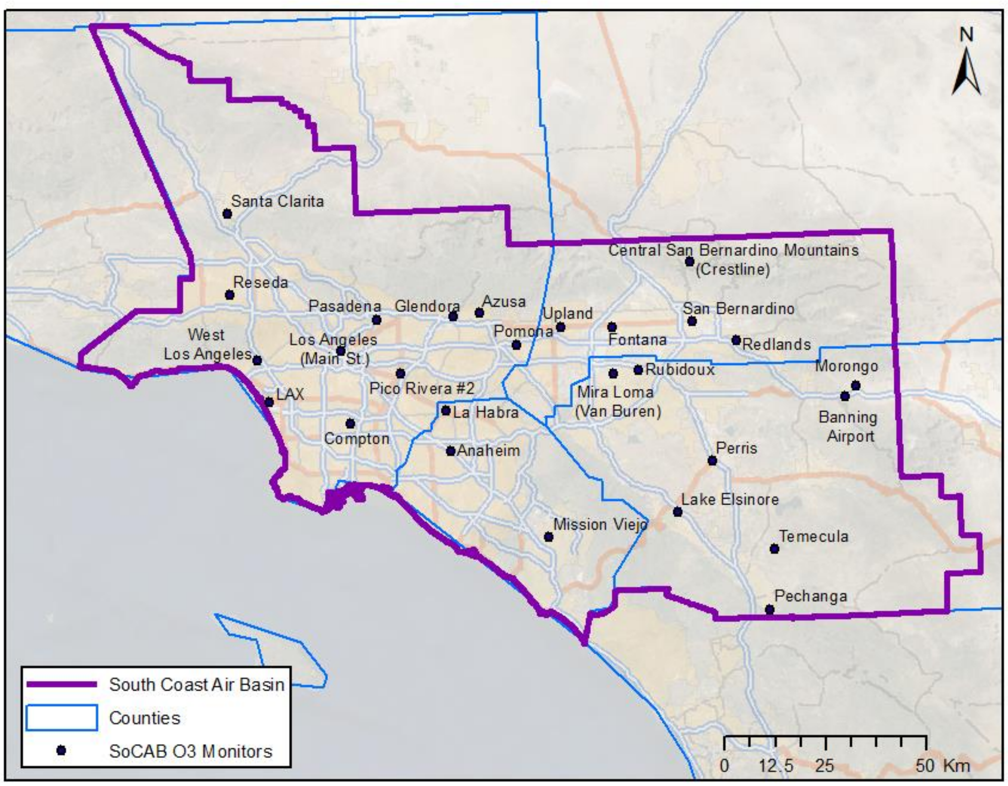

Figure 8-6. Period average 2020 COVID minus 2020 BAU MDA8 ozone concentrations (top) and monitor locations throughout the basin (bottom) focusing on the SoCAB.

Table 8-2. CMAQ impacts of the ozone response to COVID-19 emissions reductions at the SOCAB monitors (2020 COVID – 2020 BAU). Period mean, maximum and minimum impact.

AQS Number	Monitor Name	Period Average MDA8 Difference (ppb)	Period Maximum MDA8 Difference (ppb)	Period Minimum MDA8 Difference (ppb)
60370002	Azusa	0.80	2.72	-0.57
60370016	Glendora	0.77	2.77	-0.75
60370113	West Los Angeles	-0.04	0.46	-0.52
60371103	Los Angeles (Main St.)	0.46	1.17	-0.05
60371201	Reseda	-0.54	0.28	-1.45
60371302	Compton	0.27	0.98	-0.34
60371602	Pico Rivera #2	0.56	1.95	-0.31
60371701	Pomona	0.20	2.08	-1.06
60372005	Pasadena	0.55	1.98	-0.21
60375005	LAX Hastings	0.23	0.93	-0.28
60376012	Santa Clarita	-0.67	1.53	-1.70
60590007	Anaheim	0.03	1.03	-0.75
60592022	Mission Viejo	-0.26	0.74	-1.00
60595001	La Habra	0.29	1.15	-0.32
60650009	Pechanga	-0.59	0.10	-1.30
60650012	Banning Airport	-1.09	0.27	-2.30
60650016	Temecula	-0.69	0.07	-1.57
60651016	Morongo	-1.13	0.48	-2.19
60656001	Perris	-1.16	0.10	-1.98
60658001	Rubidoux	-0.50	0.72	-1.38
60658005	Mira Loma (Van Buren)	-0.42	0.90	-1.31
60659001	Lake Elsinore	-1.04	0.01	-2.21
60710005	Crestline	-0.65	2.01	-2.15
60711004	Upland	0.10	1.88	-1.29
60712002	Fontana	0.05	1.72	-1.18
60714003	Redlands	-0.76	0.75	-1.74
60719004	San Bernardino	-0.58	1.27	-1.69

8.4 Conclusions of Dynamic Evaluation

We conclude that throughout the SoCAB (but away from the three sites near the coast) CMAQ can replicate the observed ozone response to the COVID-19 emissions reductions and changes in meteorology between 2019 and 2020 within the framework of the ozone projections procedures used in a modeled ozone attainment demonstration. Frequently, the modeled ozone response is slightly weaker than the observed response with a lot of site-to-site variations. The modeled and observed ozone response between 2019 and 2020 actual conditions was mainly an increase in ozone throughout most of the SoCAB except in the eastern most regions of the modeling domain (e.g., Banning Airport) where small decreases were observed and modeled, and the discrepancy in modeled (ozone increase) of observed (ozone decrease) at the three sites near the coast (i.e., West Los Angeles, LAX and Compton). Analysis of modeled ozone changes using the ozone projection procedures using static meteorology (i.e., 2020) revealed much smaller ozone changes which suggests that differences in the 2019 and 2020 meteorology was a bigger driver for the increased ozone in 2020 than the chemistry due to the COVID caused emission reductions.

The modeling suggests that the emissions reductions caused by the response to the COVID-19 pandemic mitigation measures, (i.e., NO_X reductions), result in ozone increases on most days centered on downtown Los Angeles in south-central Los Angeles County. The spatial extent of the area of modeled ozone increases in response to the COVID caused NO_X emission reductions can extend into western San Bernardino County and varies day-to-day. The area of ozone increases due to the COVID caused NO_X emission reductions is smaller than the spatial extent of the area of ozone decreases that includes many of the monitors that historically had the highest ozone concentrations (e.g., Crestline, San Bernardino and Redlands). However, the area of ozone increases due to the NO_X controls frequently includes the locations of highest population density in the SoCAB emphasizing that an ozone attainment VOC/NO_X emissions control plan for the SoCAB should not just consider the peak downwind MDA8 ozone design value in an attainment year a decade or more in the future, but also the population exposed to ozone concentrations in excess of the health based ozone NAAQS in the intervening years before the ultimate ozone NAAQS attainment year.

9.0 ADDITIONAL 2020 AMBIENT DATA ANALYSIS

This section provides additional analysis of ambient data to better understand the causes of high ozone in 2020.

9.1 Frequency of Occurrence of Ozone Exceedance Days in 2020

The introductory Section 1.2 reported trends in SoCAB ozone and Figure 1-3 reported the number of days per year in the SoCAB that MDA8 ozone exceeded the 70 ppb ozone NAAQS. During 2020 there were 157 "bad air" days (i.e., days with at least one site with observed MDA8 ozone above the 70 ppb 2015 ozone NAAQS) in comparison to approximately 130 days on average for the prior five years. Therefore, the number of excess bad air days in 2020 was approximately 25-30 days (~20%) higher compared to recent years. To better understand this phenomenon, we first considered the seasonal timing of the excess bad air days. We obtained EPA AQS multiyear tile plots[29] for ozone AQI which are presented in Figure 9-1. These plots display the color coded AQI where green represents good, yellow is moderate, orange is unhealthy for sensitive groups and corresponds to days with ozone concentrations greater than the 70 ppb 8-hr ozone NAAQS. Orange, red, purple, and maroon colors all indicate bad air days. The upper panel is for the core-based statistical area (CBSA) based on Los-Angeles-Long Beach-Anaheim and the lower panel is for the Riverside-San Bernardino-Ontario CBSA, which extends beyond the SoCAB. Note that for all years (2015-2020), most days in June, July and August are color coded to indicate bad air days. In 2020, however, bad air days occurred with a much higher frequency in spring (e.g., May) and fall (e.g., September and October) compared to the other years. The expansion of the ozone season is one attribute believed to be influenced by climate change, although in this case year-to-year variations also probably played a role.

[29] https://www.epa.gov/outdoor-air-quality-data/air-data-multiyear-tile-plot

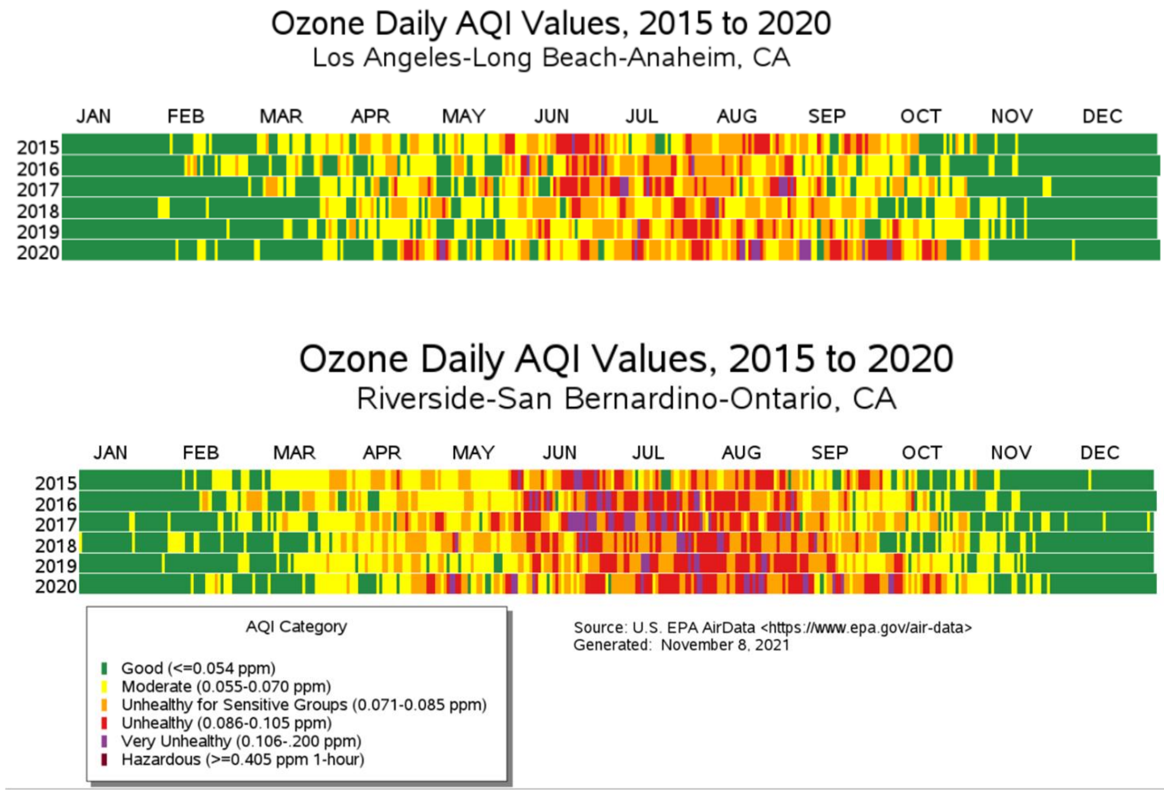

Figure 9-1. EPA AQS multiyear ozone AQI tile plot by day for 2015 – 2020. Upper panel is for the Los-Angeles-Long Beach-Anaheim CBSA and lower panel is for Riverside-San Bernardino-Ontario CBSA.

In Figure 9-2 we investigate the monthly distribution of days with ozone AQI indicative of 8-hr ozone NAAQS exceedance days (i.e., greater than 70 ppb) for the same two CBSA regions and period. These plots show that the number of exceedance days in 2020 was anomalously high for May, September, and October. June had fewer exceedance days than in most other years (although a similar number as 2019) and July and August had a typical number of exceedance days which is most days during those two months. Chapter 2.0 detailed the modeling episode selection process which was designed to: (1) be a period with non-trivial COVID-19 emissions reductions; (2) facilitate a reasonable comparison between 2019 and 2020; and (3) avoid substantial confounding factors (e.g., the atypically large wildfire season after July in 2020), therefore the modeling was performed for June and July 2019 and 2020. This ambient data analysis shows that the anomalously high number of excess bad air days that occurred in 2020 were primarily during the months outside our period of focus.

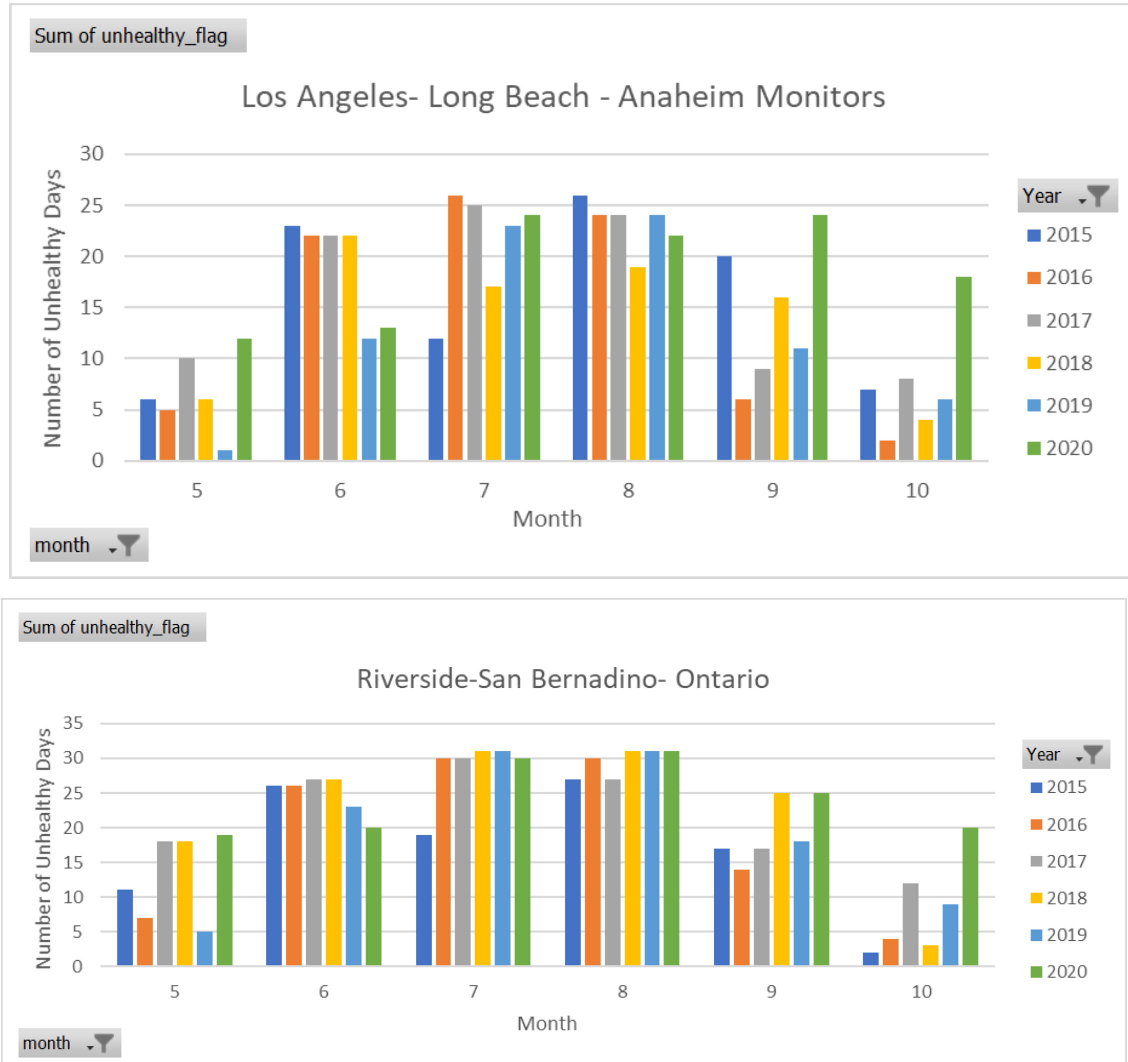

Figure 9-2. Monthly distribution of bad air days for 2015 to 2020. . Upper panel is for the Los-Angeles-Long Beach-Anaheim CBSA and lower panel is for Riverside-San Bernardino-Ontario CBSA.

9.2 2020 Ozone Formation Potential Conditions

A detailed analysis of factors that contributed to high ozone in May, September and October is beyond the scope of this study, however we examined the T850 mb temperatures by year and month which is presented in Figure 9-3 and note that the T850 mb is highest in 2020 compare to the prior 5 years for May, August, September and October which indicates that those four months were more meteorologically conducive to ozone formation than the prior 5 years, which explains the expansion of the high ozone season period compared to previous years.

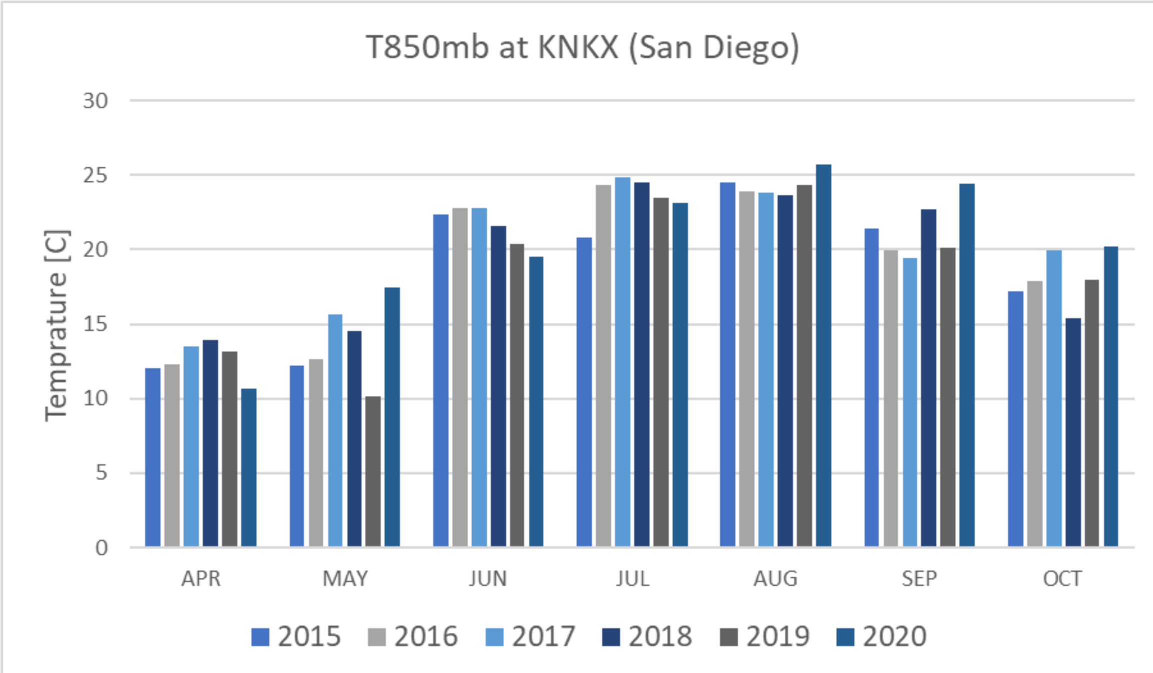

Figure 9-3. Monthly 850 millibar temperature (T850) by year at Miramar Air Force Base (KNKX) near San Diego.

The previous section investigated the high frequency of bad air days in the SoCAB basin in 2020. Another metric that describes the severity of ozone was shown in Figure 1-2 which displays the ozone DV and 4th highest maximum daily average 8-hour (4HMDA8) ozone concentration trends over the last two decades. In 2020, the highest of the 4th highest MDA8 across the basin was 125 ppb which was the highest since 2006 and occurred at the Redlands monitor. Table 9-1 reports the 4 highest MDA8 ozone values for Redlands and Figure 9-4 displays the time series of Redland MDA8 from March through October 2020. The 4 highest MDA8 ozone values all occurred between mid-August and early September. Figure 9-3 shows that September and October in 2020 were more conducive to ozone formation than those months in the prior 5 years, which may be a cause for the high ozone in 2020. Another possible reason is emissions from massive wildfires, in particular the Lake Fire in Los Angeles county[30]. Based on the timing of the high ozone and the fires, emissions from fires also likely played a role in some of the high observed ozone concentrations in August-October 2020.

Table 9-1. Redlands 4 highest MDA8 ozone concentrations in 2020 and date of occurrence.

Rank	MDA8 Ozone (ppb)	Date
1	136	8/14/202
2	134	9/4/2020
3	133	8/20/2020
4	125	8/17/2020

[30] https://en.wikipedia.org/wiki/Lake_Fire_(2020)

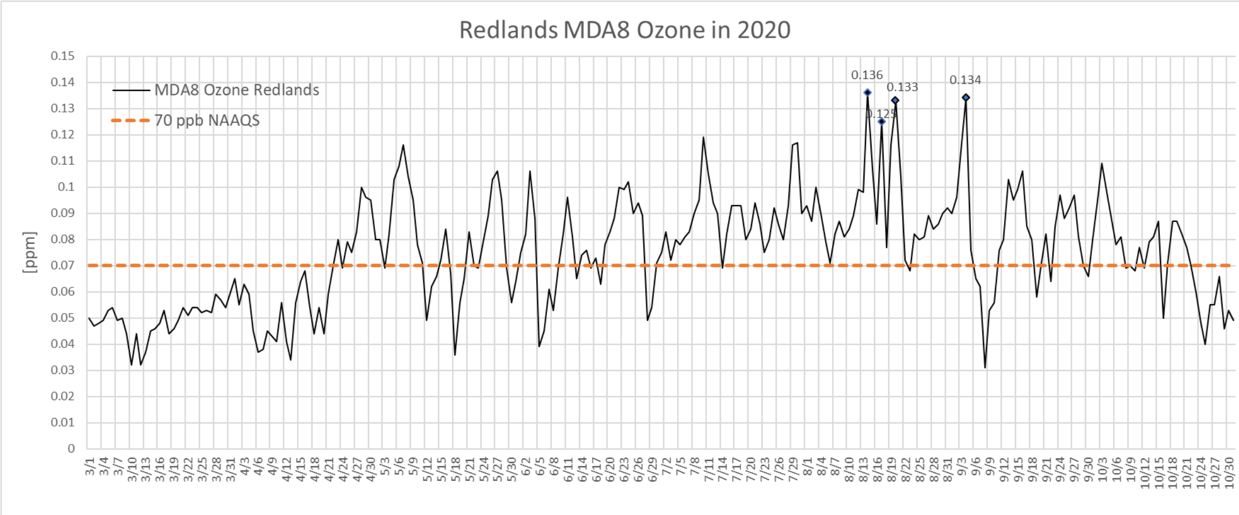

Figure 9-4. Redlands 2020 MDA8 ozone timeseries plot.

10.0 SUMMARY, CONCLUSIONS AND RECOMMENDATIONS

This Project developed a 2020 COVID-19 emissions inventory (EI) based on a recent California Air Resources Board (ARB) 2020 business as usual (BAU) EI that did not account for the effects the response to the COVID-19 pandemic had on emissions in 2020. The 2020 BAU inventory was adjusted for COVID-19 emission reductions using bottom-up, sector-by-sector, scaling approach based on differences in sector-specific activity data between 2019 and 2020. A 2019 EI was also developed by backcasting the California ARB 2020 BAU EI to 2019. The June-July modeling period in 2019 and 2020 was selected as those months exhibited fairly similar meteorological conditions between the two years. WRF meteorological modeling was performed to generate 2019 and 2020 meteorological inputs for the Community Multiscale Air Quality (CMAQ) photochemical grid model for the end of May through July period. Day-specific hourly gridded biogenic emissions were generated for the same periods using the MEGAN3.1 biogenic emissions model and the WRF output. 2019 and 2020 fire emissions inputs were also generated using the Fire Inventory from NCAR (FINN).

Three CMAQ simulations were performed for the 2019 Base, 2020 BAU and 2020 COVID emission scenarios using a 4-km grid resolution domain that covered the South Coast Air Basin (SoCAB). Boundary conditions (BCs) for the 4-km SoCAB domain were based on a CMAQ simulation of a 12-km grid resolution California domain. An operational model performance evaluation was completed for the 2019 BAU and 2020 COVID actual emission scenarios with ozone model performance compared against routinely used performance thresholds. Ozone model performance was generally within typical thresholds based on historical PGM applications. The upper range of MDA8 ozone (i.e., MDA8 greater than 80 ppb) had a negative bias as is typical in these applications with the ozone underestimation bias was larger in July than June for both years.

The CMAQ modeling of the June-July modeling period for the 2019 BAU and 2020 COVID cases was used to evaluate the procedures used to make future year ozone projections in the SoCAB air quality management plans (AQMPs). These ozone projection procedures are used to define the level of NO_X and VOC emission reductions needed to attain the ozone National Ambient Air Quality Standard (NAAQS) in a future year. The changes in the modeled and observed ozone concentrations between the 2019 and 2020 years are compared to evaluate whether the modeled ozone projection procedure responds in the same fashion as the observed ozone in response to the changes in emissions between 2019 and 2020 caused by the shelter-in-place orders due to the COVID-19 pandemic. The evaluation of whether model ozone estimates respond to changes in emissions as observed is termed a Dynamic Evaluation. We estimated that NO_X emissions would be reduced by approximately 13% due to the response to the COVID-19 pandemic. With a few exceptions, most notably three sites near the coast, both the observed and modeled change in ozone between 2019 and 2020 agreed fairly well with each other with both indicating that ozone would increase between 2019 and 2020 across most of the SoCAB. Although both modeled and observed ozone decreases were seen at the furthest downwind distances in the 4-km domain (e.g., Banning Airport). At the three sites near the coast, the model estimated ozone increases but the observed ozone was decreased between 2019 and 2020. Without these three sites, there was an average ozone increase of 7 % (i.e., RRFs = 1.07) for both the modeled and observed ozone changes between 2019 and 2020.

In order to disentangle how much of the observed and modeled increase in ozone between June-July 2019 and June-July 2020 modeling periods was due to the COVID caused NO_X emission reductions versus differences in meteorology the CMAQ modeling results for the 2020 BAU and 2020 COVID were analyzed. The primary cause of the ozone increases between 2019 and 2020 were found to be due to the changes in meteorology. Although the NO_X emission reductions due to the pandemic do cause increases in ozone in Los Angeles County that can extend into western San Bernardino County.

The key conclusions of the study are as follows:

- The observed ozone changes between 2019 and 2020 are consistent with the modeled ozone changes using procedures that are used to make future year ozone projections that lends confidence in our future year ozone projections.

- Although meteorology played a major role in the increases in ozone between 2019 and 2020, the reduction in NO_X emissions due to the response of the COVID pandemic also caused ozone increases in Los Angeles County and into western San Bernardino County, with ozone decreases further east.

- Ozone formation in parts of the SoCAB is still VOC-sensitive and the locations where NO_X reductions cause ozone increases occur in areas with some of the highest population density in the SoCAB.

- The evaluation of VOC/NO_X emission control strategies to attain the ozone NAAQS needs to examine ozone levels in the intervening years between current and the attainment year to better understand whether ozone may be getting worse or cause more population exposure to high ozone concentrations rather than focusing on just ozone levels in the attainment year.

Study limitations include: (1) a relatively small COVID-19 emissions reduction (i.e., approximately 13% decrease in total NO_X for 2020 COVID compared to 2020 BAU); (2) limited spatial and temporal resolution in the COVID-19 adjustments (i.e., no day-of-the-week effect for on-road adjustments); and (3) uncertainties in emissions, in particular for VOCs and biogenic emissions.

Recommendations for further study include:

1. Additional model performance including ozone precursor species
   a. A NO_X model performance analysis that avoids the pitfalls detailed by R. Dickerson, et.al., (2019) and considers the accuracy of commercial NOx monitors. A rigorous NOx evaluation would be helpful to assess the accuracy of the emissions inventories, which would be highly beneficial for this study
   b. A VOC evaluation based on any available observational data.
2. More rigorous WRF meteorological performance evaluation including an assessment of the simulation of the marine layer. This may provide insight into the poor performing coastal sites.
3. Evaluation and analysis of 2019 and 2020 WACCM global model simulations used as BCs for the CMAQ modeling.
4. Additional effort to improve the modeling platform based on meteorological and ozone precursor performance analysis or other insight.
   a. Conduct diagnostic tests designed to improve ozone model performance.
5. Day-of-the-week adjustments to the on-road sector to allow day of the week analysis that provides insight into the current extent of VOC-limited versus NOx-limited chemical regimes throughout the basin.

11.0 REFERENCES

Dickerson, R.R., D.C Anderson and X. Ren. 2019. On the use of data from commercial NOx analyzers for air pollution studies. *Atmos. Environ*., **215,** https://doi.org/10.1016/j.atmosenv.2019.116873

Emery, C.A., E. Tai, and G. Yarwood. 2001. Enhanced Meteorological Modeling and Performance Evaluation for Two Texas Ozone Episodes. Prepared for the Texas Natural Resource Conservation Commission (now TCEQ), by ENVIRON International Corp, Novato, CA. Available at: http://www.tceq.texas.gov/assets/public/implementation/air/am/contracts/reports/mm/EnhancedMetModelingAndPerformanceEvaluation.pdf

Emery, C.A., Z. Liu, A.G. Russell, M.T. Odman, G. Yarwood and N. Kumar. 2016. Recommendations on statistics and benchmarks to assess photochemical model performance. J. of the Air and Waste Management Assoc., Vol. 67, Issue 5. DOI: 10.1080/10962247.2016.1265027. https://www.tandfonline.com/doi/full/10.1080/10962247.2016.1265027

EPA. 2018. Modeling Guidance for Demonstrating Air Quality Goals for Ozone, PM2.5, and Regional Haze. U.S. Environmental Protection Agency, Office of Air Quality Planning and Standards, Air Quality Assessment Division. Research Triangle Park, NC. EPA 454/R-18-009. November 29. https://www3.epa.gov/ttn/scram/guidance/guide/O3-PM-RH-Modeling_Guidance-2018.pdf

Fujita, E., D. Campbell , W. Stockwell and D. Lawson. 2013. Past and future ozone trends in California's South Coast Air Basin: Reconciliation of ambient measurements with past and projected emission inventories, Journal of the Air & Waste Management Association, 63:1, 54-69, DOI: 10.1080/10962247.2012.735211

Kemball-Cook, S., Y. Jia, C. Emery, and R. Morris. 2005. Alaska MM5 Modeling for the 2002 Annual Period to Support Visibility Modeling. Prepared for the Western Regional Air Partnership, by ENVIRON International Corp., Novato, CA.

McNally, D. E. 2009. 12 km MM5 Performance Goals. Presentation to the Ad-Hoc Meteorology Group. June 25, 2009. http://www.epa.gov/scram001/adhoc/mcnally2009.pdf

Park, S., J.B. Klemp, and J. Kim. 2019: Hybrid Mass Coordinate in WRF-ARW and Its Impact on Upper-Level Turbulence Forecasting. Mon. Wea. Rev., 147, 971–985. https://doi.org/10.1175/MWR-D-18-0334.1

Ramboll. 2013. METSTAT Meteorological Model Statistical Evaluation Package. Ramboll, Novato, California. December 9. https://www.camx.com/download/support-software/

Tong D.Q., L. Lamsal, L. Pan, C. Ding, H. Kim, P. Lee, T. Chai, K.E. Pickering, I. Stajne. 2015. Long-term NOx trends over large cities in the United States during the 2008 Recession: intercomparison of satellite retrievals, ground observations, and emission inventories. Atmos. Environ., 107 (2015), pp. 70-84, 10.1016/j.atmosenv.2015.01.035

Toro, C., K. Foley, H. Simon, B. Henderson, K. Baker, A. Eyth, B. Timin, W. Appel, D. Luecken, M. Beardsley, D. Sonntag, N. Possiel and S. Roberts. 2021. Evaluation of 15 years of modeled atmospheric oxidized nitrogen compounds across the contiguous United States. *Elementa: Science of the Anthropocene.* January, 9 (1): 00158. doi: https://doi.org/10.1525/elementa.2020.00158

Wiedinmyer, C., T. Sakulyanontvittaya and A. Guenther. 2007. MEGAN FORTRAN code V2.04 User Guide. NCAR, Boulder, CO. October 29. http://acd.ucar.edu/~guenther/MEGAN/MEGANguideFORTRAN204.pdf

APPENDIX A.
ADDITIONAL EMISSIONS PLOTS

Appendix A. Additional Emissions Plots

This Appendix presents additional emissions plots for informational purposes.

air	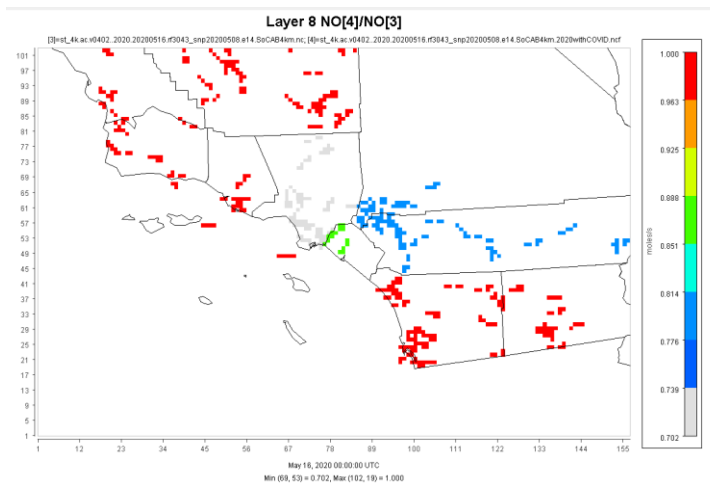
Area	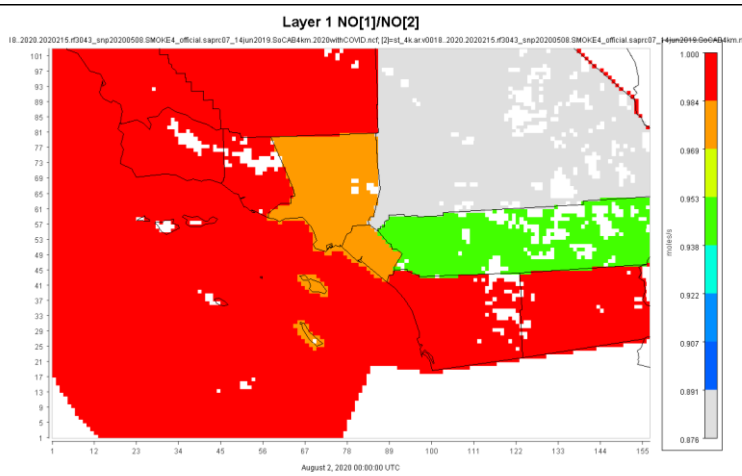
Consumer_Products	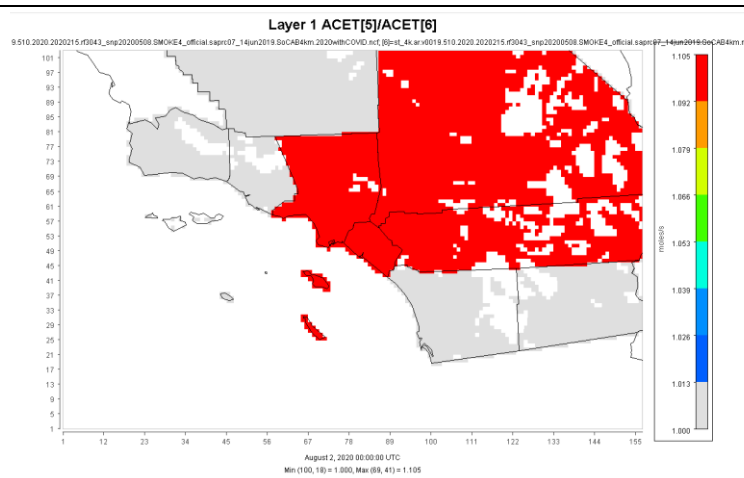

Onroad	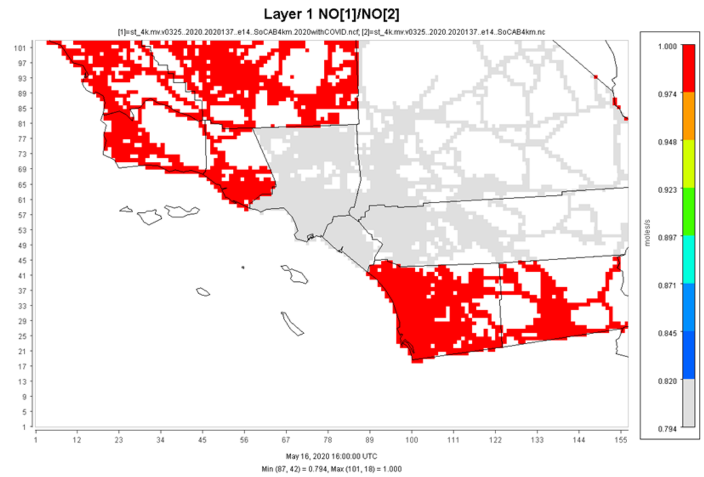
Fertilizer	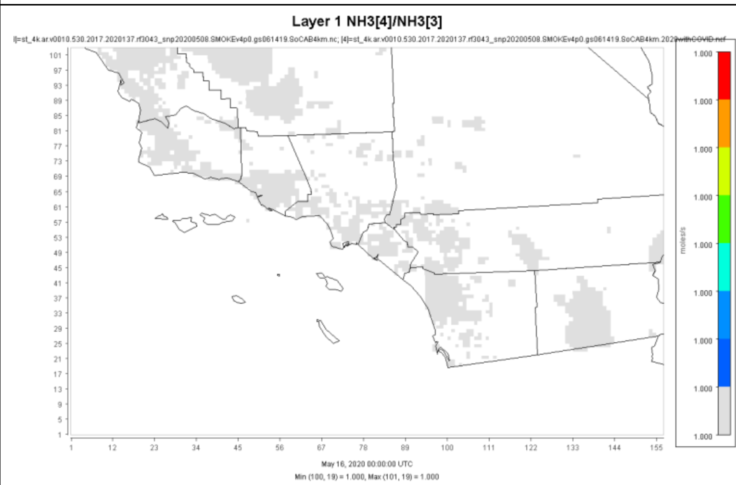
Livestock	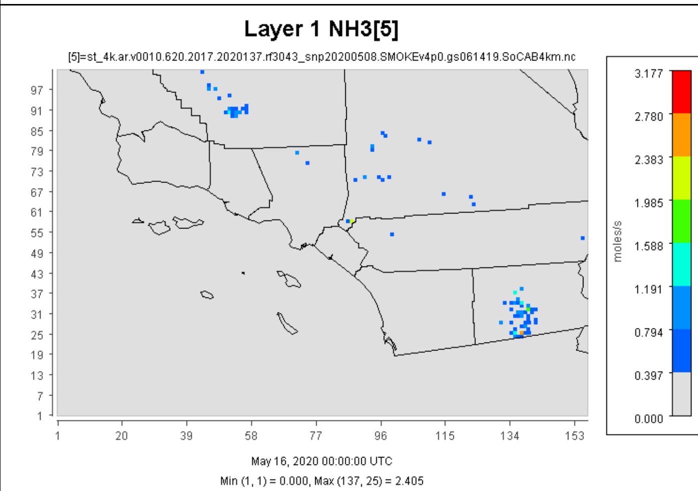

Lvst_a2p (No COVID adjustment)	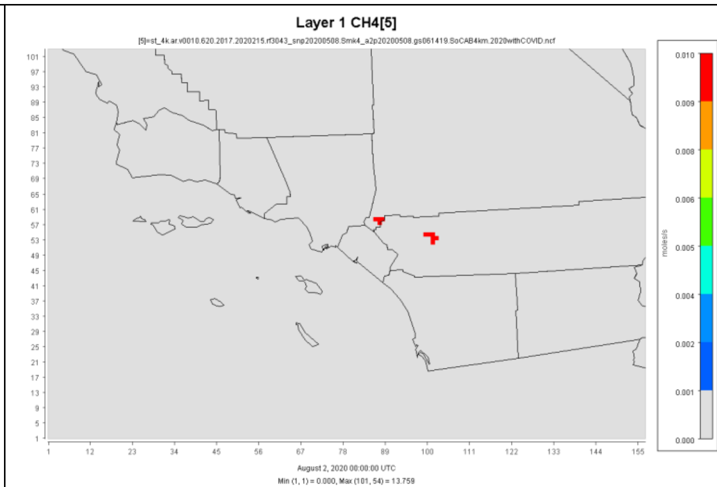
Ogv_area	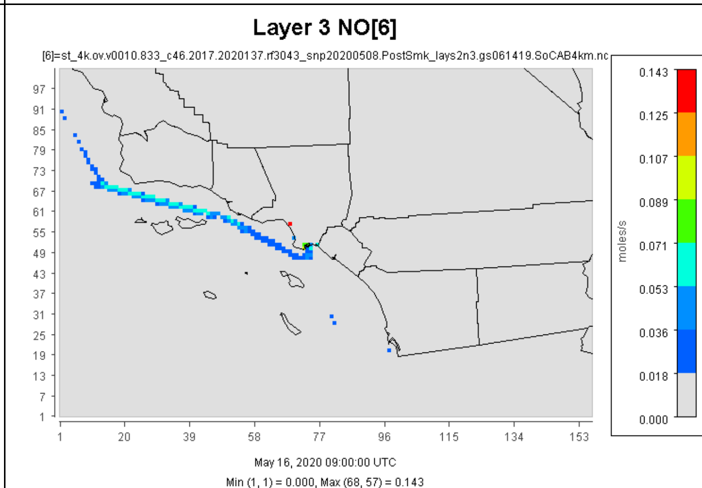
Biogenic - ISOP	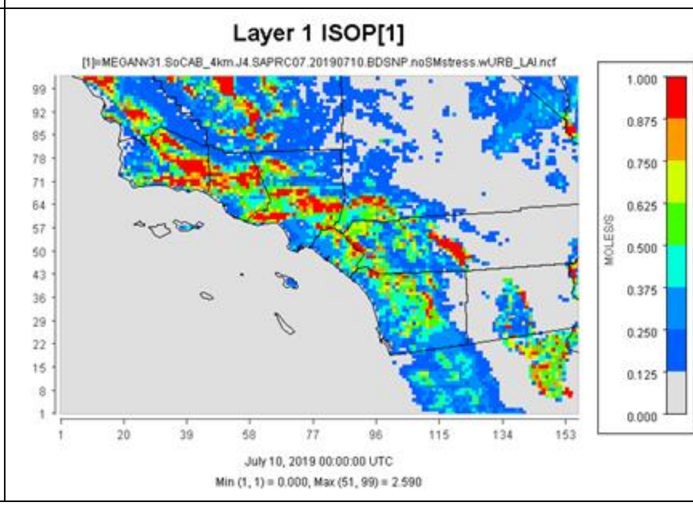

Biogenic -NOx	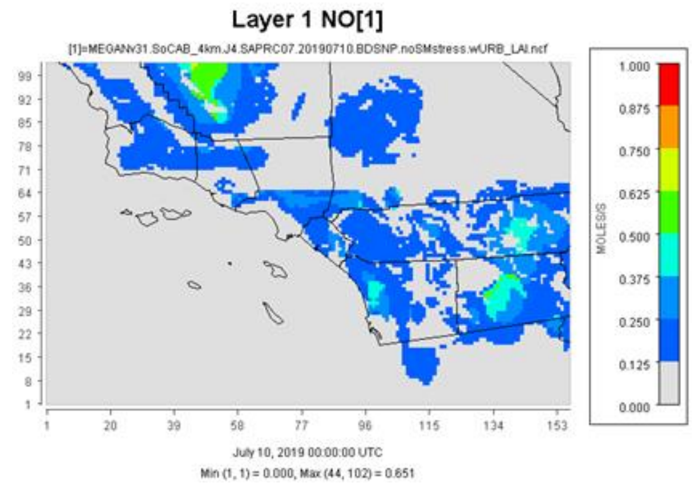
Inln_point	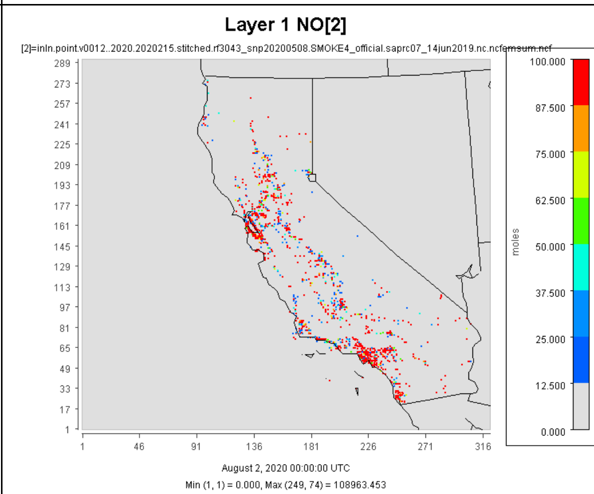
Inln_ogv	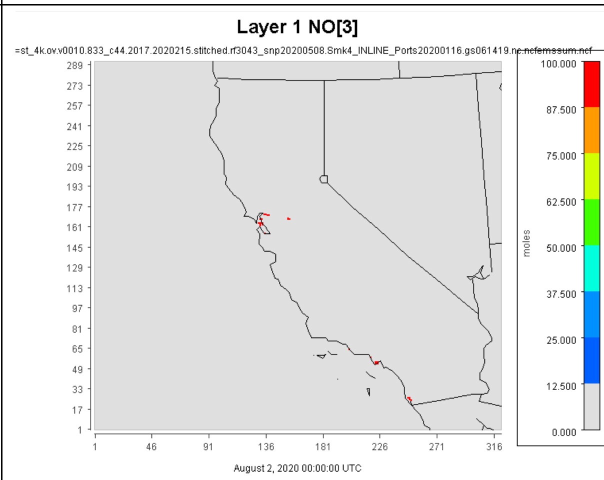

Figure A - 1. Spatial plots of model-ready emissions for various sectors and model species,

<table>
<tr><th>FINN Fires Monthly</th><th>June</th><th>July</th></tr>
<tr><td>2019</td><td>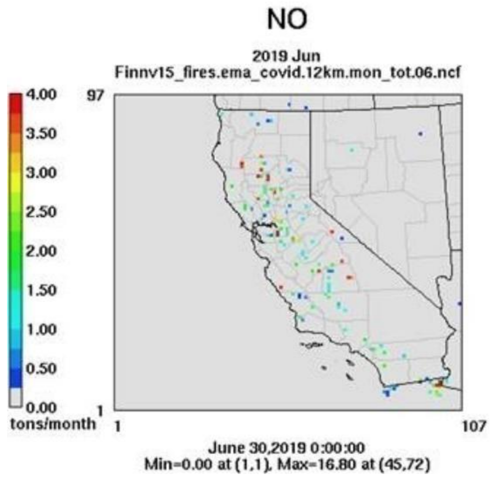
</td><td>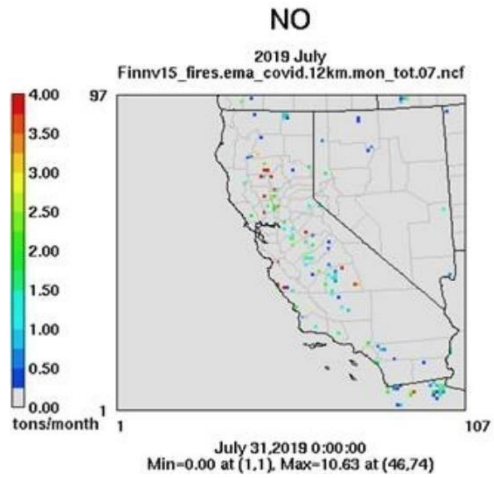
</td></tr>
<tr><td>2020</td><td>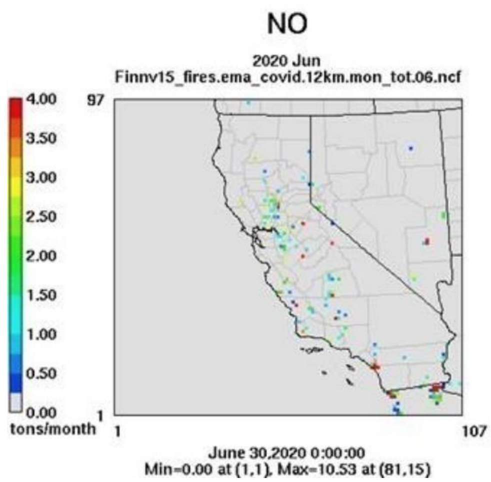
</td><td>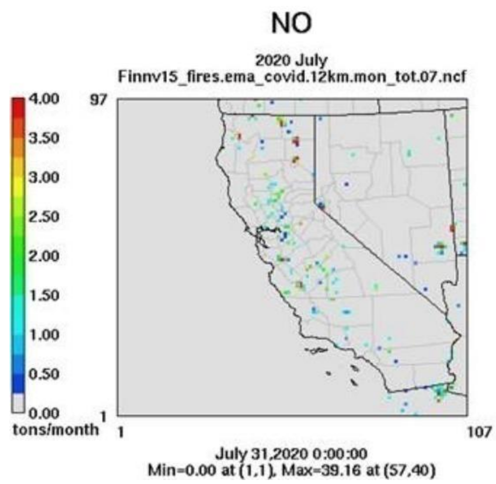
</td></tr>
</table>

Figure A - 2. Spatial summary plots of FINN fire emissions, by month and by year.

APPENDIX B

SCAQMD MONITORING NETWORK

Appendix B. SCAQMD Monitoring Network

This Appendix presents relevant excerpts from the SCAQMD's 2016 AQMP[31] monitoring network sections for informational purposes.

Air Quality Monitoring Network Plan – July 1, 2021

TABLE 1. List of Monitoring Sites

	Location	AQS No.	Criteria Pollutants Monitored	Start Date
1	Anaheim	060590007	CO, NO2, O3, PM10, PM2.5	08/01
2	Anaheim Route 5 Near Road	060590008	CO, NO2	01/14
3	ATSF (Exide)	060371406	Pb	01/99
4	Azusa	060370002	CO, NO2, O3, PM10, PM2.5	01/57
5	Banning Airport	060650012	NO2, O3, PM10, PM2.5	04/97
6	Big Bear	060718001	PM2.5	02/99
7	Central San Bernardino Mountains	060710005	O3, PM10, PM2.5	10/73
8	Closet World (Quemetco)	060371404	Pb	10/08
9	Compton	060371302	CO, NO2, O3, Pb, PM2.5	01/04
10	Fontana	060712002	CO, NO2, SO2, O3, PM10, PM2.5	08/81
11	Glendora	060370016	CO, NO2, O3, PM10, PM2.5	08/80
12	Indio	060652002	O3, PM10, PM2.5	01/83
13	La Habra	060595001	CO, NO2, O3	08/60
14	Lake Elsinore	060659001	CO, NO2, O3, PM10, PM2.5	06/87
15	LAX Hastings	060375005	CO, NO2, O3, PM10, Pb	04/04
16	Long Beach (North)	060374002	PM2.5	10/62
17	Long Beach Route 710 Near Road	060374008	NO2, PM2.5	01/15
18	Long Beach (South)	060374004	PM10, Pb, PM2.5	06/03
19	Los Angeles (Main St.)	060371103	CO, NO2, SO2, O3, PM10, Pb, PM2.5	09/79
20	Mecca (Saul Martinez)	060652005	PM10	01/11
21	Mira Loma (Van Buren)	060658005	CO, NO2, O3, PM10, PM2.5	11/05
22	Mission Viejo	060592022	CO, O3, PM10, PM2.5	06/99
23	Norco	060650003	PM10	12/80
24	North Hollywood	060374010	NO2, O3, PM2.5	01/2020
25	Ontario Etiwanda Near Road	060710026	CO, NO2	06/14
26	Ontario Route 60 Near Road	060710027	NO2, PM2.5	01/15
27	Palm Springs	060655001	CO, NO2, O3, PM10, PM2.5	04/71
28	Pasadena	060372005	CO, NO2, O3, PM2.5	04/82
29	Perris	060656001	O3, PM10	05/73
30	Pico Rivera #2	060371602	CO, NO2, O3, PM10, Pb, PM2.5	09/05
31	Pomona	060371701	CO, NO2, O3	06/65
32	Redlands	060714003	O3, PM10	09/86
33	Rehrig (Exide)	060371405	Pb	11/07
34	Reseda	060371201	CO, NO2, O3, PM2.5	03/65
35	Rubidoux	060658001	CO, NO2, SO2, O3, PM10, Pb, PM2.5	09/72
36	San Bernardino	060719004	CO, NO2, O3, PM10, Pb, PM2.5	05/86
37	Santa Clarita	060376012	CO, NO2, O3, PM10, PM2.5	05/01
38	Signal Hill	060374009	NO2, O3,	01/2020
39	Temecula	060650016	O3, PM2.5	06/10
40	Uddeholm (Trojan Battery)	060371403	Pb	11/92
41	Upland	060711004	CO, NO2, O3, PM10, PM2.5	03/73
42	West Los Angeles	060370113	CO, NO2, O3	05/84

[31] http://www.aqmd.gov/home/air-quality/clean-air-plans/air-quality-mgt-plan/final-2016-aqmp


Ozone (O3) Monitoring Stations
LEGEND
O3 Monitoring Station
South Coast Air Basin (Basin)
County Lines
0
20 Miles
Santa Clarita
Reseda
North Hollywood
Pasadena
Azusa
Glendora
Los Angeles
West Los Angeles
Pomona
Pico Rivera
Lax Hastings
Compton
La Habra
Signal Hill
Anaheim
Central San Bernardino Mountains
Upland
Fontana
San Bernardino
Redlands
Mira Loma
Rubidoux
Banning
Palm Springs
Perris
Indio
Lake Elsinore
Mission Viejo
Temecula
Last Updated: April 24, 2020

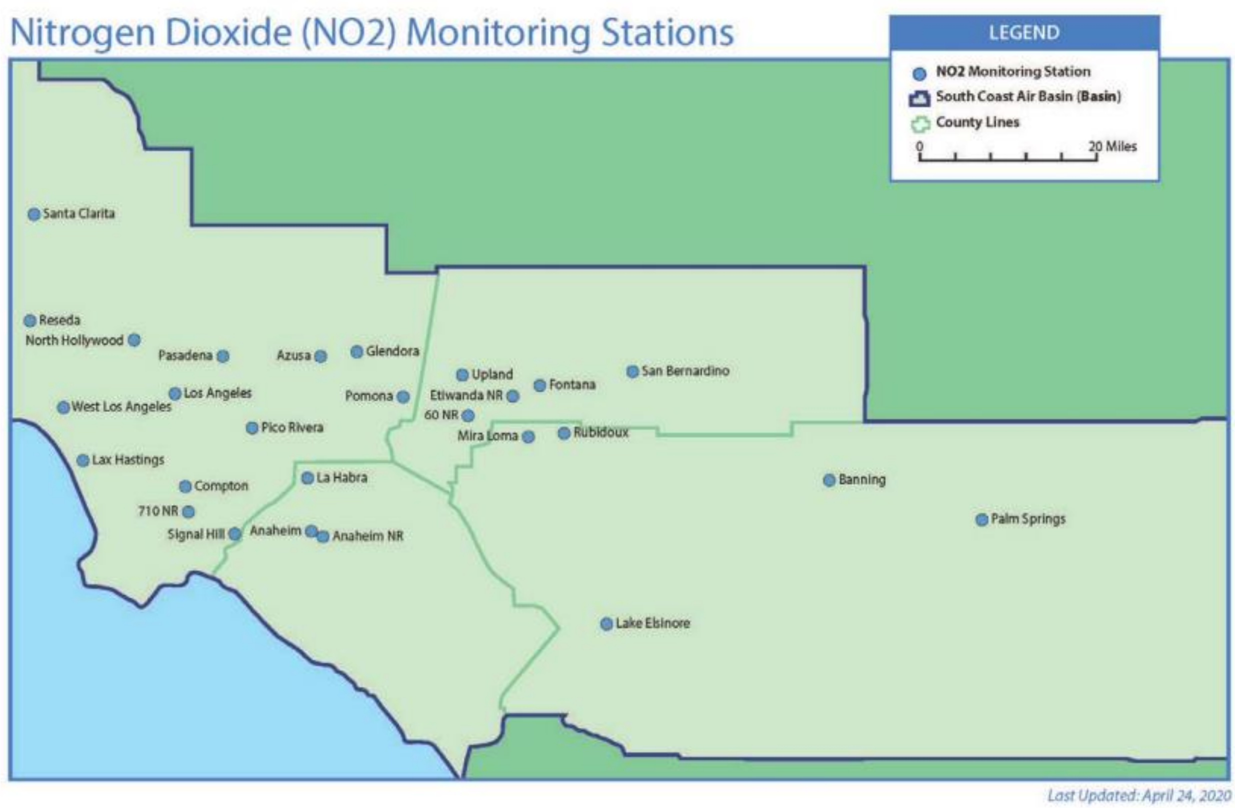
Nitrogen Dioxide (NO2) Monitoring Stations
LEGEND
NO2 Monitoring Station
South Coast Air Basin (Basin)
County Lines
0
20 Miles
Santa Clarita
Reseda
North Hollywood
Pasadena
Azusa
Glendora
Los Angeles
West Los Angeles
Pomona
Etiwanda NR
60 NR
Upland
Fontana
San Bernardino
Pico Rivera
Mira Loma
Rubidoux
Lax Hastings
Compton
La Habra
710 NR
Signal Hill
Anaheim
Anaheim NR
Banning
Palm Springs
Lake Elsinore
Last Updated: April 24, 2020

APPENDIX C
ADDITIONAL MPE

Appendix C. Additional MPE

This Appendix provides additional model performance plots for MDA8 ozone for 2019 for the selected sites shown in Chapter 7, as well as NOx model performance spatial plots.

LAX (06-037-5005)

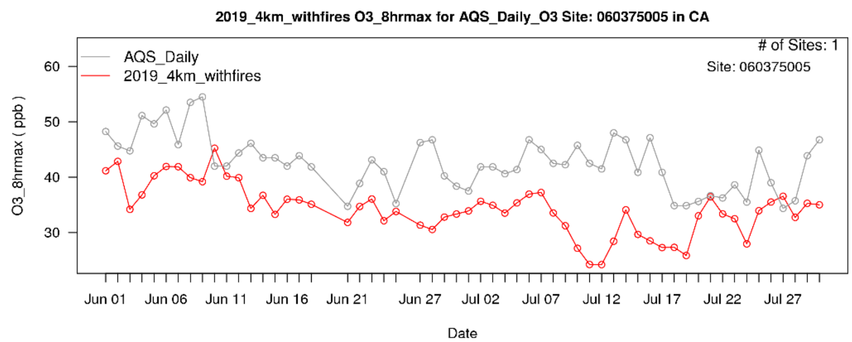

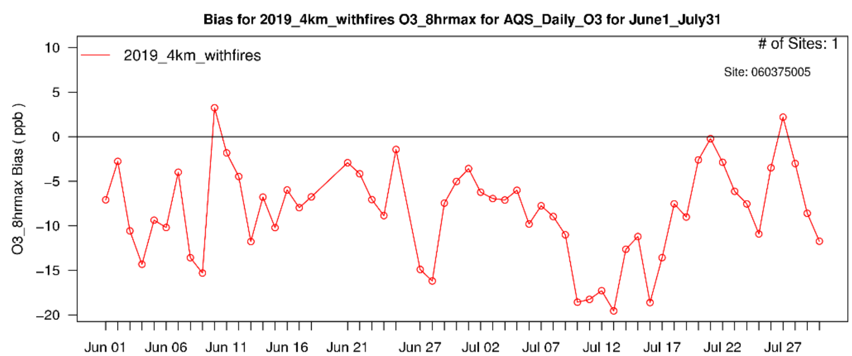

Los Angeles Main (06-037-1103)

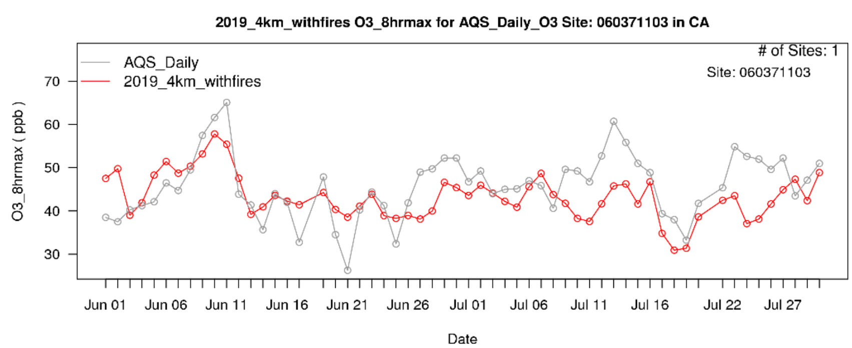

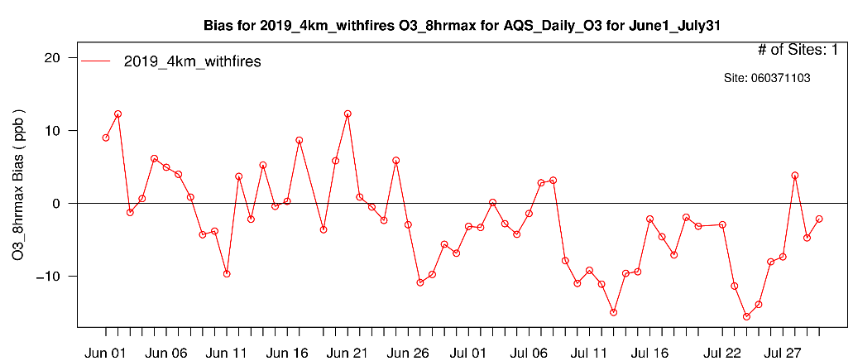

Figure C - 1. LAX and Los Angeles Main 2019 timeseries plots.

Azusa (06-037-0002)	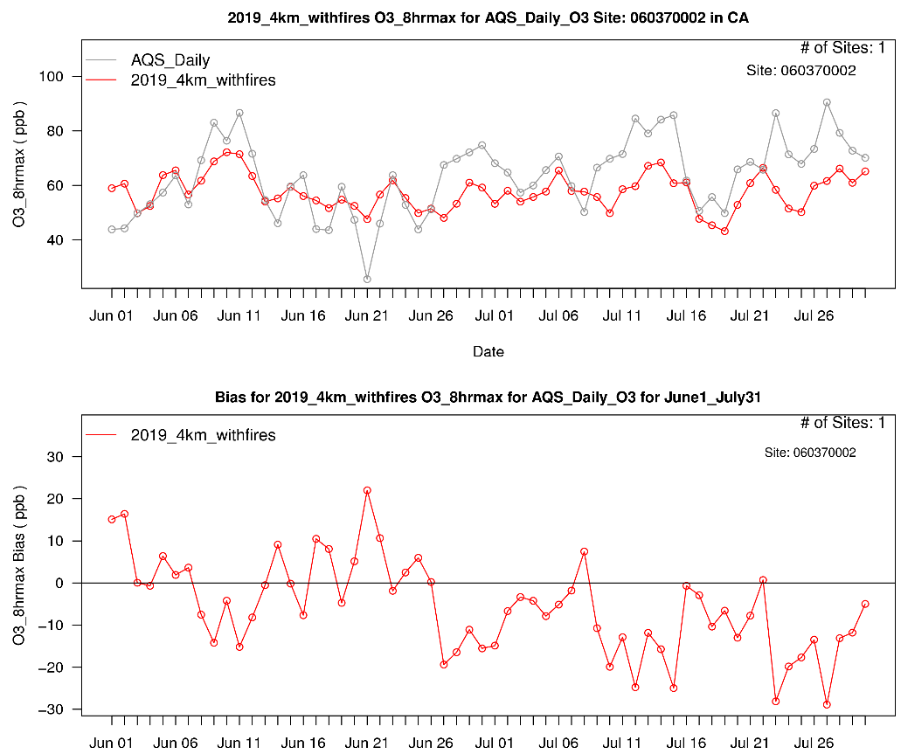
Glendora (06-037-0016)	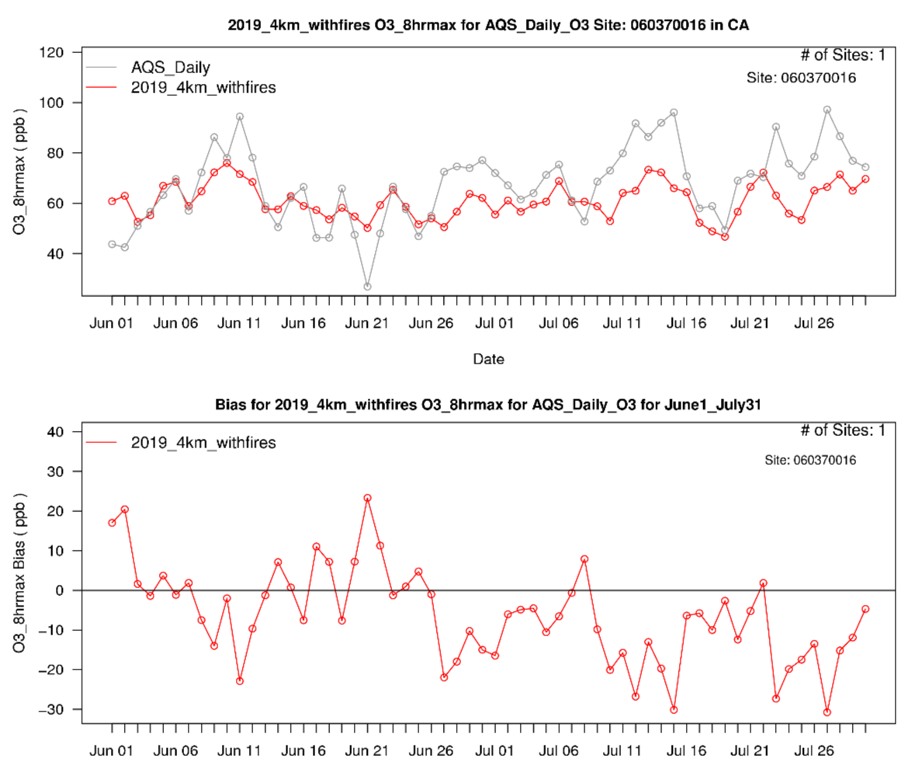

Figure C - 2. Azusa and Glendora 2019 timeseries plots.

Pomona (06-037-1701)	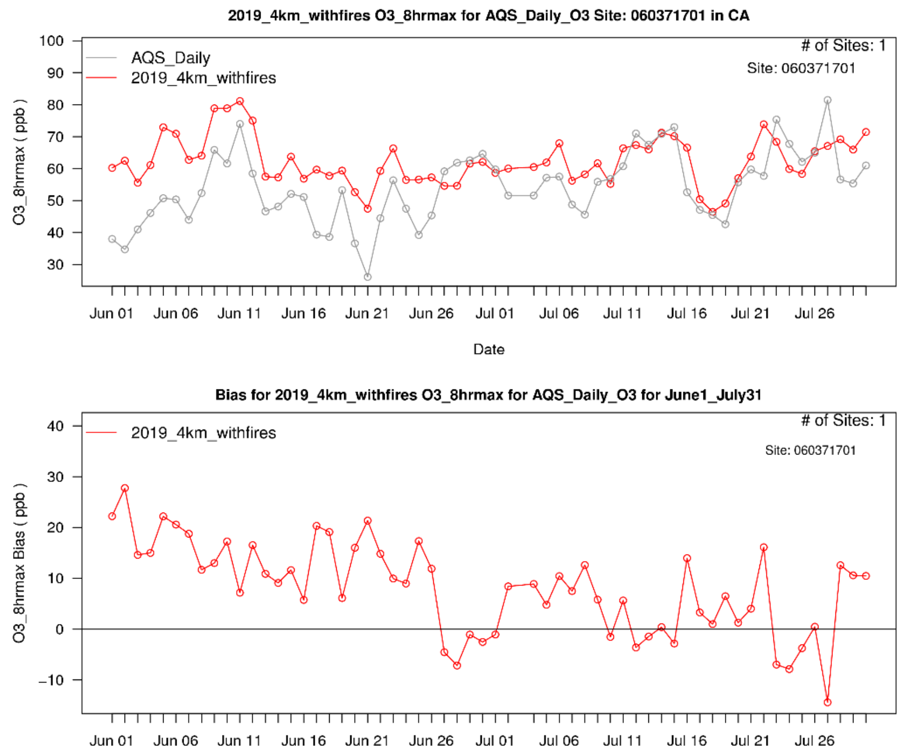
Uplands (06-071-1004)	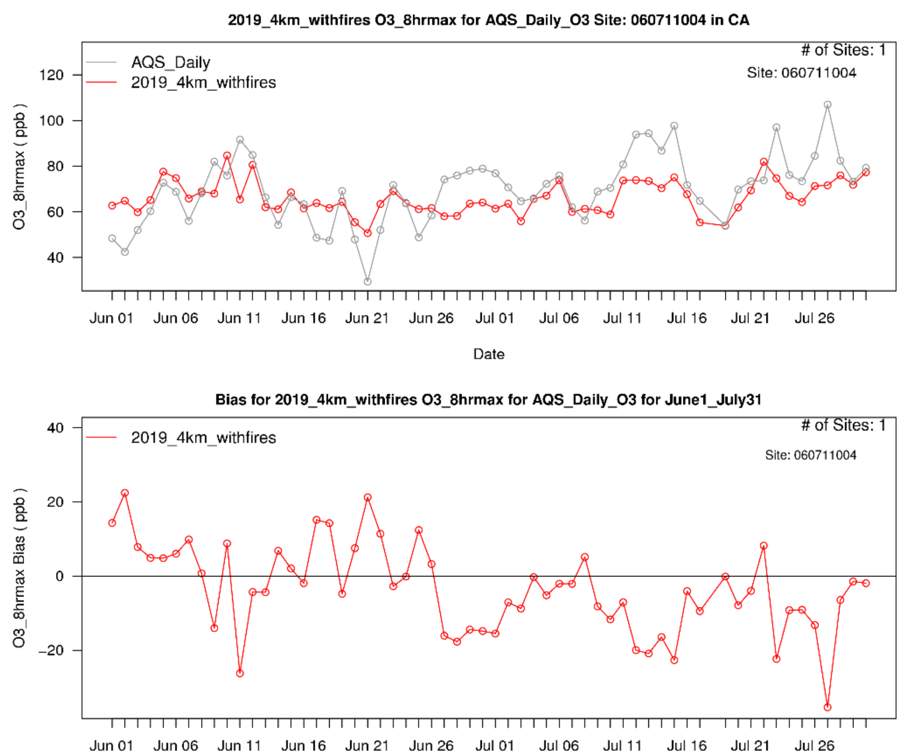

Figure C - 3. Pomona and Uplands 2019 timeseries plots.

Fontana (06-071-2002)	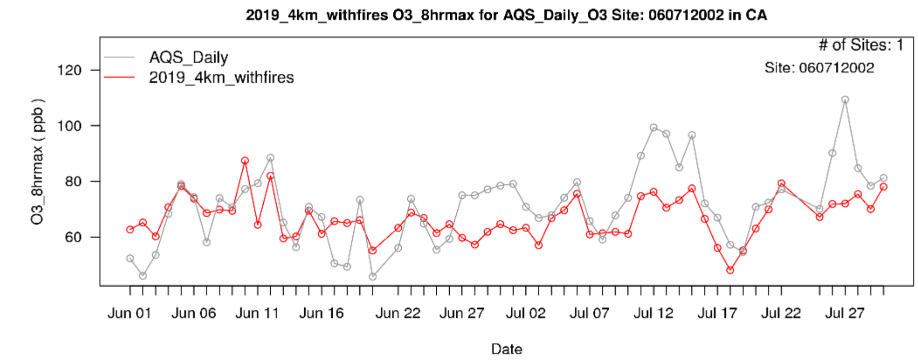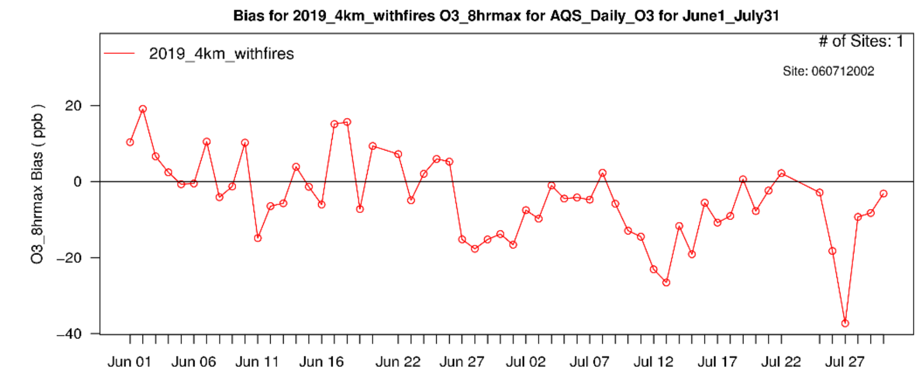
Crestline (06-071-0005)	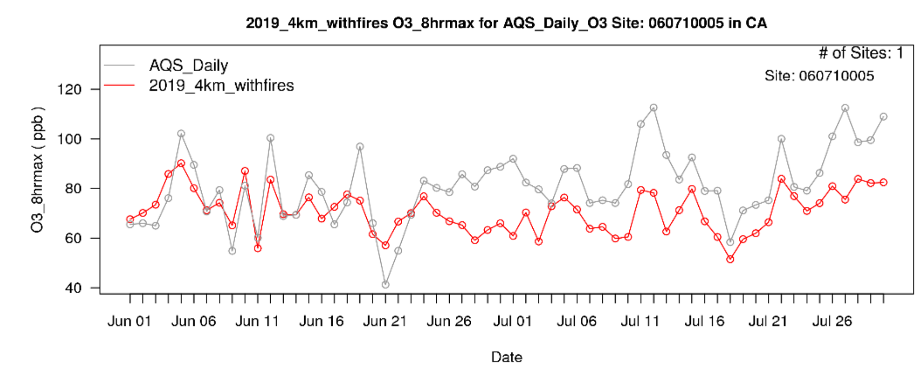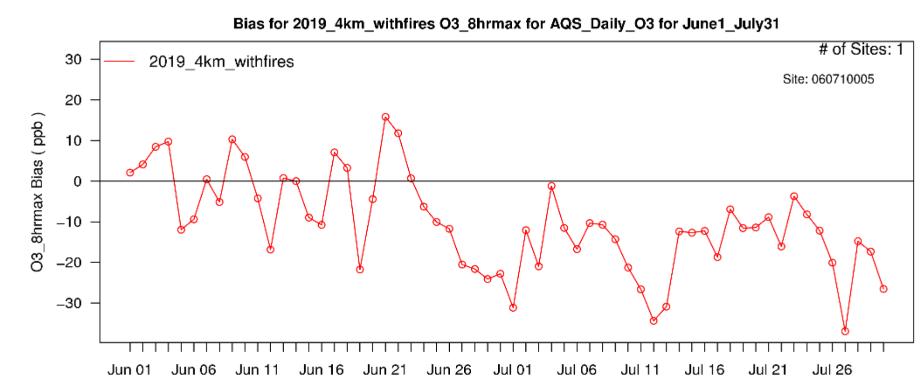

Figure C - 4. Fontana and San Bernardino 2019 timeseries plots.

San Bernardino (06-071-9004)	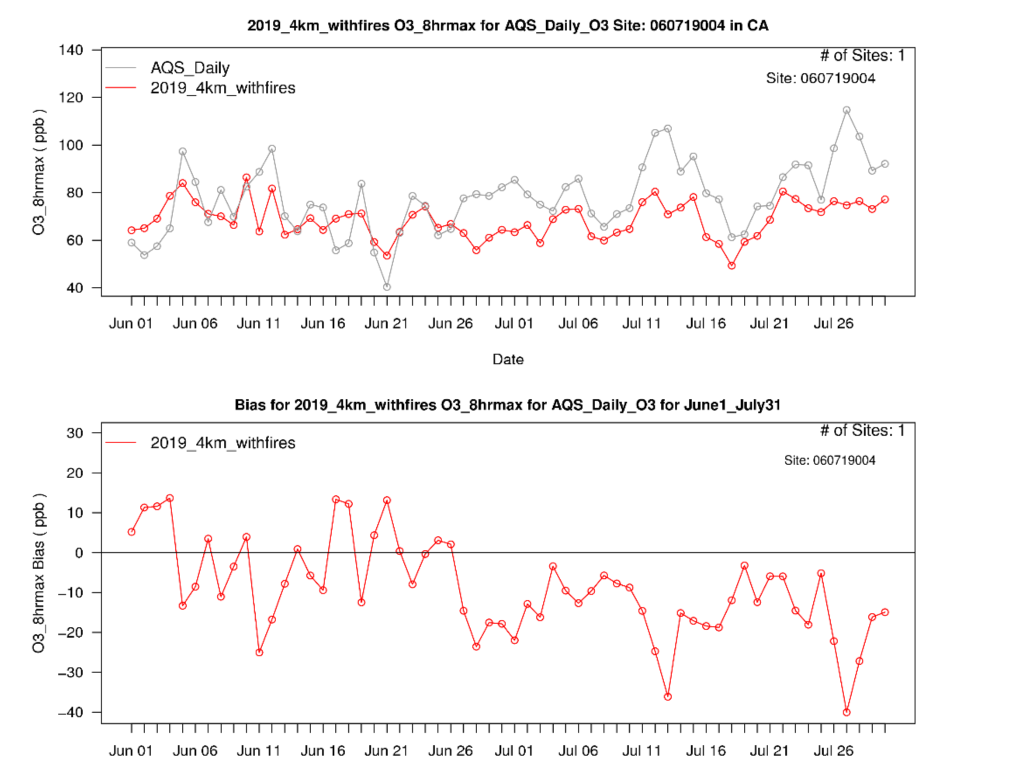
Redlands (06-071-4003)	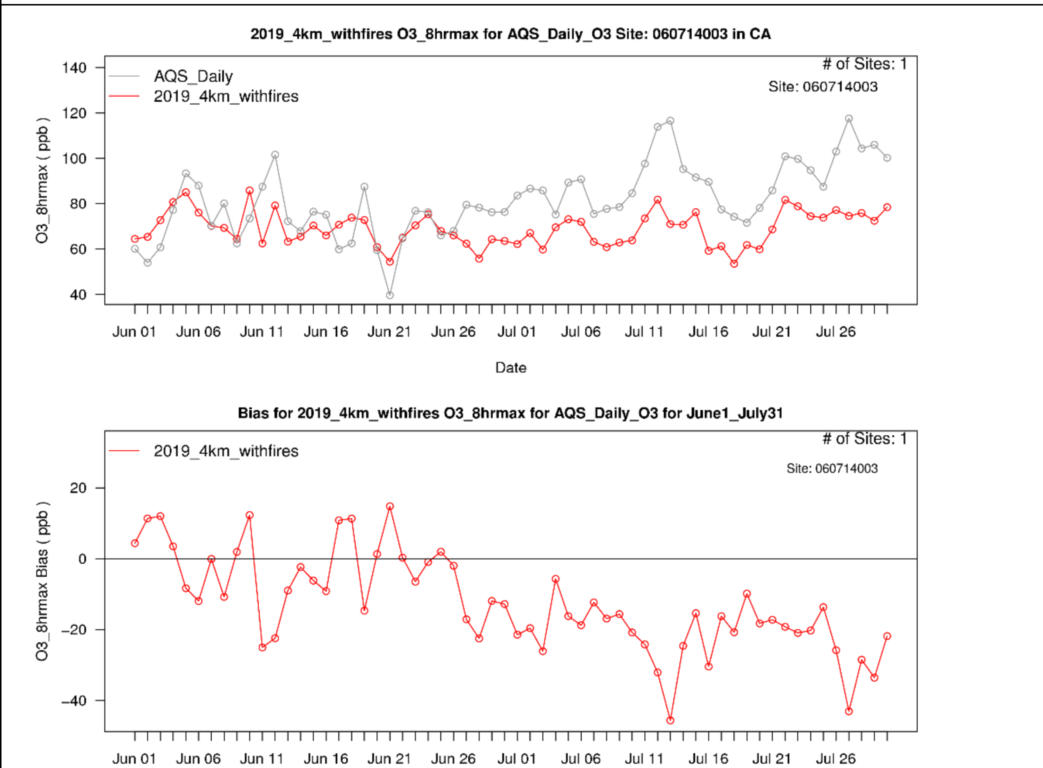

Figure C - 5. San Bernardino and Redlands 2019 timeseries plots.

APPENDIX D
CMAQ RUNSCRIPT

Appendix D. CMAQ Runscript

```
#!/bin/csh -f

# ===================== CCTMv5.2 Run Script =========================
# Usage: run.cctm >&! cctm_v52b.log &
#
# To report problems or request help with this script/program:
#           http://www.epa.gov/cmaq    (EPA CMAQ Website)
#           http://www.cmascenter.org  (CMAS Website)
#
=================================================================
====

#
=================================================================
===
#> Runtime Environment Options
#
=================================================================
===

#> Choose compiler and set up CMAQ environment with correct
#> libraries using config.cmaq. Options: intel | gcc | pgi
 if ( ! $?compiler ) then
   #setenv compiler intel
   setenv compiler pgi
 endif

#> Source the config.cmaq file to set the build environment
 #cd ../..
 #source ./config_cmaq.csh $compiler
 source /disk40/ema_covid/cmaq/CMAQ-5.2.1/config_cmaq.csh $compiler 13.4
 #cd CCTM/scripts

#> Set General Parameters for Configuring the Simulation
 set VRSN      = v521                         #> Code Version
 set PROC      = mpi                          #> serial or mpi
 set MECH      = saprc07tc_ae6_aq             #> Mechanism ID
 set EMIS      = ema_covid          #> Emission Inventory Details
 set APPL      = saprc07tc_ae6_aq   #> Application Name (e.g. Gridname)

#> Define RUNID as any combination of parameters above or others. By default,
#> this information will be collected into this one string, $RUNID, for easy
#> referencing in output binaries and log files as well as in other scripts.
 setenv RUNID  ${VRSN}_${compilerString}_${APPL}

#> Set the build directory (this is where the CMAQ executable
#> is located by default).
```

```
 set BASE     = /disk40/ema_covid/cmaq/CMAQ-5.2.1/CCTM/scripts
 set BLD      = ${BASE}/BLD_CCTM_${VRSN}_${compiler}
 set EXEC     = CCTM_${VRSN}.exe
 cat $BLD/CCTM_${VRSN}.cfg; echo "    "; set echo

#> Set Working, Input, and Output Directories
 setenv WORKDIR /disk40/ema_covid/runfiles/4km/2020COVID_withfires       #> Working Directory.
Where the runscript is.
 setenv OUTDIR /qhex1c/ema_covid/cmaq/outputs/4km/2020COVID_withfires
 setenv INPDIR  "Not_Available"    #> Input Directory
# setenv LOGDIR  ${OUTDIR}/LOGS     #> Log Directory Location
 setenv NMLpath ${BLD}             #> Location of Namelists. Common places are:
                               #>   ${WORKDIR} | ${CCTM_SRC}/MECHS/${MECH} | ${BLD}

#
==================================================================
======
#> CCTM Configuration Options
#
==================================================================
======

#> Set Start and End Days for looping
 #setenv NEW_START TRUE            #> Set to FALSE for model restart
 setenv NEW_START FALSE
 #set START_DATE = "2020-05-21"     #> beginning date (July 1, 2011)
 #set END_DATE   = "2020-05-21"
 set START_DATE = "2020-07-10"
 set END_DATE   = "2020-08-01"     #> ending date    (July 14, 2011)

#> Set Timestepping Parameters
set STTIME     = 0            #> beginning GMT time (HHMMSS)
set NSTEPS     = 240000           #> time duration (HHMMSS) for this run
set TSTEP      = 010000           #> output time step interval (HHMMSS)

#> Horizontal domain decomposition
if ( $PROC == serial ) then
   setenv NPCOL_NPROW "1 1"; set NPROCS   = 1 # single processor setting
else
   @ NPCOL  =  6; @ NPROW =  4
   @ NPROCS = $NPCOL * $NPROW
   setenv NPCOL_NPROW "$NPCOL $NPROW";
endif

#> Vertical extent
set NZ         = "No_need"

setenv LOGFILE $WORKDIR/$RUNID.log  #> log file name; uncomment to write standard output to a
log, otherwise write to screen
```

```
setenv GRID_NAME SoCAB_4km      #> check GRIDDESC file for GRID_NAME options
setenv GRIDDESC /disk40/ema_covid/inputs/mcip/GRIDDESC   #> grid description file

#> Output Species and Layer Options
#>   CONC file species; comment or set to "ALL" to write all species to CONC
    setenv CONC_SPCS "O3"
    #setenv CONC_BLEV_ELEV " 1 4" #> CONC file layer range; comment to write all layers to CONC

#>   ACONC file species; comment or set to "ALL" to write all species to ACONC
    #setenv AVG_CONC_SPCS "O3 NO CO NO2 ASO4I ASO4J NH3"
    setenv AVG_CONC_SPCS "ALL"
    setenv ACONC_BLEV_ELEV " 1 1" #> ACONC file layer range; comment to write all layers to
ACONC
    #setenv ACONC_END_TIME Y      #> override default beginning ACON timestamp [ default: N ]

setenv EXECUTION_ID $EXEC    #> define the model execution id

#> Sychronization Time Step and Tolerance Options
setenv CTM_MAXSYNC 720       #> max sync time step (sec) [ default: 720 ]
setenv CTM_MINSYNC  60       #> min sync time step (sec) [ default: 60 ]
setenv SIGMA_SYNC_TOP 0.7    #> top sigma level thru which sync step determined [ default: 0.7 ]
#setenv ADV_HDIV_LIM 0.95     #> maximum horiz. div. limit for adv step adjust [ default: 0.9 ]
setenv CTM_ADV_CFL 0.95      #> max CFL [ default: 0.75]
#setenv RB_ATOL 1.0E-09       #> global ROS3 solver abs tol [ default: 1.0E-07 ]

#> Science Options
setenv CTM_WB_DUST N         #> use inline windblown dust emissions [ default: Y ]
setenv CTM_ERODE_AGLAND Y    #> use agricultural activity for windblown dust
                       #>    [ default: N ]; ignore if CTM_WB_DUST = N
setenv CTM_WBDUST_BELD BELD3 #> landuse database for identifying dust source regions
                       #>    [ default: BELD3 ]; ignore if CTM_WB_DUST = N
setenv CTM_LTNG_NO N         #> turn on lightning NOx [ default: N ]
setenv CTM_WVEL N            #> save derived vertical velocity component to conc
                       #>    file [ default: N ]
setenv KZMIN Y               #> use Min Kz option in edyintb [ default: Y ],
                       #>    otherwise revert to Kz0UT
setenv CTM_ILDEPV Y          #> calculate in-line deposition velocities [ default: Y ]
setenv CTM_MOSAIC N          #> landuse specific deposition velocities [ default: N ]
setenv CTM_FST N             #> mosaic method to get land-use specific stomatal flux
                       #>    [ default: N ]
setenv CTM_ABFLUX N          #> ammonia bi-directional flux for in-line deposition
                       #>    velocities [ default: N ]; ignore if CTM_ILDEPV = N
setenv CTM_HGBIDI N          #> mercury bi-directional flux for in-line deposition
                       #>    velocities [ default: N ]; ignore if CTM_ILDEPV = N
setenv CTM_SFC_HONO Y        #> surface HONO interaction [ default: Y ]; ignore if CTM_ILDEPV = N
setenv CTM_GRAV_SETL Y       #> vdiff aerosol gravitational sedimentation [ default: Y ]
setenv CTM_BIOGEMIS N        #> calculate in-line biogenic emissions [ default: N ]
setenv CTM_PT3DEMIS Y        #> calculate in-line plume rise for elevated point emissions
```

```
                         #>    [ default: N ]
setenv CTM_ZERO_PCSOA N      #> turn off the emissions of the VOC precursor to pcSOA.
                         #>    The CMAQ dev team recommends leaving pcSOA mass in the
                         #>    model for production runs. [ default: N ]

#> Process Analysis Options
setenv CTM_PROCAN N         #> use process analysis [ default: N]
#> process analysis global column, row and layer ranges
#> user must check GRIDDESC for validity!
setenv PA_BCOL_ECOL "10 320"
setenv PA_BROW_EROW "10 195"
setenv PA_BLEV_ELEV "1  4"

#> I/O Controls
setenv IOAPI_LOG_WRITE F     #> turn on excess WRITE3 logging [ options: T | F ]
setenv FL_ERR_STOP N         #> stop on inconsistent input files
setenv PROMPTFLAG F          #> turn on I/O-API PROMPT*FILE interactive mode [ options: T | F ]
setenv IOAPI_OFFSET_64 NO    #> support large timestep records (>2GB/timestep record) [ options:
YES | NO ]
setenv CTM_EMISCHK N         #> Abort CMAQ if missing surrogates from emissions Input files

#> Aerosol Diagnostic Controls
setenv CTM_AVISDIAG N        #> Aerovis diagnostic file [ default: N ]
setenv CTM_PMDIAG Y          #> What is this [ default: Y ]
setenv CTM_APMDIAG Y         #> What is this [ default: Y ]
setenv APMDIAG_BLEV_ELEV "1 3" #> layer range for average pmdiag
setenv APMDIAG_BLEV_ELEV ""  #> layer range for average pmdiag = NLAYS
setenv AVG_FILE_ENDTIME N    #> What is this [ default: N ]

#> Diagnostic Output Flags
setenv CTM_CKSUM Y           #> cksum report [ default: Y ]
setenv CLD_DIAG N            #> cloud diagnostic file [ default: N ]
setenv CTM_AERDIAG N         #> aerosol diagnostic file [ default: N ]
setenv CTM_PHOTDIAG N        #> photolysis diagnostic file [ default: N ]
setenv CTM_SSEMDIAG N        #> sea-salt emissions diagnostic file [ default: N ]
setenv CTM_DUSTEM_DIAG Y     #> windblown dust emissions diagnostic file [ default: N ]; ignore if
CTM_WB_DUST = N
setenv CTM_DEPV_FILE N       #> deposition velocities diagnostic file [ default: N ]
setenv VDIFF_DIAG_FILE N     #> vdiff & possibly aero grav. sedimentation diagnostic file [ default: N
]
setenv LTNGDIAG N            #> lightning diagnostic file [ default: N ]
setenv CTM_AOD N             #> AOD diagnostic file [ default: N ]
setenv B3GTS_DIAG Y          #> beis mass emissions diagnostic file [ default: N ]
setenv PT3DDIAG N            #> optional 3d point source emissions diagnostic file [ default: N]; ignore
if CTM_PT3DEMIS = N
setenv PT3DFRAC N            #> optional layer fractions diagnostic (play) file(s) [ default: N]; ignore if
CTM_PT3DEMIS = N
setenv REP_LAYER_MIN -1      #> Minimum layer for reporting plume rise info [ default: -1 ]
```

set DISP = delete #> [delete | keep] existing output files

#
==
#> Input Directories and Filenames
#
==

set ICpath = /disk40/ema_covid/inputs/icbc_4km_from12km/2020_withfires #> initial conditions input directory
set BCpath = /disk40/ema_covid/inputs/icbc_4km_from12km/2020_withfires #> boundary conditions input directory
set EMISpath = /disk40/ema_covid/emis/emis_proc_round2/4km/5.mrggrid_withCOVID/outputs/2020 #> surface emissions input directory
set IN_PTpath = /disk40/ema_covid/emis/emis_proc_round2/4km/4.adjustpoints/output/x2q_inln #> elevated emissions input directory (in-line point only)
set IN_PTpath2 = /disk40/ema_covid/emis/emis_proc_round2/4km/4.adjustpoints/output/add25th_hour
set IN_PTpath3 = /disk40/ema_covid/emis/FINN/outputs/model_ready/cmaq/2020
#set IN_LTpath = #> lightning NOx input directory
set METpath = /disk40/ema_covid/inputs/mcip #> meteorology input directory
#set JVALpath = $INPDIR/jproc #> offline photolysis rate table directory
set OMIpath = $BLD #> ozone columne data for the photolysis model
#set LUpath = #> BELD landuse data for windblown dust model
set SZpath = /disk40/ema_covid/inputs/ocean #> surf zone file for in-line seasalt emissions

set ICBC_CASE = "No_need" #> Version label for the ICBCs
set EMIS_CASE = "No_need" #> Version Label for the Emissions

#
==
#> Begin Loop Through Simulation Days
#
==

set TODAYG = ${START_DATE}
set TODAYJ = `date -ud "${START_DATE}" +%Y%j` #> Convert YYYY-MM-DD to YYYYJJJDEC_FBKS_SIPDEC_FBKS_SIP
set STOP_DAY = `date -ud "${END_DATE}" +%Y%j` #> Convert YYYY-MM-DD to YYYYJJJ

while ($TODAYJ <= $STOP_DAY) #>Compare dates in terms of YYYYJJJ

#> Retrieve Calendar day Information

```
 set YYYYMMDD = `date -ud "${TODAYG}" +%Y%m%d` #> Convert YYYY-MM-DD to YYYYMMDD
 set YYMMDD = `date -ud "${TODAYG}" +%y%m%d`   #> Convert YYYY-MM-DD to YYMMDD
 set YYYYJJJ = $TODAYJ

 #> Calculate Yesterday's Date
 set YESTERDAY = `date -ud "${TODAYG}-1days" +%Y%m%d` #> Convert YYYY-MM-DD to YYYYJJJ

#
=================================================================
======
#> Input Files (Some are Day-Dependent)
#
=================================================================
======

 #> Initial conditions
 if ($NEW_START == true || $NEW_START == TRUE ) then
    setenv ICFILE ICON_v52_SoCAB_4km_${YYYYMMDD}
    setenv INITIAL_RUN Y #related to restart soil information file
#     rm -rf $LOGDIR/CTM_LOG*${RUNID}*  # Remove all Log Files Since this is a new start
    mkdir -p $OUTDIR
 else
    set ICpath = $OUTDIR
    setenv ICFILE CCTM_CGRID_${RUNID}_${YESTERDAY}.nc
    setenv INITIAL_RUN N
 endif

 #> Boundary conditions
 set BCFILE = BCON_v52_SoCAB_4km_${YYYYMMDD}

 #> Off-line photolysis rates
 #set JVALfile  = JTABLE_${YYYYJJJ}

 #> Ozone column data
 set OMIfile   = OMI_1979_to_2015.dat

 #> Optics file
 set OPTfile = PHOT_OPTICS.dat

 #> MCIP meteorology files
 setenv GRID_CRO_2D $METpath/${YYYYMMDD}/GRIDCRO2D_SoCAB_4km.${YYYYMMDD}
 setenv GRID_DOT_2D $METpath/${YYYYMMDD}/GRIDDOT2D_SoCAB_4km.${YYYYMMDD}
 setenv MET_CRO_2D $METpath/${YYYYMMDD}/METCRO2D_SoCAB_4km.${YYYYMMDD}
 setenv MET_CRO_3D $METpath/${YYYYMMDD}/METCRO3D_SoCAB_4km.${YYYYMMDD}
 setenv MET_DOT_3D $METpath/${YYYYMMDD}/METDOT3D_SoCAB_4km.${YYYYMMDD}
 setenv MET_BDY_3D $METpath/${YYYYMMDD}/METBDY3D_SoCAB_4km.${YYYYMMDD}

 setenv LAYER_FILE $MET_CRO_3D  # Deprecated: MET_CRO_3D is now read directly in CCTM
```

```
 #> Emissions files
 if ( $CTM_PT3DEMIS == 'N' ) then
    #> Offline 3d emissions file name
    #set EMISfile  = emis.2020noCOVID_ANT+OGV+MEX+BIOwURB_LAI.${YYYYMMDD}.ncf
    if ( ! -f $EMISpath/$EMISfile ) then
      if ( -f $EMISpath/${EMISfile}.gz ) then
        echo "unzipping emissions"
        cat $EMISpath/${EMISfile}.gz | gunzip > $EMISpath/${EMISfile}
      else
        echo "CAN'T FIND EMIS FILE OR ZIP"
        exit
      endif
    endif
 else
    #> In-line emissions configuration
    set EMISfile  = emis.ARB_griddedANTH+MEX+BIO_4kmSoCAB_2020withCOVID.${YYYYMMDD}.ncf
#> Surface emissions
    setenv NPTGRPS 3          #> Number of elevated source groups

    setenv STK_GRPS_01 $IN_PTpath2/point/stkgrps.point.ncf
    setenv STK_GRPS_02 $IN_PTpath2/ogv_inln/stkgrps.ogv_inln.ncf
    setenv STK_GRPS_03
$IN_PTpath3/cmaq.stack_groups.ema_covid.finnv15_fires.${YYYYMMDD}.saprc07tc.12km.ncf
    setenv LAYP_STTIME $STTIME
    setenv LAYP_NSTEPS $NSTEPS

    setenv STK_EMIS_01
$IN_PTpath2/point/cmaq.inline_pt.point.${YYYYMMDD}.stitched_windowed_scaled_wCOVID.SoCAB_4
km.25hrs.nc
    setenv STK_EMIS_02
$IN_PTpath2/ogv_inln/cmaq.inline_pt.ogv_inln.${YYYYMMDD}.stitched_windowed_scaled_wCOVID.So
CAB_4km.25hrs.nc
    setenv STK_EMIS_03
$IN_PTpath3/cmaq.inline_pts.ema_covid.finnv15_fires.${YYYYMMDD}.saprc07tc.12km.ncf
    setenv LAYP_STDATE $YYYYJJJ
 endif

 #> Lightning NOx configuration
 if ( $CTM_LTNG_NO == 'Y' ) then
    setenv LTNGNO "InLine"    #> set LTNGNO to "Inline" to activate in-line calculation

 #> In-line lightning NOx options
    setenv USE_NLDN  Y        #> use hourly NLDN strike file [ default: Y ]
    setenv LTNGPARAM Y        #> use lightning parameter file [ default: Y ]
    if ( $USE_NLDN == Y ) then
      setenv NLDN_STRIKES $INPDIR/lightning/NLDN.12US1.${YYYYMMDD}_bench.nc
    else
      setenv LOG_START 2.0   #> RC value to transit linear to log linear
```

```
    endif
    setenv LTNGPARMS_FILE $INPDIR/lightning/LTNG_AllParms_12US1_bench.nc #> lightning
parameter file; ignore if LTNGPARAM = N
  endif


  #> In-line biogenic emissions configuration
  if ( $CTM_BIOGEMIS == 'Y' ) then
    set IN_BEISpath = ${INPDIR}/land
    set GSPROpath   = ${IN_BEISpath}
    setenv GSPRO      $GSPROpath/gspro_biogenics_1mar2017.txt
    setenv B3GRD      $IN_BEISpath/b3grd_bench.nc
    setenv BIOG_SPRO  B10C6 #> speciation profile to use for biogenics
    setenv BIOSW_YN   Y     #> use frost date switch [ default: Y ]
    setenv BIOSEASON  $IN_BEISpath/bioseason.cmaq.2011_12US1_wetland100.ghrsst_bench.ncf
#> ignore season switch file if BIOSW_YN = N
    setenv SUMMER_YN  Y     #> Use summer normalized emissions? [ default: Y ]
    setenv PX_VERSION Y     #> MCIP is PX version? [ default: N ]
    setenv SOILINP    $OUTDIR/CCTM_SOILOUT_${RUNID}_${YESTERDAY}.nc
                      #> Biogenic NO soil input file; ignore if INITIAL_RUN = Y
  endif

  #> Windblown dust emissions configuration
  if ( $CTM_WB_DUST == 'Y' ) then
    # Input variables for BELD3 Landuse option
    setenv DUST_LU_1 $LUpath/beld3_12US1_459X299_output_a_bench.nc
    setenv DUST_LU_2 $LUpath/beld4_12US1_459X299_output_tot_bench.nc
    setenv MODIS_FPAR $LUpath/modis_bench.nc

    if ( $CTM_ERODE_AGLAND == 'Y' ) then
      setenv CROPMAP01 ${INPDIR}/land/BeginPlanting_12km_bench.nc
      setenv CROPMAP04 ${INPDIR}/land/EndPlanting_12km_bench.nc
      setenv CROPMAP08 ${INPDIR}/land/EndHarvesting_12km_bench.nc
    endif
  endif

  #> In-line sea salt emisisions configuration
  setenv OCEAN_1 $SZpath/ocean_scos_4km_156x102.ncf #> horizontal grid-dependent surf zone file

  #> Bidiretional ammonia configuration
  if ( $CTM_ABFLUX == 'Y' ) then
    setenv E2C_Soilfile  ${INPDIR}/land/2011_US1_soil_bench.nc
    setenv E2C_Fertfile  ${INPDIR}/land/2011_US1_time${YYYYMMDD}_bench.nc
    setenv B4LU_file     ${INPDIR}/land/beld4_12kmCONUS_2006nlcd_bench.nc
    setenv E2C_SOIL ${E2C_Soilfile}
    setenv E2C_FERT ${E2C_Fertfile}
    setenv BELD4_LU ${B4LU_file}
  endif
```

```
#
=================================================================
======
#> Output Files
#
=================================================================
======
  #> set output file name extensions
  setenv CTM_APPL ${RUNID}_${YYYYMMDD}
  #> set output file names
  setenv S_CGRID         "$OUTDIR/CCTM_CGRID_${CTM_APPL}.nc"         #> 3D Inst.
Concenctrations
  setenv CTM_CONC_1      "$OUTDIR/CCTM_CONC_${CTM_APPL}.nc -v"       #> On-Hour
Concentrations
  setenv A_CONC_1        "$OUTDIR/CCTM_ACONC_${CTM_APPL}.nc -v"      #> Hourly Avg.
Concentrations
  setenv MEDIA_CONC      "$OUTDIR/CCTM_MEDIA_CONC_${CTM_APPL}.nc -v" #> NH3 Conc. in
Media
  setenv CTM_DRY_DEP_1   "$OUTDIR/CCTM_DRYDEP_${CTM_APPL}.nc -v"     #> Hourly Dry
Deposition
  setenv CTM_DEPV_DIAG   "$OUTDIR/CCTM_DEPV_${CTM_APPL}.nc -v"       #> Dry Deposition
Velocities
  setenv CTM_PT3D_DIAG   "$OUTDIR/CCTM_PT3D_${CTM_APPL}.nc -v"       #>
  setenv B3GTS_S         "$OUTDIR/CCTM_B3GTS_S_${CTM_APPL}.nc -v"    #> Biogenic Emissions
  setenv SOILOUT         "$OUTDIR/CCTM_SOILOUT_${CTM_APPL}.nc"       #> Soil Emissions
  setenv CTM_WET_DEP_1   "$OUTDIR/CCTM_WETDEP1_${CTM_APPL}.nc -v"    #> Wet Dep From All
Clouds
  setenv CTM_WET_DEP_2   "$OUTDIR/CCTM_WETDEP2_${CTM_APPL}.nc -v"    #> Wet Dep From
SubGrid Clouds
  setenv CTM_VIS_1       "$OUTDIR/CCTM_PMVIS_${CTM_APPL}.nc -v"      #> On-Hour Visibility
  setenv CTM_AVIS_1      "$OUTDIR/CCTM_APMVIS_${CTM_APPL}.nc -v"     #> Hourly-Averaged
Visibility
  setenv CTM_PMDIAG_1    "$OUTDIR/CCTM_PMDIAG_${CTM_APPL}.nc -v"     #> On-Hour Particle
Diagnostics
  setenv CTM_APMDIAG_1   "$OUTDIR/CCTM_APMDIAG_${CTM_APPL}.nc -v"    #> Hourly Avg.
Particle Diagnostic
  setenv CTM_RJ_1        "$OUTDIR/CCTM_PHOTDIAG1_${CTM_APPL}.nc -v"  #> Photolysis Rxn
Diagnostics
  setenv CTM_RJ_2        "$OUTDIR/CCTM_PHOTDIAG2_${CTM_APPL}.nc -v"  #> Photolysis Rates
Output
  setenv CTM_SSEMIS_1    "$OUTDIR/CCTM_SSEMIS_${CTM_APPL}.nc -v"     #> Sea Spray
Emissions
  setenv CTM_DUST_EMIS_1 "$OUTDIR/CCTM_DUSTEMIS_${CTM_APPL}.nc -v"   #> Dust Emissions
  setenv CTM_IPR_1       "$OUTDIR/CCTM_PA_1_${CTM_APPL}.nc -v"       #> Process Analysis
  setenv CTM_IPR_2       "$OUTDIR/CCTM_PA_2_${CTM_APPL}.nc -v"       #> Process Analysis
  setenv CTM_IPR_3       "$OUTDIR/CCTM_PA_3_${CTM_APPL}.nc -v"       #> Process Analysis
  setenv CTM_IRR_1       "$OUTDIR/CCTM_IRR_1_${CTM_APPL}.nc -v"      #> Chem Process Analysis
  setenv CTM_IRR_2       "$OUTDIR/CCTM_IRR_2_${CTM_APPL}.nc -v"      #> Chem Process Analysis
  setenv CTM_IRR_3       "$OUTDIR/CCTM_IRR_3_${CTM_APPL}.nc -v"      #> Chem Process Analysis
```

```
  setenv CTM_DRY_DEP_MOS "$OUTDIR/CCTM_DDMOS_${CTM_APPL}.nc -v"      #> Dry Dep
  setenv CTM_DRY_DEP_FST "$OUTDIR/CCTM_DDFST_${CTM_APPL}.nc -v"      #> Dry Dep
  setenv CTM_DEPV_MOS    "$OUTDIR/CCTM_DEPVFST_${CTM_APPL}.nc -v"    #> Dry Dep Velocity
  setenv CTM_DEPV_FST    "$OUTDIR/CCTM_DEPVMOS_${CTM_APPL}.nc -v"    #> Dry Dep Velocity
  setenv CTM_VDIFF_DIAG  "$OUTDIR/CCTM_VDIFF_DIAG_${CTM_APPL}.nc -v" #> Vertical
Dispersion Diagnostic
  setenv CTM_VSED_DIAG   "$OUTDIR/CCTM_VSED_DIAG_${CTM_APPL}.nc -v"  #> Particle Grav.
Settling Velocity
  setenv CTM_AOD_1       "$OUTDIR/CCTM_AOD_DIAG_${CTM_APPL}.nc -v"   #> Aerosol Optical
Depth Diagnostic
  setenv CTM_LTNGDIAG_1  "$OUTDIR/CCTM_LTNGHRLY_${CTM_APPL}.nc -v"   #> Hourly Avg
Lightning NO
  setenv CTM_LTNGDIAG_2  "$OUTDIR/CCTM_LTNGCOL_${CTM_APPL}.nc -v"    #> Column Total
Lightning NO

  #> set floor file (neg concs)
  setenv FLOOR_FILE ${OUTDIR}/FLOOR_${CTM_APPL}.txt

  #> create output directory
  if ( ! -d "$OUTDIR" ) mkdir -p $OUTDIR

  #> look for existing log files and output files
  set log_test = `ls CTM_LOG_???.${CTM_APPL}`
  set OUT_FILES = (${FLOOR_FILE} ${S_CGRID} ${CTM_CONC_1} ${A_CONC_1} ${MEDIA_CONC}
\
           ${CTM_DRY_DEP_1} $CTM_DEPV_DIAG $CTM_PT3D_DIAG $B3GTS_S $SOILOUT
$CTM_WET_DEP_1\
           $CTM_WET_DEP_2 $CTM_VIS_1 $CTM_AVIS_1 $CTM_PMDIAG_1 $CTM_APMDIAG_1
\
           $CTM_RJ_1 $CTM_RJ_2 $CTM_SSEMIS_1 $CTM_DUST_EMIS_1 $CTM_IPR_1 $CTM_IPR_2
\
           $CTM_IPR_3 $CTM_IRR_1 $CTM_IRR_2 $CTM_IRR_3 $CTM_DRY_DEP_MOS                  \
           $CTM_DRY_DEP_FST $CTM_DEPV_MOS $CTM_DEPV_FST $CTM_VDIFF_DIAG
$CTM_VSED_DIAG    \
           $CTM_AOD_1 $CTM_LTNGDIAG_1 $CTM_LTNGDIAG_2)
  set OUT_FILES = `echo $OUT_FILES | sed "s; -v;;g" `
  echo $OUT_FILES
  set out_test = `ls $OUT_FILES`

  #> delete previous output if requested
  if ( $DISP == 'delete' ) then
     #> remove previous log files
     echo " ancillary log files being deleted"
     foreach file ( $log_test )
        echo " deleting $file"
        /bin/rm -f $file
     end

     #> remove previous output files
```

```
    echo " output files being deleted"
    foreach file ( $out_test )
      echo " deleting $file"
      /bin/rm -f $file
    end

 else
    #> remove previous log files
    if ( "$log_test" != "" ) then
      echo "*** Logs exist - run ABORTED ***"
      echo "*** To overide, set $DISP == delete in run_cctm.csh ***"
      echo "*** and these files will be automatically deleted. ***"
      exit 1
    endif

    #> remove previous output files
    if ( "$out_test" != "" ) then
      echo "*** Output Files Exist - run will be ABORTED ***"
      foreach file ( $out_test )
        echo " cannot delete $file"
        /bin/rm -f $file
      end
      echo "*** To overide, set $DISP == delete in run_cctm.csh ***"
      echo "*** and these files will be automatically deleted. ***"
      exit 1
    endif
 endif

 #> for the run control ...
 setenv CTM_STDATE      $YYYYJJJ
 setenv CTM_STTIME      $STTIME
 setenv CTM_RUNLEN      $NSTEPS
 setenv CTM_TSTEP       $TSTEP
 setenv EMIS_1 $EMISpath/$EMISfile
 setenv INIT_GASC_1 $ICpath/$ICFILE
 setenv INIT_AERO_1 $INIT_GASC_1
 setenv INIT_NONR_1 $INIT_GASC_1
 setenv INIT_TRAC_1 $INIT_GASC_1
 setenv BNDY_GASC_1 $BCpath/$BCFILE
 setenv BNDY_AERO_1 $BNDY_GASC_1
 setenv BNDY_NONR_1 $BNDY_GASC_1
 setenv BNDY_TRAC_1 $BNDY_GASC_1
 setenv OMI $OMIpath/$OMIfile
 setenv OPTICS_DATA $OMIpath/$OPTfile
 #setenv XJ_DATA $JVALpath/$JVALfile
 set TR_DVpath = $METpath
 set TR_DVfile = $MET_CRO_2D

 #> species defn & photolysis
```

```
 setenv gc_matrix_nml ${NMLpath}/GC_$MECH.nml
 setenv ae_matrix_nml ${NMLpath}/AE_$MECH.nml
 setenv nr_matrix_nml ${NMLpath}/NR_$MECH.nml
 setenv tr_matrix_nml ${NMLpath}/Species_Table_TR_0.nml

 #> check for photolysis input data
 setenv CSQY_DATA ${NMLpath}/CSQY_DATA_$MECH

 if (! (-e $CSQY_DATA ) ) then
    echo " $CSQY_DATA  not found "
    exit 1
 endif
 if (! (-e $OPTICS_DATA ) ) then
    echo " $OPTICS_DATA  not found "
    exit 1
 endif

#
=================================================================
====
#> Execution Portion
#
=================================================================
====

 #> Print attributes of the executable
 ls -l $BLD/$EXEC; size $BLD/$EXEC
 unlimit
 limit

 set RUN_LOG = $WORKDIR/stdout.$APPL
 date > $RUN_LOG

 #> Executable call for single PE, uncomment to invoke
 # /usr/bin/time  $BLD/$EXEC

 #> Executable call for multi PE, configure for your system
 set MPI = /usr/local/mpich3/bin
 set MPIRUN = $MPI/mpiexec
 $MPIRUN -n $NPROCS $BLD/$EXEC < /dev/null >>& $RUN_LOG

 if ( -f $EMISpath/${EMISfile}.gz ) then
    if ( -f $EMISpath/$EMISfile ) then
       echo "archive exists, removing expanded emissions"
       ls -l $EMISpath/${EMISfile}.gz
       ls -l $EMISpath/${EMISfile}
       rm -v $EMISpath/${EMISfile}
    endif
  endif
```

```
  date >> $RUN_LOG

  mv -f $LOGFILE $WORKDIR/LOGS/log.$APPL.$CTM_APPL
  mv -f $RUN_LOG $WORKDIR/LOGS/stdout.$APPL.$CTM_APPL
  mv -f CTM_LOG_* $WORKDIR/LOGS/
  mv -f FLOOR_* $WORKDIR/LOGS/

#
=================================================================
====
#> Finalize Run for This Day and Loop to Next Day
#
=================================================================
====

  #> Save Log Files and Move on to Next Simulation Day
#  if (! -e $LOGDIR ) then
#    mkdir $LOGDIR
#  endif
#  mv CTM_LOG_???.${CTM_APPL} $LOGDIR

  #> The next simulation day will, by definition, be a restart
  setenv NEW_START false

  #> Increment both Gregorian and Julian Days
  set TODAYG = `date -ud "${TODAYG}+1days" +%Y-%m-%d` #> Add a day for tomorrow
  set TODAYJ = `date -ud "${TODAYG}" +%Y%j` #> Convert YYYY-MM-DD to YYYYJJJ

end  #Loop to the next Simulation Day

exit
```